Seismic Hazard Assessment of Dhaka, Chittagong and Sylhet City Corporation Area of Bangladesh

June 2009

Printing supported by:

Comprehensive Disaster Management Programme
Ministry of Disaster Management and Relief

UKaid from the British people
European Union
NORWEGIAN EMBASSY
SWEDEN
Australian AID
UNDP
Empowered lives.
Resilient nations.

Seismic Hazard Assessment of Dhaka, Chittagong and Sylhet City Corporation Area of Bangladesh

Comprehensive Disaster Management Programme (CDMP)
Ministry of Food and Disaster Management (MoFDM)
Government of the People's Republic of Bangladesh

Seismic Hazard Assessment of Dhaka, Chittagong and Sylhet City Corporation Area of Bangladesh

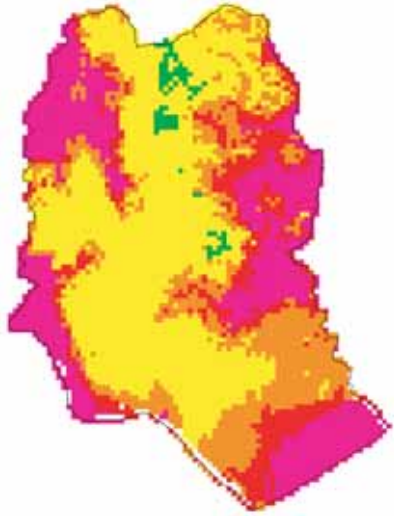

DF, PBF-1, PBF-2, PBF-3

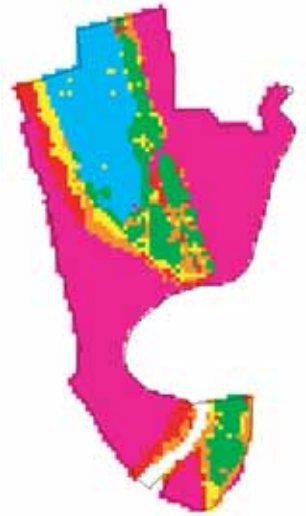

MF, DF, PBF-2, PBF-3

MF, PBF-1, PBF-3

June 2009

Comprehensive Disaster Management Programme (CDMP)
Ministry of Food and Disaster Management (MoFDM)
Government of the People's Republic of Bangladesh

SEISMIC HAZARD MAP

FOR

SEISMIC HAZARD

AND VULNERABILITY ASSESSMENT

OF

DHAKA, CHITTAGONG AND SYLHET

CITY CORPORATION AREA

Table of Contents

List of Figure

List of Table

Executive Summary

1. Baserock and Seismic Motion Analysis (Chapter 1 and Chapter 2)

The deterministic approach was adopted for the earthquake motion estimation in this study. The earthquake motion for engineering seismic baserock and sub-surface layer amplification were determined separately. An empirical method is used to calculate the earthquake motion for engineering baserock. Four formulas from NGA project are applied and average value was used. The stochastic Green's function study was also conducted for verification. The amplification by sub-surface soil layers was evaluated by the amplification factor which was decided by average shear wave velocity from ground surface to 30 meters depth. The ground of each grid was classified based on the modified NEHRP Provisions. The amplification factors of NEHRP Provisions were verified by the response analysis at 19 points, where PS loggings were conducted in this study, and the applicability of the amplification factor to Bangladesh was verified.

The PGA, PGV and Sa (h=5%, T=0.3 and 1.0 sec) at engineering seismic baserock (Vs30=760m/sec) were calculated. The most important earthquake in Dhaka is MF and the PGA in Dhaka is 130 to 230 gals. The most important earthquake in Chittagong is PBF-1 and PGA is 650 to 770 gal. The most important earthquakes in Sylhet are DF and PBF-2. PGA by DF is 180 to 240 gal and 160 to 240 gal by PBF-2.

The PGA, PGV and Sa (h=5%, T=0.3 and 1.0 sec) at ground surface were calculated. The PGA in Dhaka by MF is 220 to 410 gal. The PGA in Chittagong by PBF-1 is 600 to 770 gal and the effect of non-linearity of soils is remarkable. The PGA in Sylhet by DF is 270 to 420 gal and 230 to 420 gal by PBF-2.

2. Liquefaction Analysis (Chapter3 - Section 3.1)

The liquefaction potential was evaluated based on the procedure following HAZUS with geologic / geomorphic condition, PGA, magnitude (Mw) and groundwater depth. At first, liquefaction susceptibility is evaluated by geologic / geomorphic data and information of geological age. Secondary, liquefaction probability is estimated by inputting PGA, Mw and groundwater level into the above evaluated liquefaction susceptibility map.

The probability of liquefaction was calculated and classified from 1 (very low) to 5 (very high) and none (no distribution of saturated soft soil). The most severe scenario for Dhaka is MF and the ratio of rank 5 (very high) is 32%. For Chittagong, the most hazardous scenario is PBF-1 and the ratio of rank 5 is 11%. The impacts by DF and PBF-2 to Chittagong are almost same and the ratio of rank 5 is 6%.

3. Slope Failure Analysis (Chapter 3 - Section 3.2)

The probability of slope Failure was estimated by Fs, which is less than 1.2. As the results, Dhaka has low possibilities of slope failure in any scenario earthquakes.

For Chittagong, the most hazardous scenario is PBF-1, and FS which is less than 1.2 are found in 20-40% slopes of several grids in hill side. For Sylhet, the most hazardous scenario is DF and PBF-2, and Fs which is less than 1.2 are found in 10-20% slopes of several grids in hill side.

1. Baserock Motion Analysis

1.1. Outline

The approaches of earthquake motion estimation in hazard analysis are roughly classified into two groups. One is called “Deterministic study” and the other is called “Probabilistic study”. Result by the deterministic study is the seismic motion distribution in case a certain scenario earthquake may occur. Output of the probabilistic analysis is expressed as, for example, the seismic motion distribution with 10% probability of exceedance in 50 years exposure time. The probabilistic distribution of earthquake motion is, unlike that in the case where certain earthquakes actually occur, a compilation on a drawing of evaluated earthquake motion for each point.

The probabilistic study results can be applied to seismic microzoning map and seismic regulation for building or facility construction such as building codes, it cannot be used for damage/vulnerability assessment and mapping because the probabilistic seismic motion distribution cannot be realized in the future. Therefore, the deterministic approach was mainly adopted in this study. The probabilistic study was also tried; however, the result should be refined in future using the precise information about fault activity, such as recurrence interval and latest event period which are available through paleoseismic study including trenching survey. In this report, the methodology and preparation of source models are written.

The earthquake motion was determined by separately calculating earthquake motion for engineering seismic baserock and evaluating subsurface layer amplification (Figure 1-1). This is due to necessity to deal with this differently from the calculation for engineering seismic baserock since characteristics of subsurface layer amplification vary widely with soil properties near the ground surface. An empirical method is used to calculate the earthquake motion for engineering seismic baserock. The stochastic Green’s function study was also conducted for verification; however most of the necessary parameters are not available in Bangladesh and standard value are used, therefore the result should be refined in future.

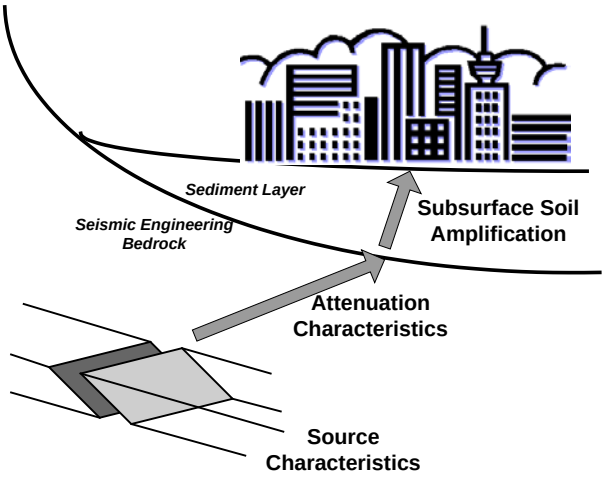

Figure 1-1 Schematic Figure of Seismic Wave Propagation and Amplification

1.2 Deterministic Method

The seismic motion at engineering seismic baserock was calculated by empirical attenuation relation and analytical stochastic Green's function method.

1.2.1 Fault Model

The fault models of scenario earthquakes were already set up in "Time-Predictable Fault Modeling Report" and shown in Figure 1-2. The shaded area is the surface projection of the faults and the lines next to the area mean the intersection of the fault surface extended to the ground surface. The necessary parameters of the faults to calculate the seismic motion by the empirical attenuation relations are shown in Table 1-1.

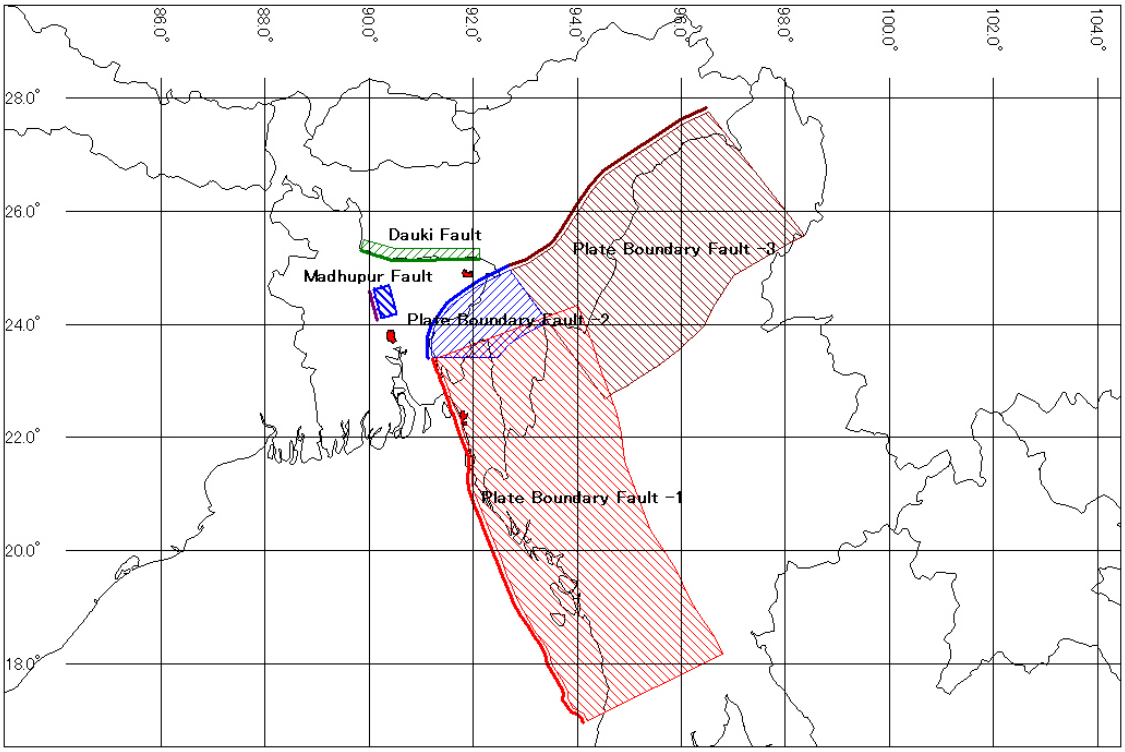

Figure 1-2 Scenario Earthquake Fault Model

Table 1-1 Fault Parameters for Empirical Attenuation Analysis

Fault	Mw	Depth to top of fault (km)	Dip (degree)	Down-dip rupture width (km)	Fault Type
Madhupur Fault (MF)	7.5	10	45	42	Reverse
Dauki Fault (DF)	8.0	3	60	43	Reverse
Plate Boundary Fault -1 (PBF-1)	8.5	3	20/30	337	Reverse
Plate Boundary Fault -2 (PBF-2)	8.0	3	20	137	Reverse
Plate Boundary Fault -3 (PBF-3)	8.3	3	20/30	337	Reverse

1.2.2. Attenuation Formula

The earthquake motion is affected by source characteristics and path effects as well as the magnitude and distance. Therefore, the selection of attenuation formula is most important because each formula is more or less affected by the characteristics of used data to derive it. Hence, it is preferable to use the attenuation formula which was derived from the observed data in and around Bangladesh, however no attenuation formula is proposed yet. The second best is to select suitable attenuation formula from existing ones which meet the observed

strong motion records in Bangladesh. There installed some strong motion seismometer in Bangladesh and several events are said to be recorded by them, however they are not accessible at this moment.

Therefore, the recently developed formulas in NGA project through comprehensive survey based on the world wide strong motion records are applied in this study. The "Next Generation of Ground-Motion Attenuation Models" (NGA) project is a multidisciplinary research program coordinated by the Lifelines Program of the Pacific Earthquake Engineering Research Center (PEER) in US, in partnership with the U.S. Geological Survey and the Southern California Earthquake Center. The comprehensive study was conducted over five years and principal results are published in 2008. The NGA attenuation relations are for shallow crustal earthquakes and similar active tectonic regions. The scenario earthquakes of MF and DF are shallow crustal earthquakes. The PBF1, PBF-2 and PBF-3 are interface earthquakes but the three study sites are located on hanging wall block and most of the propagation path is in shallow crust. The similarity of attenuation of interface motion for larger events to those of California crustal events is also shown by Atkinson and Boore (2003). Therefore, the results of NGA project are adopted in this study.

In this study, following four relations from NGA project are applied and the average value by these four formulas was used.

AS08: Abrahamson N. and W. Silva (2008)
BA08: Boore D. M. and G. M. Atkinson (2008)
CB08: Campbell K. W. and Y. Bozorgnia (2008)
CY08: Chiou B. S.-J. and R. R. Youngs (2008)

Among many new features of NGA, it is emphasized that the PGA and acceleration response spectra (Sa) saturates with increasing magnitude over 7 in the near field.

Figure 1-3 shows the PGA value for vertical reverse fault by four attenuation relations with distance and magnitude. Figure 1-4 shows the Sa (h=5%) value for vertical reverse fault at 20 km distance by four attenuation relations with magnitude.

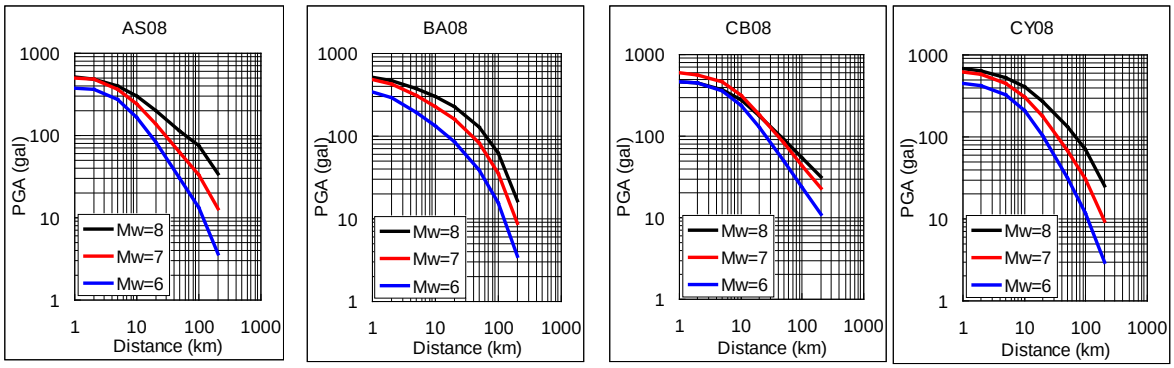

Figure 1-3 PGA Attenuation Relationships for Reverse Fault at Vs30=760 m/sec Condition

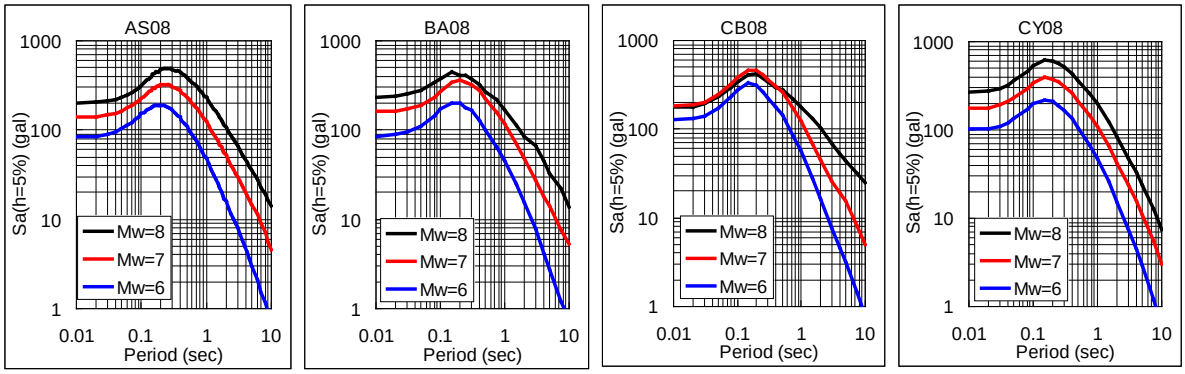

Figure 1-4 Acceleration Response Spectra (h=5%) for Reverse Fault at Vs30=760 m/sec Condition

1.2.3. Baserock Motion

The distance from each 250 meters square grid center in Dhaka, Chittagong and Sylhet to source fault models were calculated and PGA, PGV and Sa (h=5%, T=0.3 and 1.0 sec) were calculated at engineering seismic baserock for five scenario earthquakes. The PGA, PGV and Sa (h=5%, T=0.3 and 1.0 sec) are necessary parameters to calculate the damage of buildings and infrastructures by HAZUS in the task of vulnerability assessment and loss estimation. The engineering seismic baserock is defined as Vs30=760m/sec following the NEHRP provisions because the amplification of surface soft soil layer is evaluated based on the amplification factor of NEHRP provisions in Chapter 2.

The maps for Dhaka are shown in Figure 1-5 to Figure 1-8. The most important earthquake is MF and the PGA in Dhaka is 130 to 230 gal.

The maps for Chittagong are shown in Figure 1-9 to Figure 1-12. The most important earthquake is PBF-1 and the PGA in Chittagong reaches 650 to 770 gal.

The maps for Sylhet are shown in Figure 1-13 to Figure 1-16. The most important earthquakes are DF and PBF-2. PGA by DF is 180 to 240 gal and 160 to 240 gal by PBF-2.

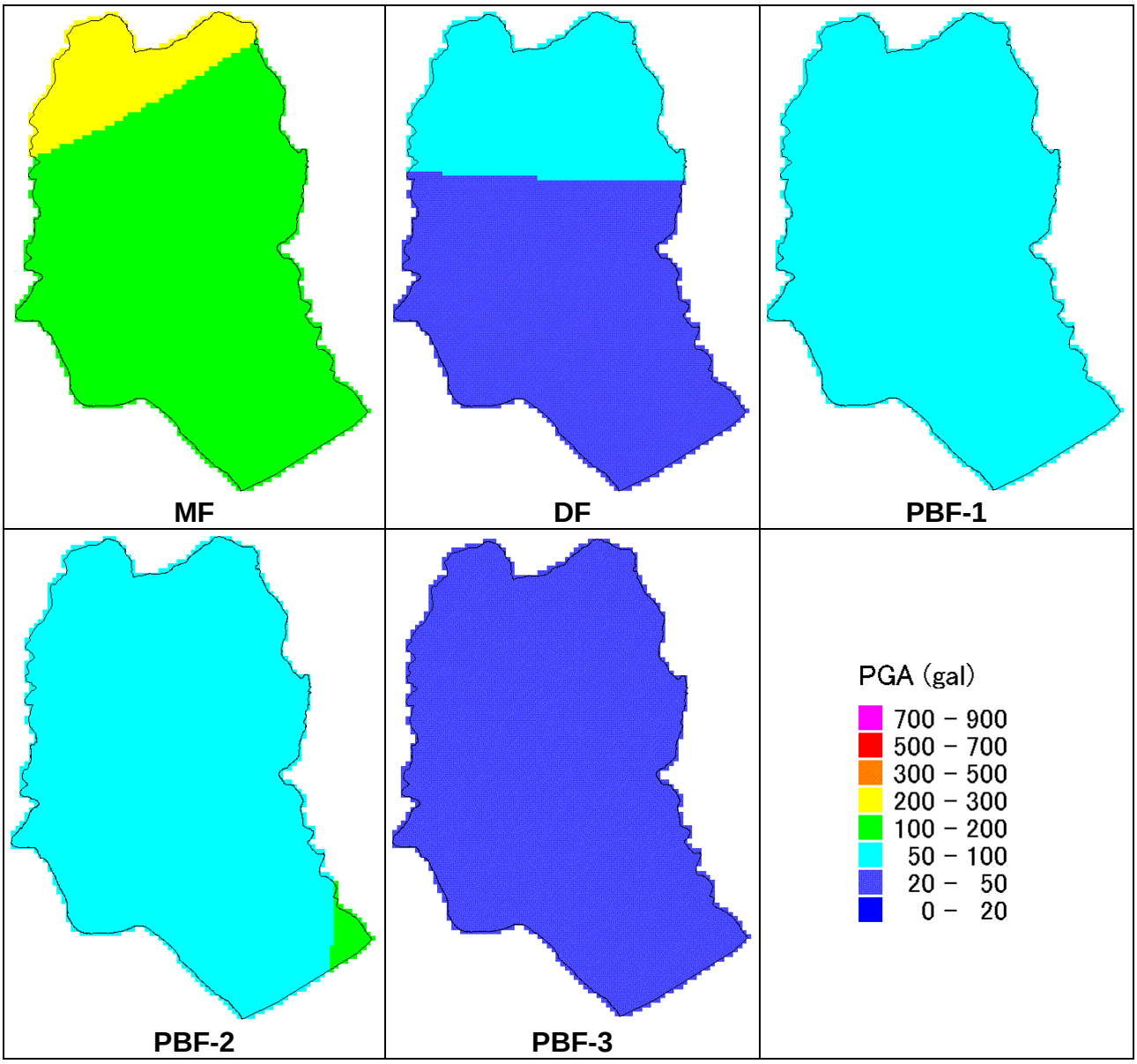

Figure 1-5 PGA at Engineering Seismic Baserock (Vs30=760 m/sec) in Dhaka

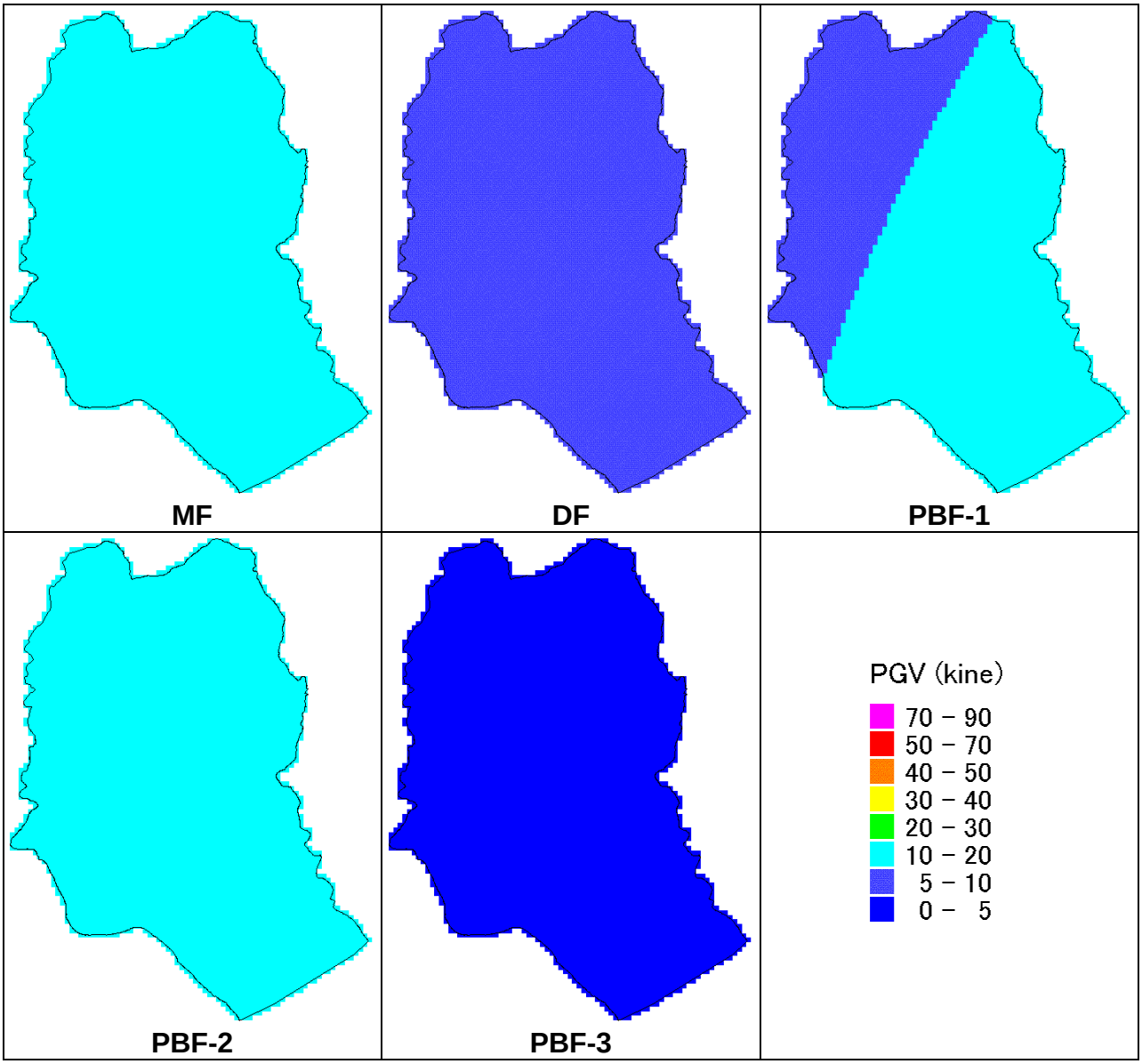

Figure 1-6 PGV at Engineering Seismic Baserock (Vs30=760 m/sec) in Dhaka

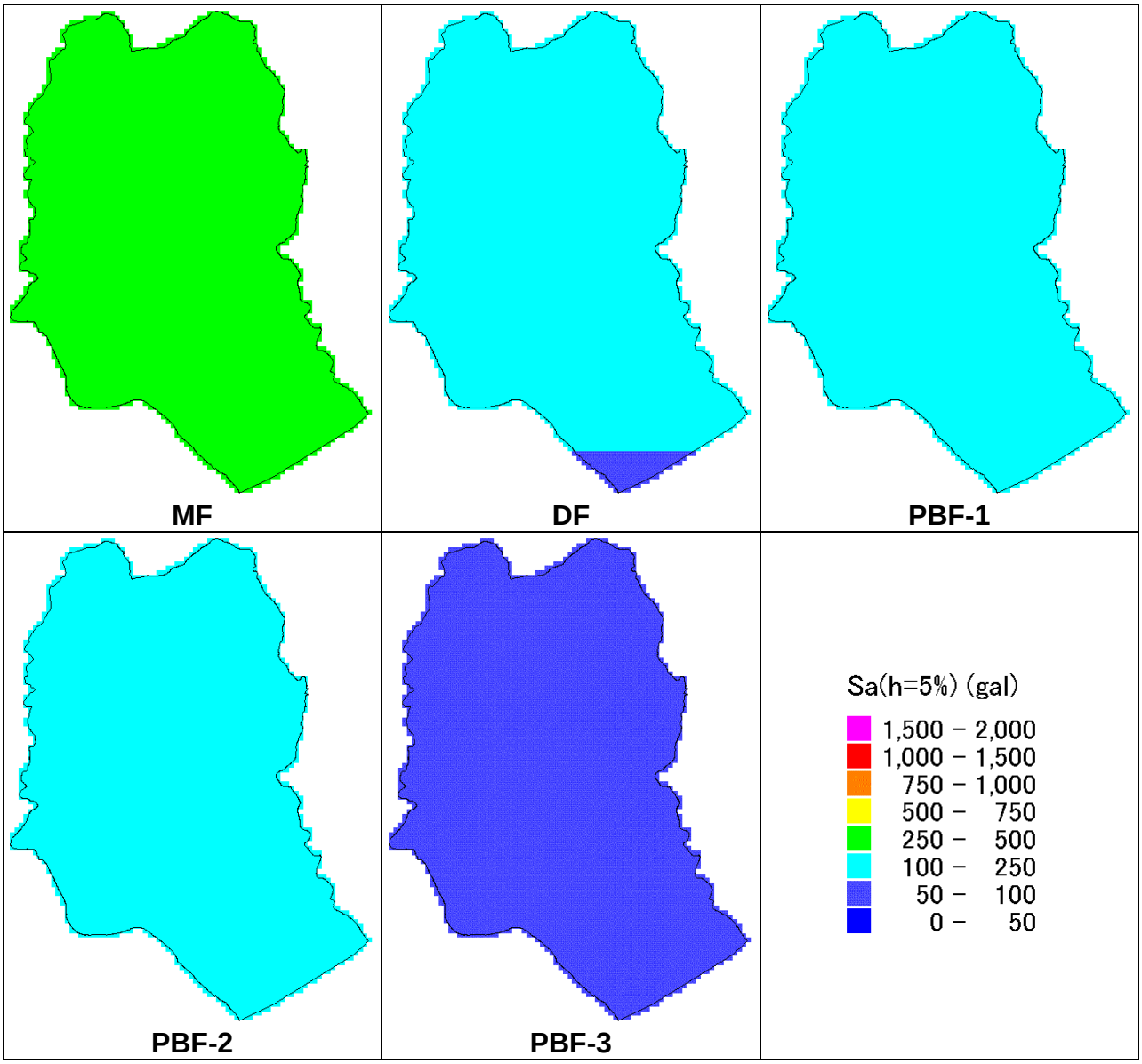

Figure 1-7 Sa (h=5%) for T=0.3 sec at Engineering Seismic Baserock (Vs30=760 m/sec) in Dhaka

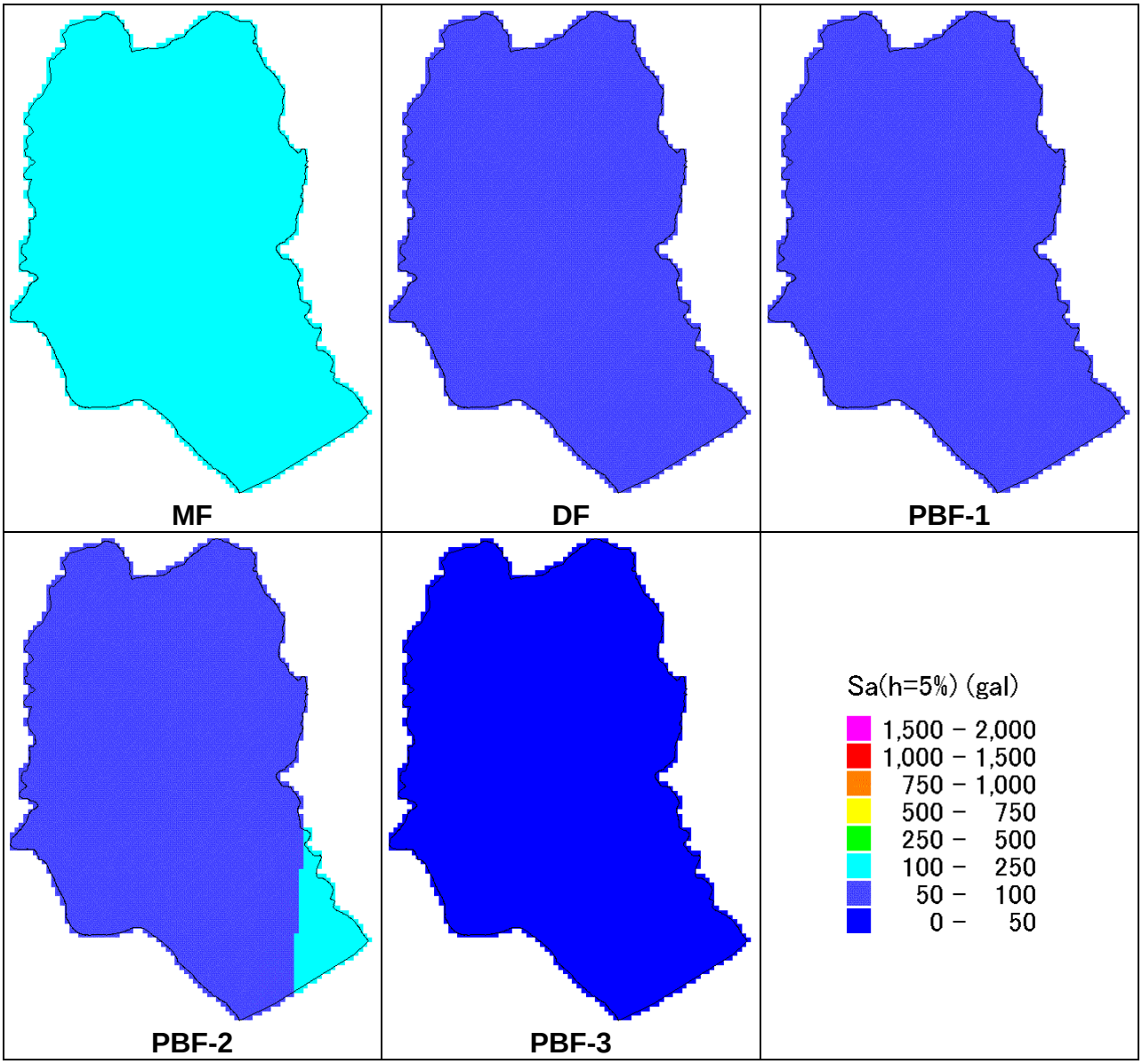

Figure 1-8 Sa (h=5%) for T=1.0 sec at Engineering Seismic Baserock (Vs30=760 m/sec) in Dhaka

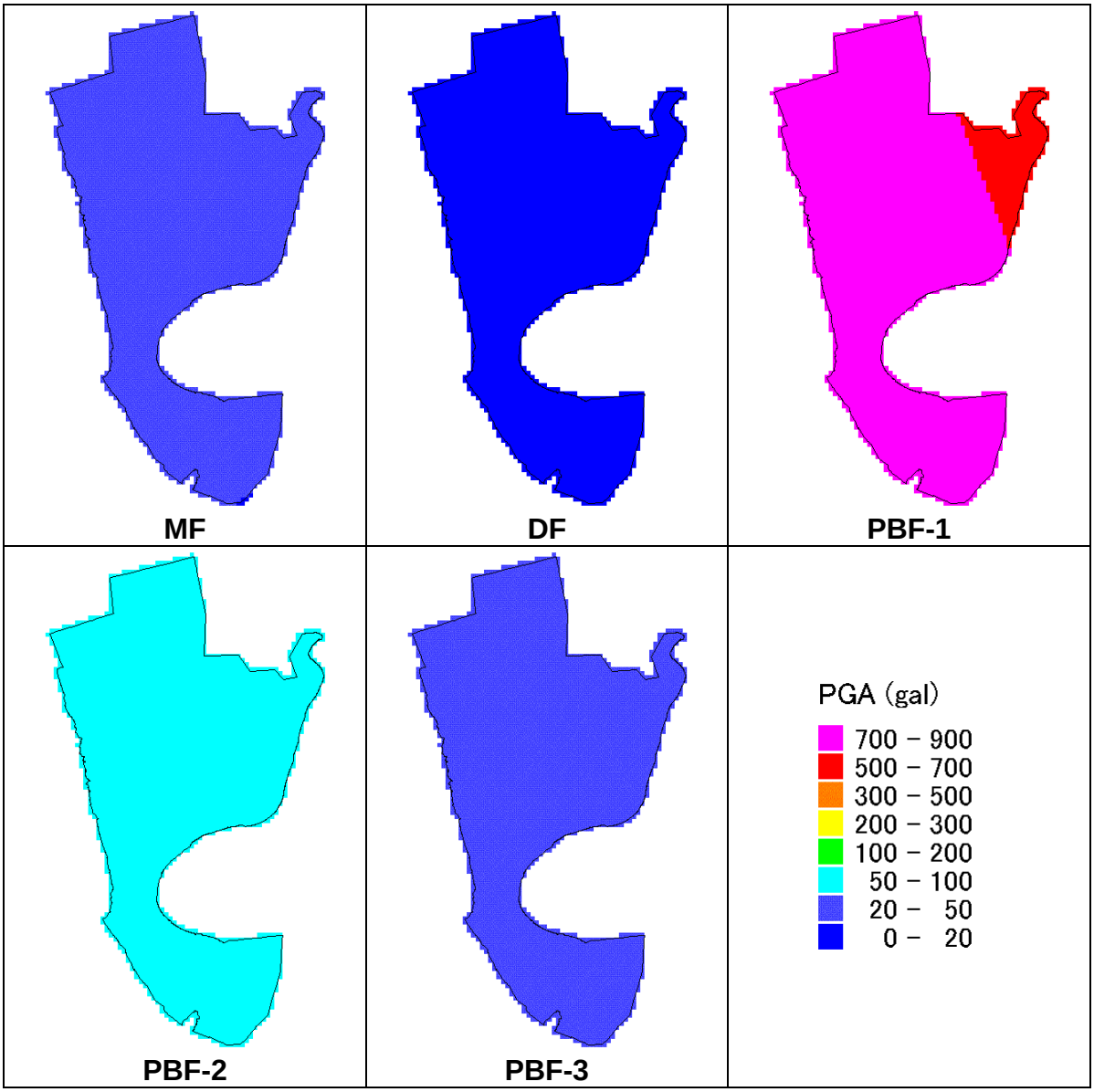

Figure 1-9 PGA at Engineering Seismic Baserock (Vs30=760 m/sec) in Chittagong

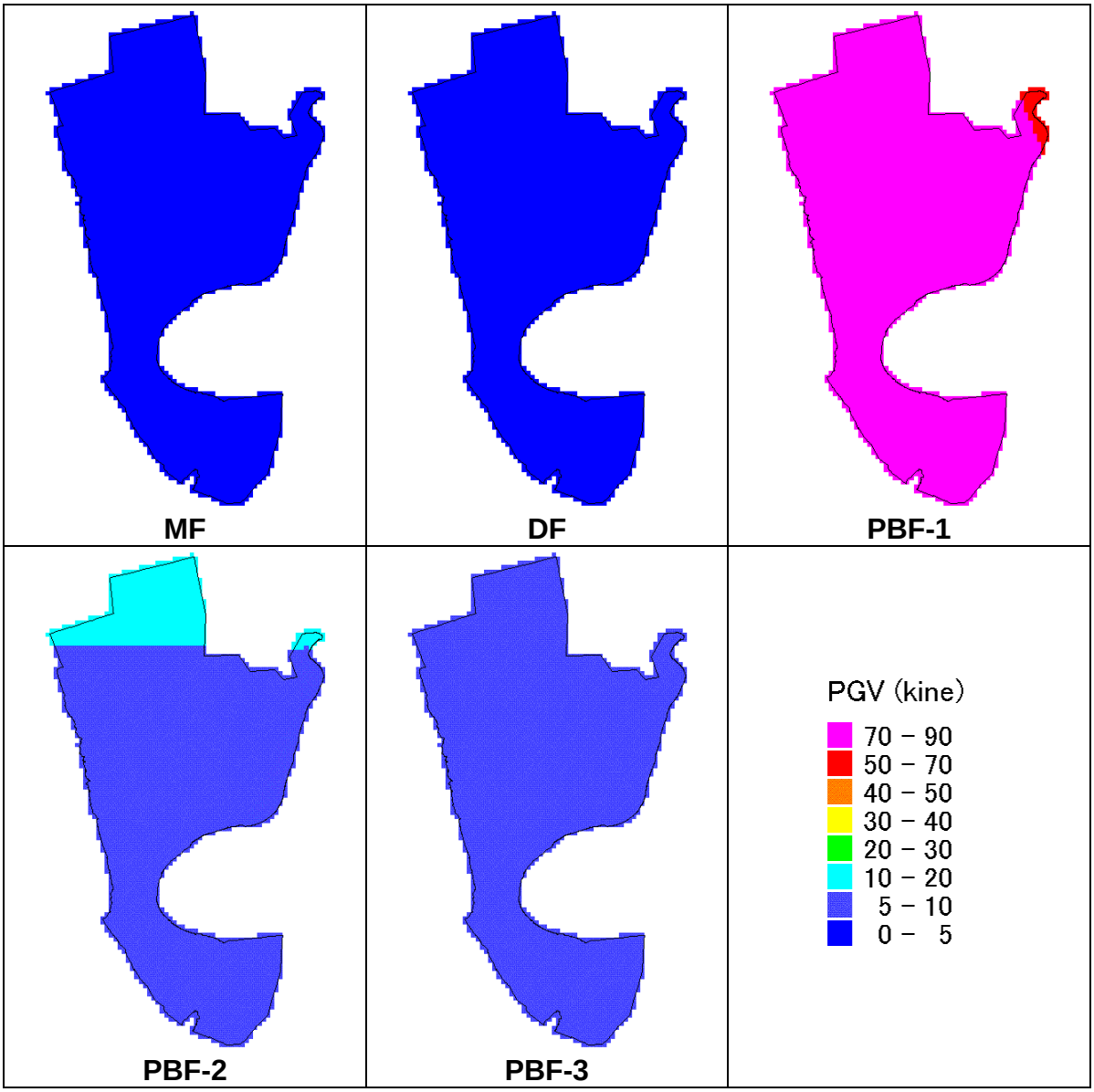

Figure 1-10 PGV at Engineering Seismic Baserock (Vs30=760 m/sec) in Chittagong

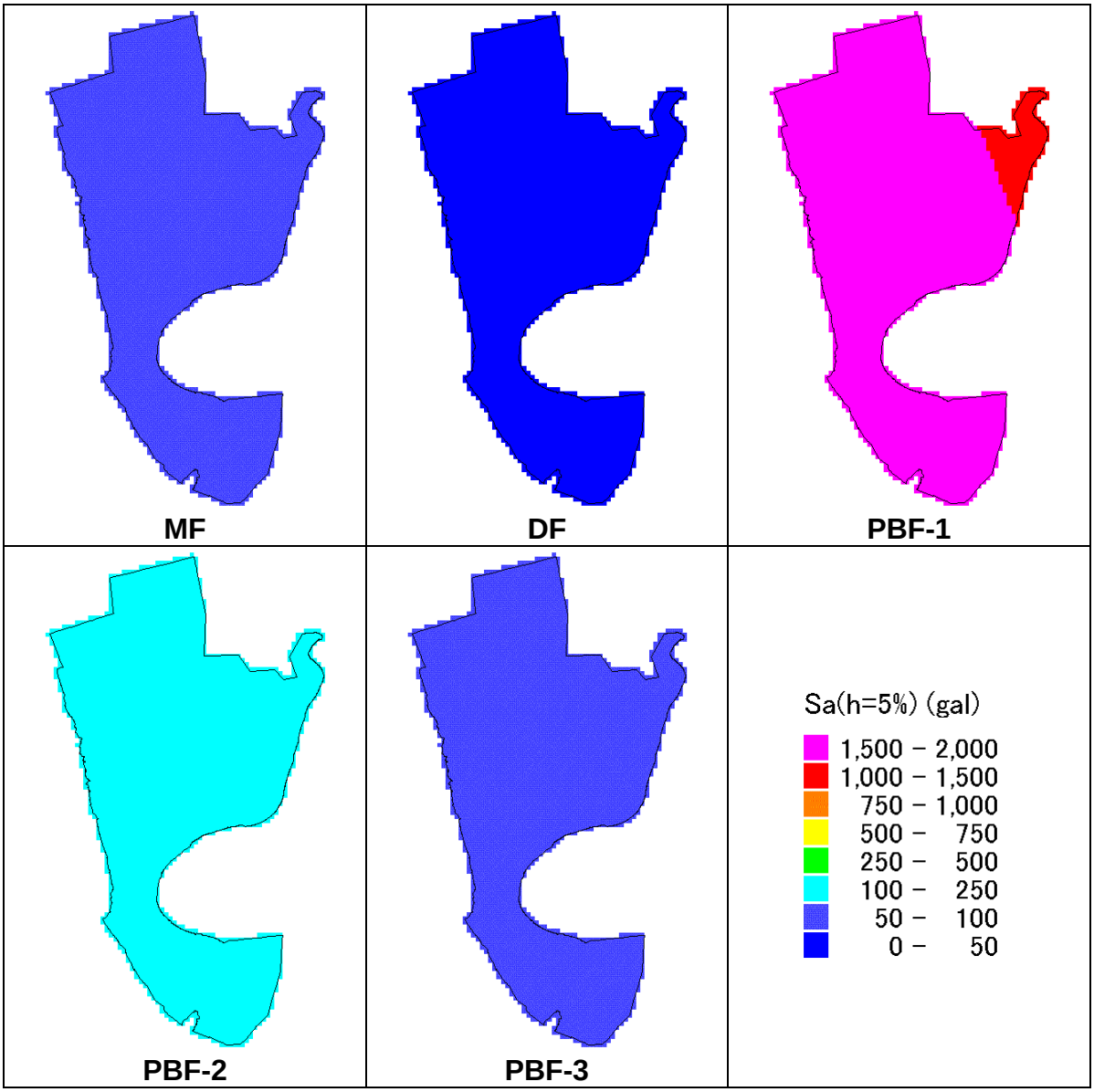

Figure 1-11 Sa (h=5%) for T=0.3 sec at Engineering Seismic Baserock (Vs30=760 m/sec) in Chittagong

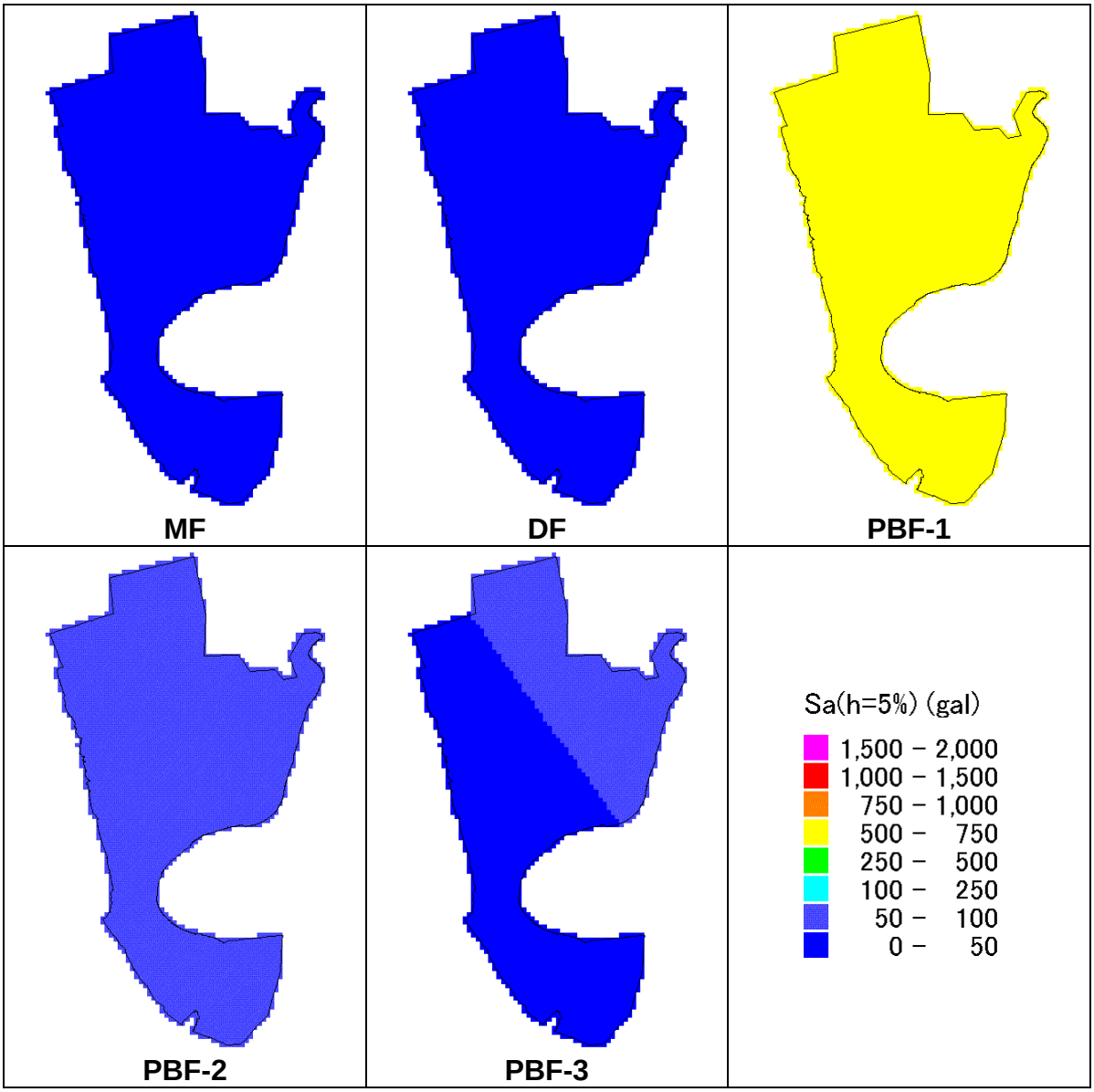

Figure 1-12 Sa (h=5%) for T=1.0 sec at Engineering Seismic Baserock (Vs30=760 m/sec) in Chittagong

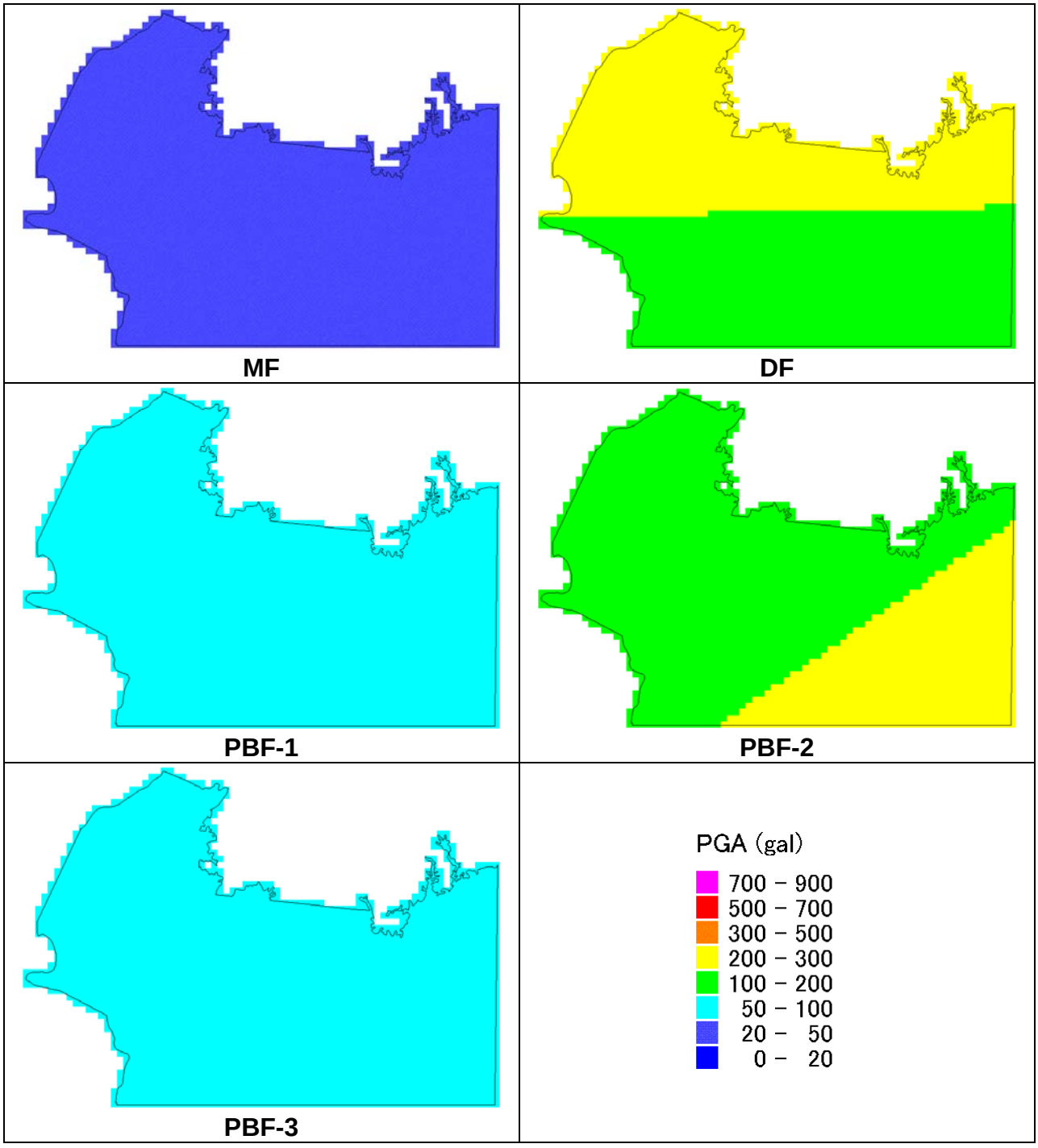

Figure 1-13 PGA at Engineering Seismic Baserock (Vs30=760 m/sec) in Sylhet

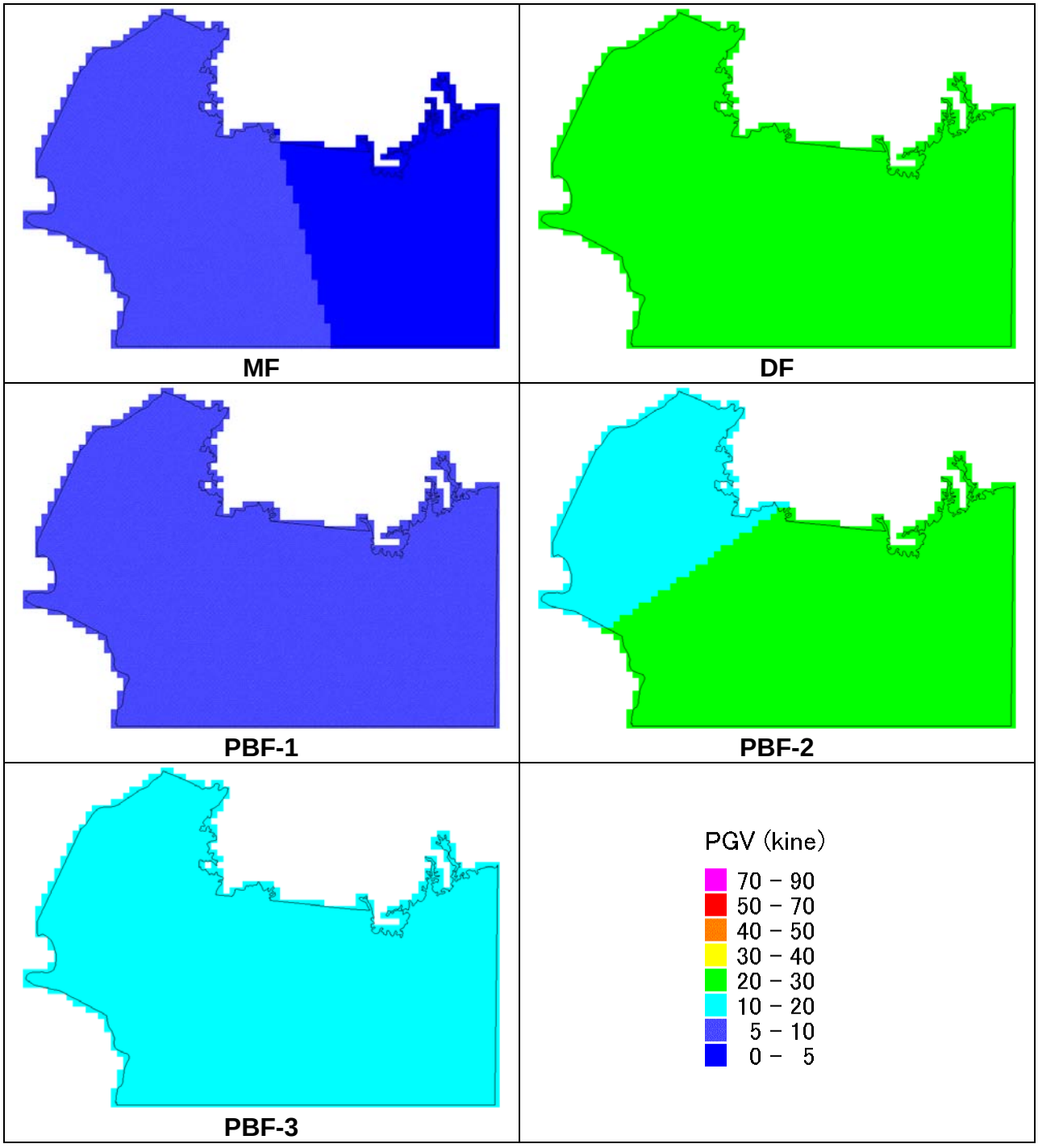

Figure 1-14 PGV at Engineering Seismic Baserock (Vs30=760 m/sec) in Sylhet

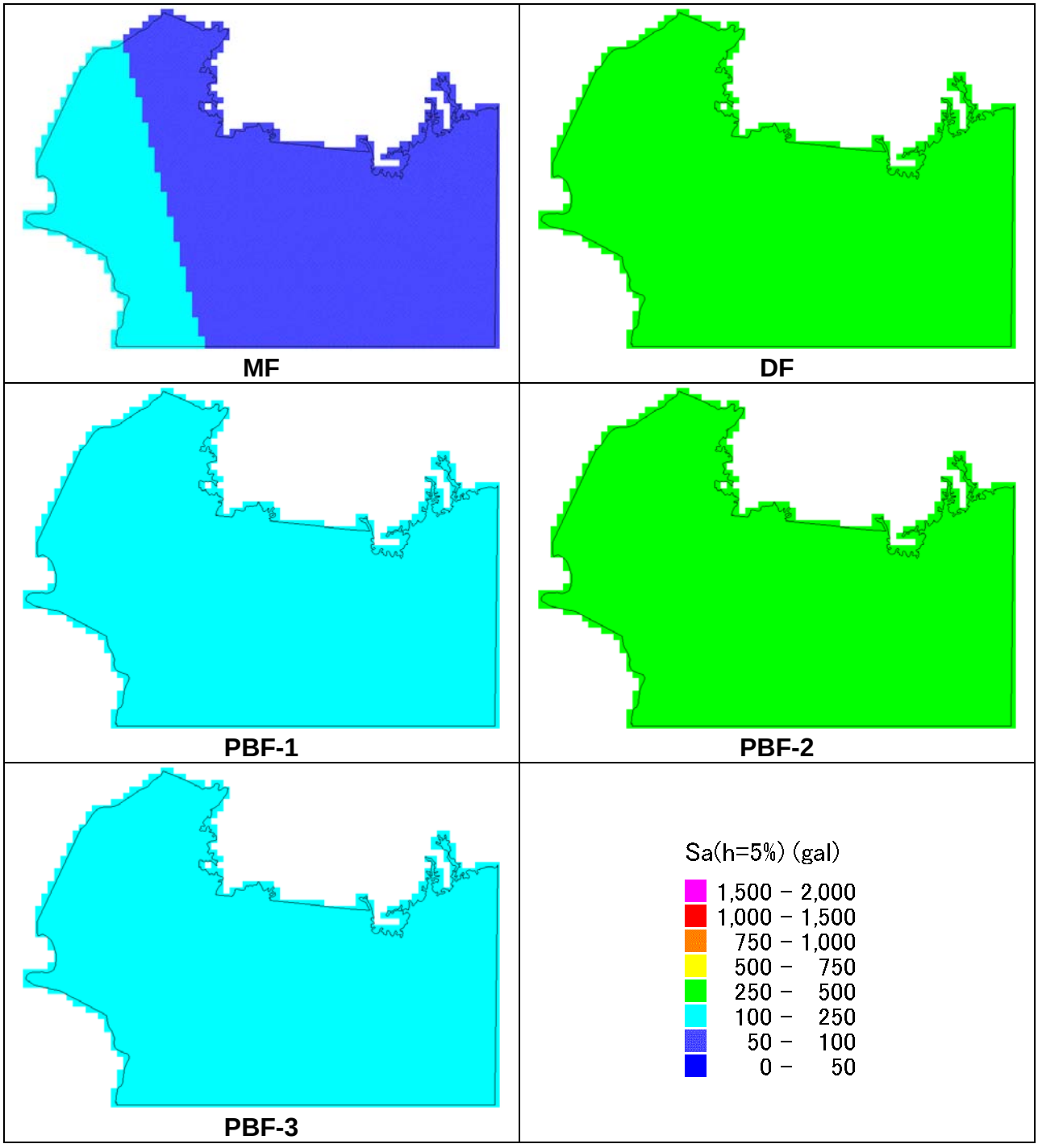

Figure 1-15 Sa (h=5%) for T=0.3 sec at Engineering Seismic Baserock (Vs30=760 m/sec) in Sylhet

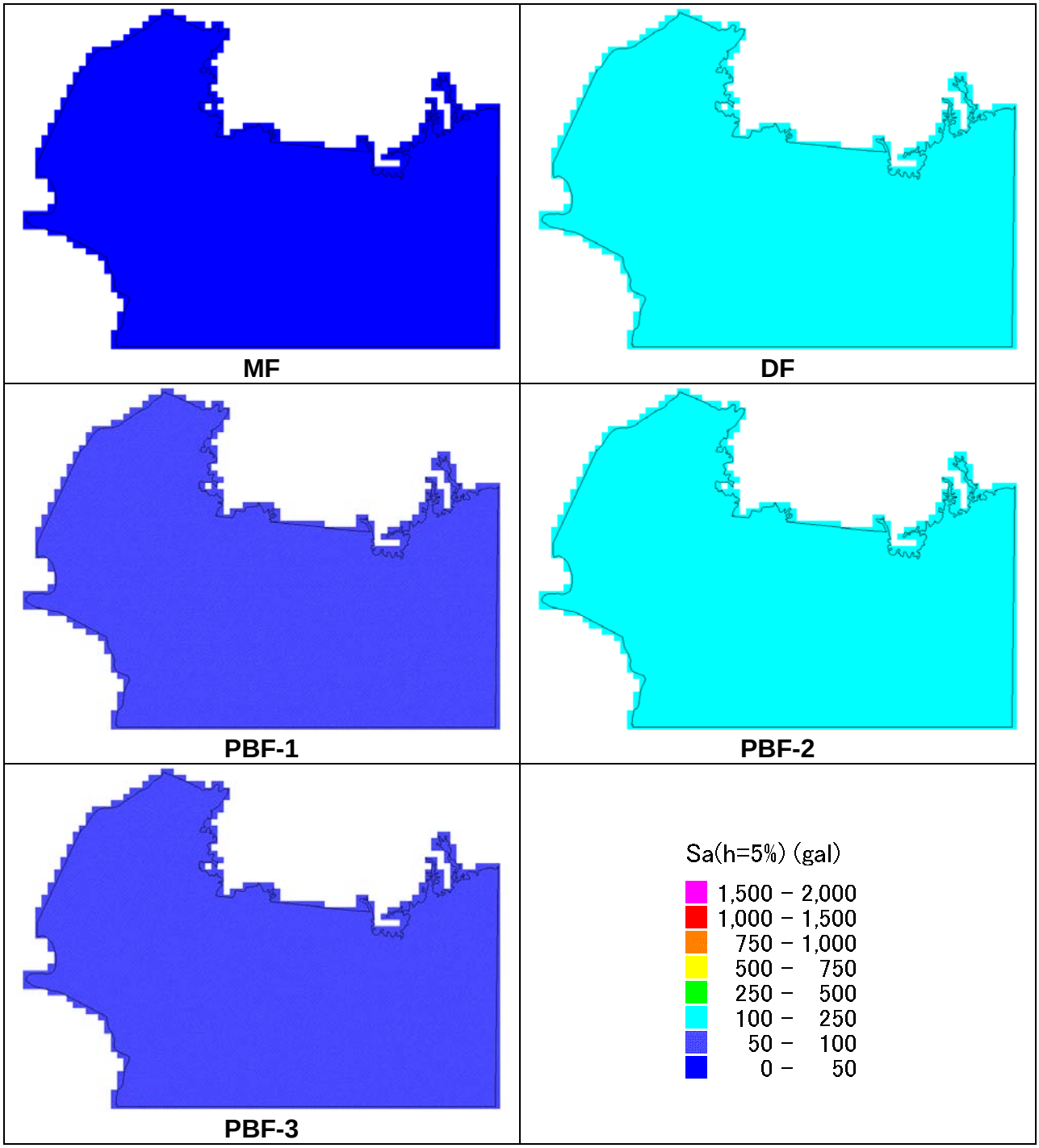

Figure 1-16 Sa (h=5%) for T=1.0 sec at Engineering Seismic Baserock (Vs30=760 m/sec) in Sylhet

1.2.4. Stochastic Green's Function Analysis

(1) Methodology

The seismic wave at the baserock was analyzed by stochastic Green's function method. The observed earthquake motion can be modeled by the convolution of slip distribution in time and space domains at the fault surface and the response of materials in propagation pass for unit slip (Green's function). The stochastic Green's function method uses stochastically derived small events from the theoretical source model of dynamic features. This method was advocated by Dr. Irikura (for example, Kamae et al. (1991)) and adopted in the seismic microzonation project within Japan by the Cabinet Office of Japan. The schematic flow chart and conceptual figure are shown in Figure 1-17.

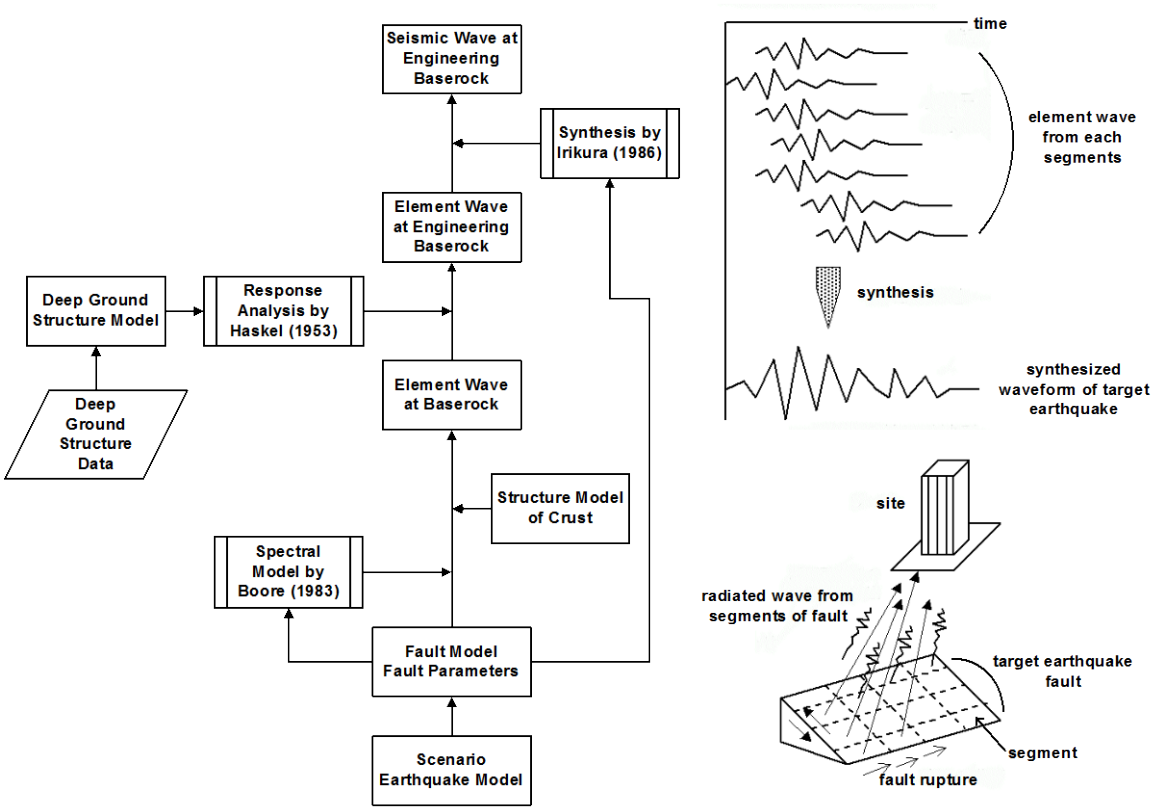

Figure 1-17 Schematic Flowchart of Stochastic Green's Function Method

The procedure of the analysis is as follows;

(a) The fault plane of scenario earthquake is divided to small rectangular elements. The amplification spectrum at the bedrock of study area by each element is derived based on the theoretical model by Boore (1983) following theorem.

The amplification spectrum for bedrock layer is as follows;

$$S_A(\omega) = \frac{R_{\phi\theta}}{4\pi\rho\beta^3} Mo \cdot \frac{\omega^2}{1+(\omega/\omega_c)^2} \cdot \frac{1}{1+(\omega/\omega_{\max})^2} \frac{e^{-\omega R/2Q\beta}}{R}$$

$$\omega_c = 2\pi f_c, \quad f_c = 4.9\times10^6 \beta(\Delta\sigma/Mo)^{1/3}$$

$R_{\phi\theta}$: radiation pattern
Mo : seismic moment
ρ : density
β : S wave velocity
$\Delta\sigma$: stress drop
Q : dumping factor
R : distance

(b) The radiation pattern is evaluated using the direction from element source to calculation point and also the radiation angle. The seismic moment and stress drop are decided based on the asperity distribution. The asperity*) of each fault is shown in Figure 1-18 by green rectangles. The crustal velocity structure model (Table 1-2) is considered in the process of spectrum calculation. The layers of deeper than 1km are based on Parvez et al. (2003) (Figure 1-19) and the estimated Quaternary and Tertiary layers are added to the top. The depth of Tertiary layer was estimated refer to the survey results of array microtremor.

(c) To obtain the element wave form at bedrock, the phase spectrum is evaluated following Boore (1983). In this process, the random number is used to generate the wave form. Several wave forms are generated using several random numbers and average amplitude wave form is selected.

(d) The element wave form at engineering seismic bedrock is calculated by 1D response analysis using the deep ground structure model. In this analysis, the incident angle to the deep ground is considered.

(e) The element wave forms are used to synthesize the scenario earthquake wave form following Irikura (1986). The formula to synthesize the wave form is as follows;

*) An asperity is an area on a fault that is stuck or locked. In the Earth, tectonic earthquakes are caused by slip along a fault plane, where two rock bodies are in rigid contact. The friction along the fault plane is not uniform in strength, so overall movement involves slip on one or more asperities, or "stuck patches" where the friction is highest. Most of the energy that is released by earthquakes comes from the patches that become "unstuck." (after IRIS Homepage)

$$A(t) = \sum_{1}^{N^2} (r / r_i) F(t - t_i) * a(t),$$

$$F(t) = \delta(t) + (1/n') \sum_{j=1}^{(N-1)n'} \delta[t - (j-1)T/(N-1)n'],$$

$$N = \left(M_O / m_O \right)^{1/3} = L/l = W/w$$

$$t_i = r_i / Vc + \xi_i / Vr$$

$A(t), a(t)$: seismogram for target and element event
M_o, m_o : seismic moment for target and element event
L, l : fault length for target and element event
W, w : fault width for target and element event
r : hypocentral distance from observation point to element event
r_i : hypocentral distance from observation point to i - th fault segment
ξ_i : distance from rupture start point to the i - th fault segment
Vc : shear wave velocity
Vr : rupture velocity
T : rise time of target event
n': appropriate integer to eliminate spuriois periodicity
* : convolution

In this process, the difference of propagation time from each element sources to the target point and the differences of the elapsed time to rupture the element sources from initial break time are considered.

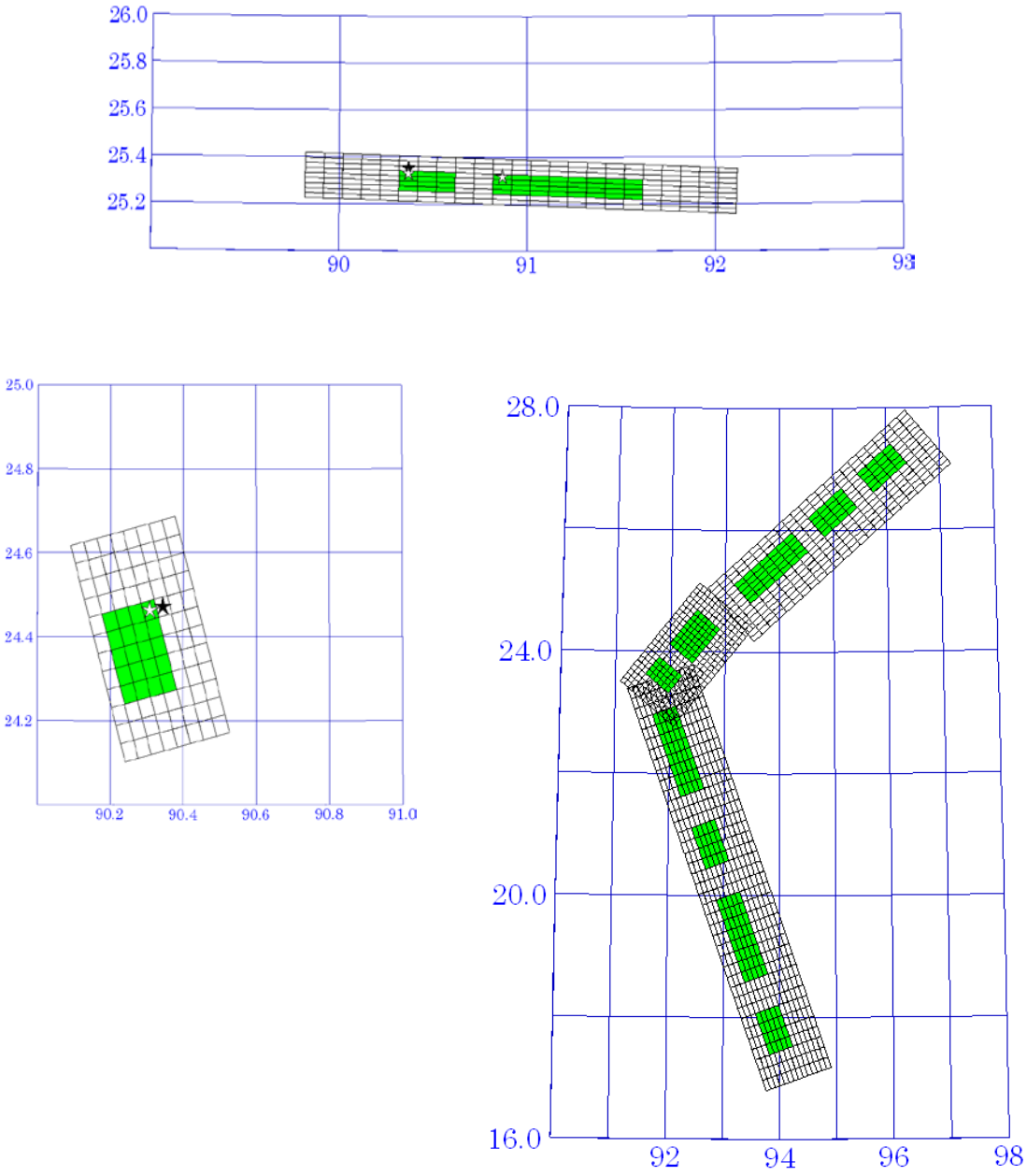

Figure 1-18 Asperity Distribution for Stochastic Green's Function Method

Table 1-2 Velocity Structure Model for the Analysis

Dhaka (No.7 + Surface Model)

Dep1(km)	Dep2(km)	Vs(km/s)	Vp(km/s)	Vp/Vs	Qs=Vs/15
0	0.1	0.4	1.2	3	27
0.1	0.5	0.76	2	2.631579	51
0.5	1	1.5	3	2	100
1	2	2.5	4.3	1.72	167
2	4	3	5.2	1.733333	200
4	8	3.5	6	1.714286	233
8	15	3.6	6.1	1.694444	240
15	28	3.7	6.3	1.702703	247
28	40	4	6.8	1.7	267
40	100	4.5	7.75	1.722222	300

Chittagong (No.6 + Surface Model)

Dep1(km)	Dep2(km)	Vs(km/s)	Vp(km/s)	Vp/Vs	Qs=Vs/15
0	0.1	0.4	1.2	3	27
0.1	0.5	0.76	2	2.631579	51
0.5	1	1.5	3	2	100
1	2	2.6	4.5	1.730769	173
2	9	3.1	5.3	1.709677	207
9	15	3.2	5.5	1.71875	213
15	33	3.8	6.5	1.710526	253
33	50	4.25	7.25	1.705882	283
50	100	4.5	7.8	1.733333	300

Sylhet (No.7 + Surface Model)

Dep1(km)	Dep2(km)	Vs(km/s)	Vp(km/s)	Vp/Vs	Qs=Vs/15
0	0.05	0.4	1.2	3	27
0.05	0.5	0.76	2	2.631579	51
0.5	1	1.5	3	2	100
1	2	2.5	4.3	1.72	167
2	4	3	5.2	1.733333	200
4	8	3.5	6	1.714286	233
8	15	3.6	6.1	1.694444	240
15	28	3.7	6.3	1.702703	247
28	40	4	6.8	1.7	267
40	100	4.5	7.75	1.722222	300

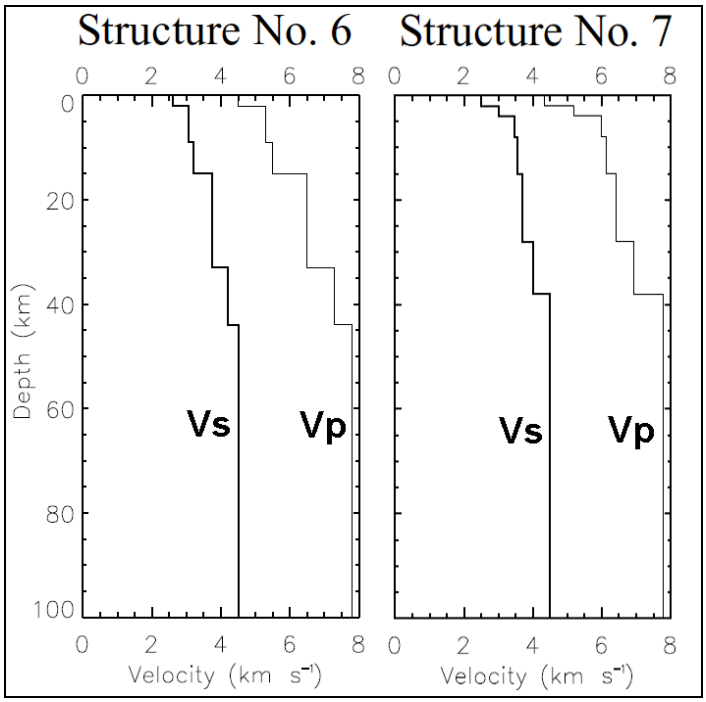

Figure 1-19 Velocity Structure Model by Parvez et al. (2003)

(2) Baserock Motion

The analysis was conducted at the points around Dhaka, Chittagong and Sylhet in 0.05 degree spacing considering the accuracy of the methodology reflecting the difference of the lay path and radiation angle from source to the points. The PGA value at the point between the calculated points can be interpolated. The PGA values for five scenario earthquakes at the ground of Vs=400 m/sec was calculated and shown in Figure 1-20 to Figure 1-22. In the analysis of engineering geology mapping in separate volume, the engineering seismic baserock is found that Vs is around 400m/sec. Therefore, the PGA value in Figure 1-20to Figure 1-22 can be used as the input value of the analysis to evaluate the amplification by surface layers shallower than engineering seismic baserock. The color of the circle shows the PGA at the center of the circle. The examples of acceleration waveform are shown in Figure 1-23. These waveforms are used as the input waves for the response analysis in Section 2.2.

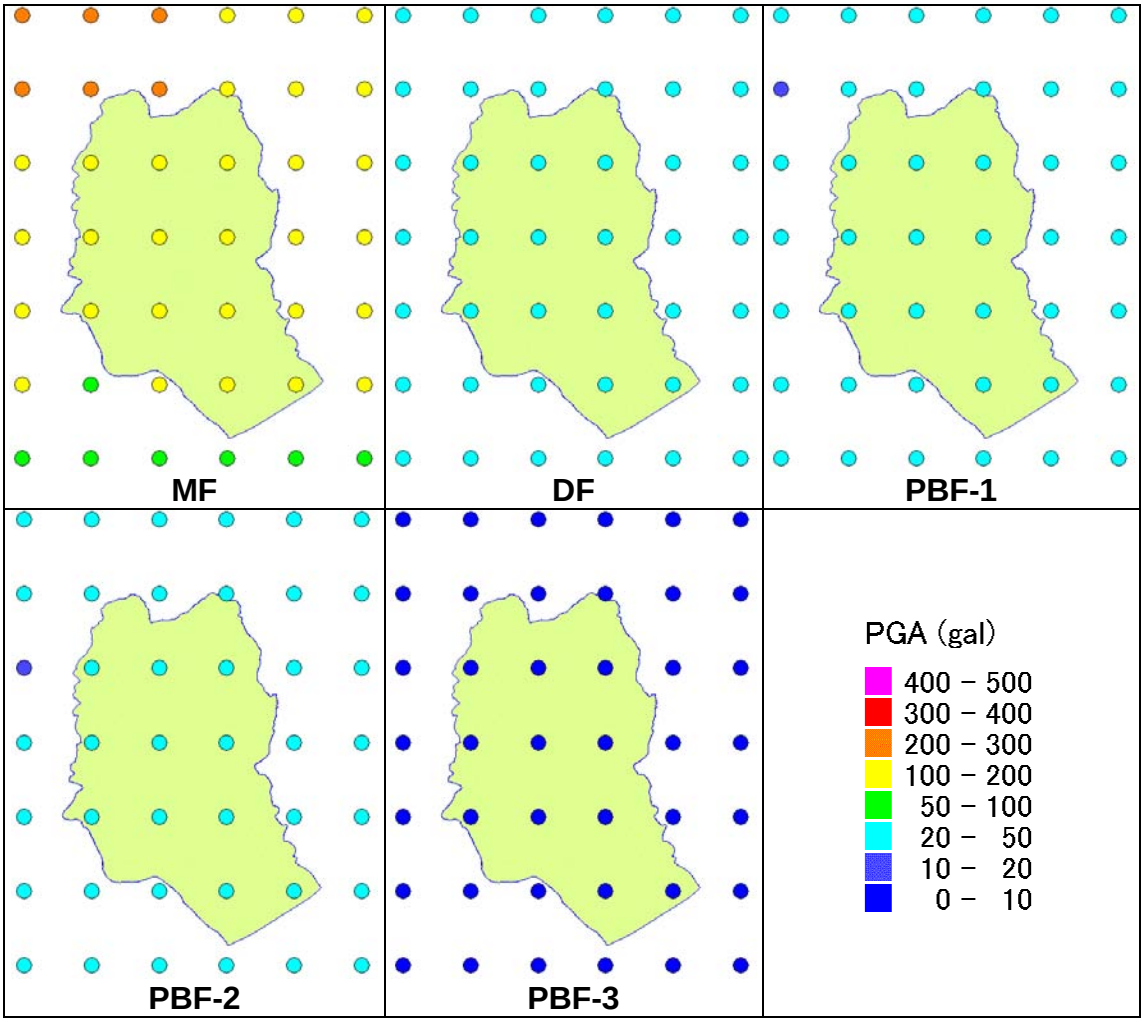

Figure 1-20 PGA at Ground of Vs=400 m/sec in Dhaka

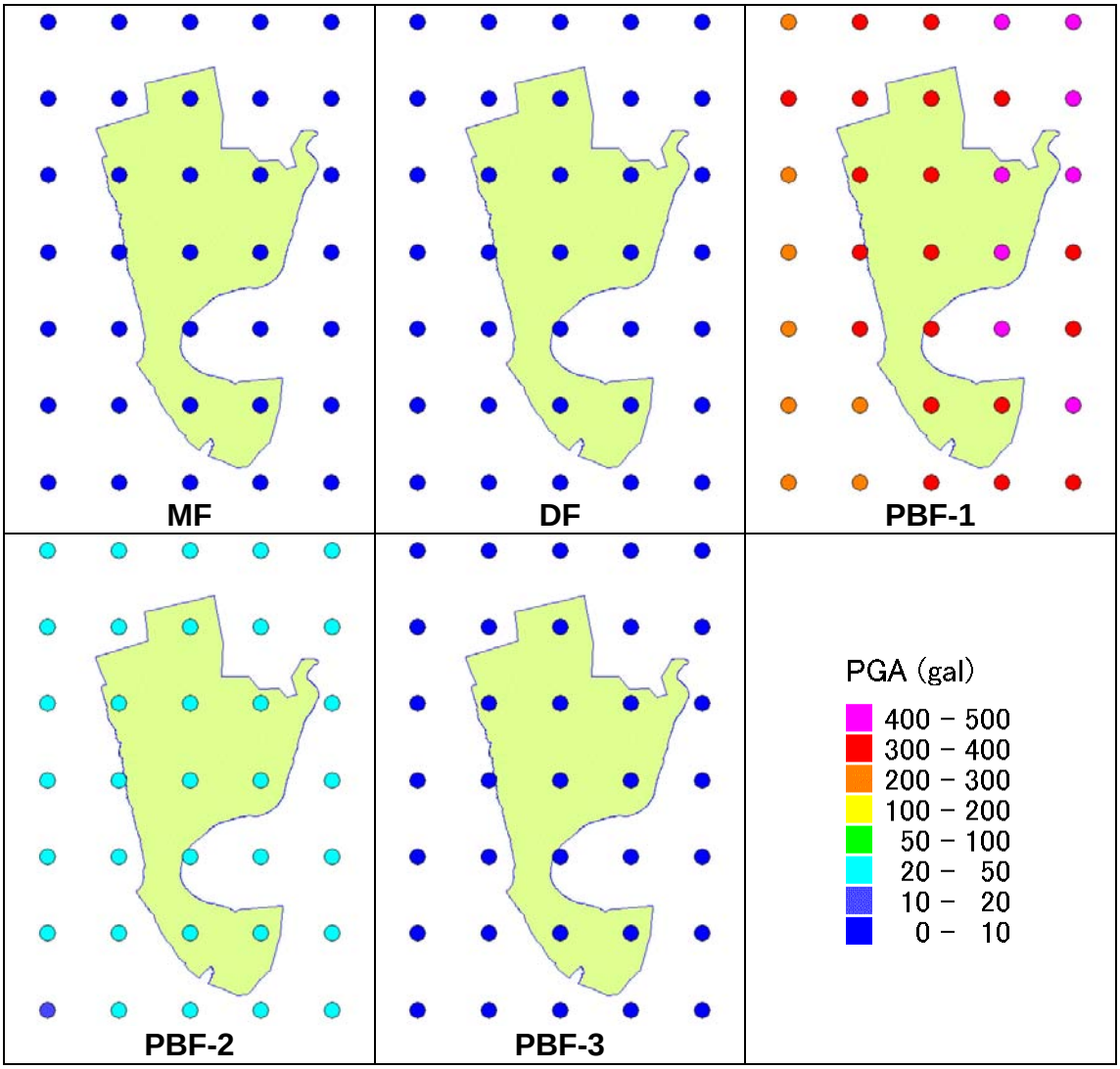

Figure 1-21 PGA at Ground of Vs=400 m/sec in Chittagong

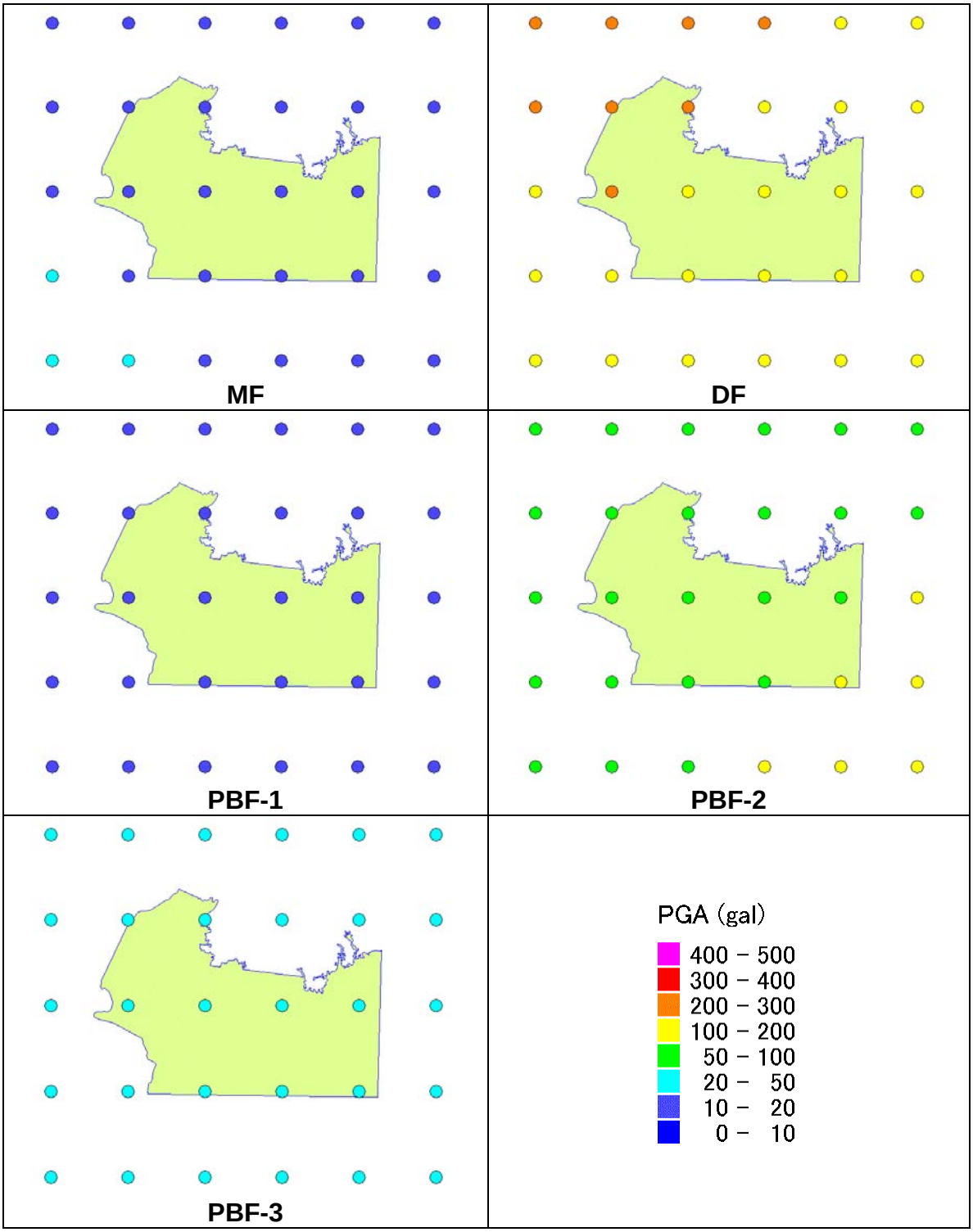

Figure 1-22 PGA at Ground of Vs=400 m/sec in Sylhet

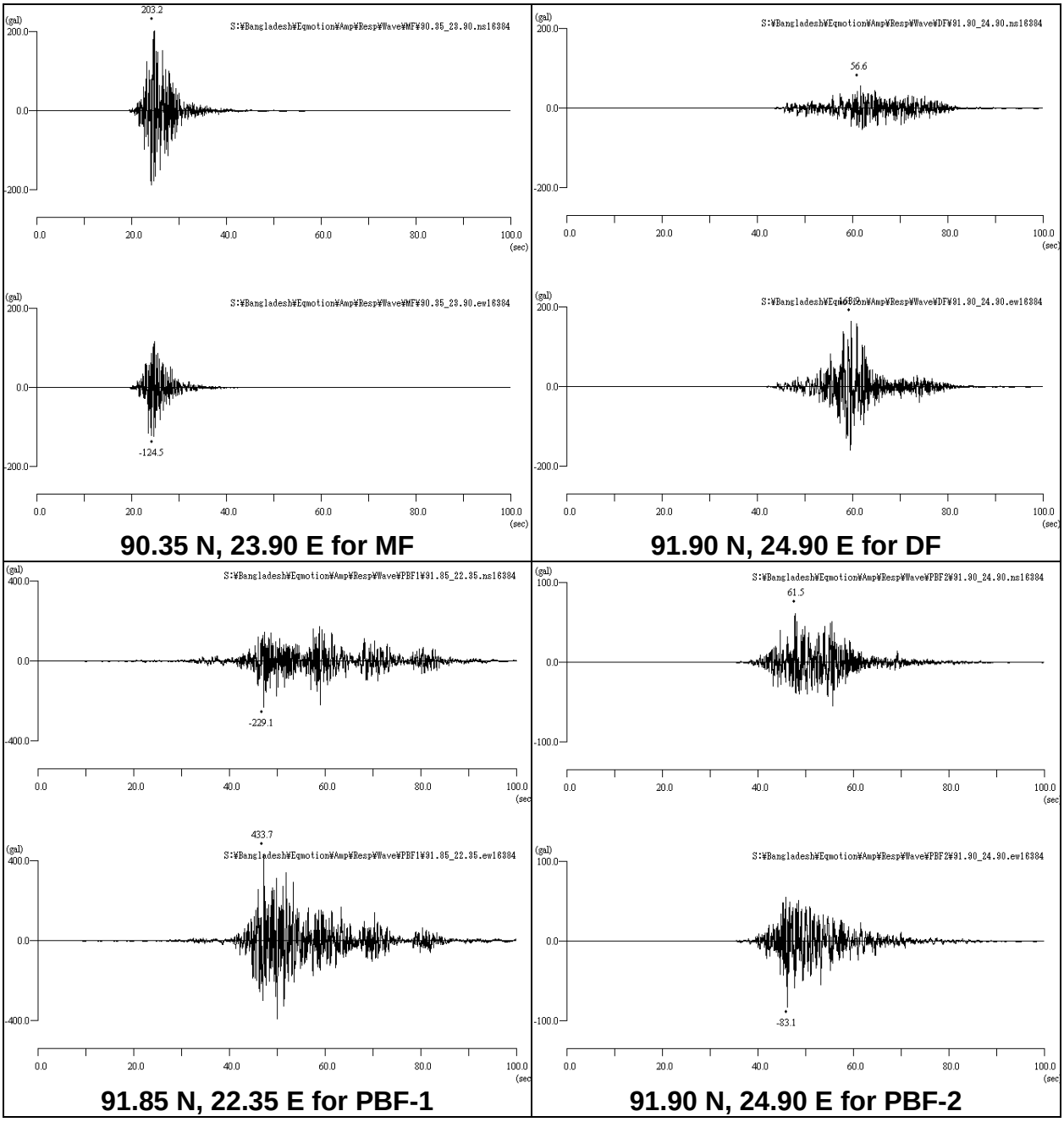

Figure 1-23 Example of Waveforms

1.3. Probabilistic Analysis

The following steps are taken for Probabilistic Analysis. The flow chart is shown in Figure 1-24.

(a) Define the possible seismic sources where an earthquake will be a significant hazard to Bangladesh. The seismic sources include the active faults and the background activities/ area sources that the location is uncertain.

(b) Determine the seismicity of each area seismic sources based on the recent and historical seismic catalogue.

(c) Determine the fault source activity based on the trenching survey result, GPS measurement and earthquake catalogue.

(d) Find the seismic hazard to Bangladesh from the sum of the contributions of all seismic sources with attenuation formula of ground motion. In this approach, seismic hazard is given by ground motion with given probability of exceedance.

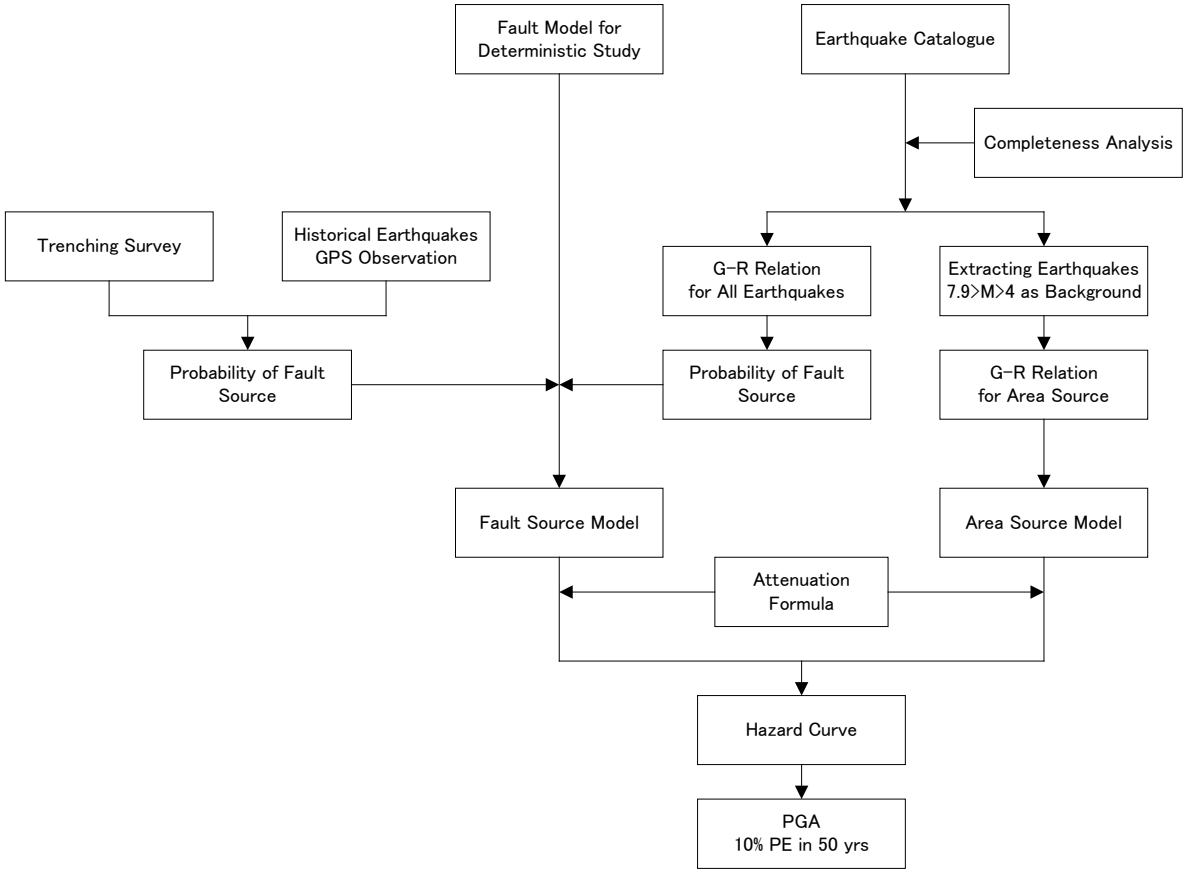

Figure 1-24 Flow Chart of Probabilistic Analysis

1.3.1. Methodology

The probabilistic analysis was performed using the code EZ-FRISK (Ver. 7.32) developed by Risk Engineering Inc., which was formed by Dr. Robin K. McGuire, who first developed and published many of the methods taken today as requirements for advanced probabilistic seismic risk analysis. This program calculates seismic hazard using the standard methodology for probabilistic seismic hazard analysis. The probabilistic seismic hazard calculations can be represented by the following equation, which is an application of the total probability theorem.

$$H(a) = \sum_i v_i \iint P[A > a \mid m, r] f_{M_i}(m) f_{R_i|M_i}(r, m) dr dm$$

$H(a)$: annual frequency of earthquakes that produce a ground motion amplitude A higher than a

A, a : peak ground acceleration, peak ground velocity or spectral acceleration for a given frequency

v_i : annual rate of i - th earthquake

m : magnitude

r : distance

$f_{M_i}(m)$: probability density function on magnitude

$f_{R_i|M_i}(r, m)$: probability density function on distance for the condition that magnitude is m

$P[A > a \mid m, r]$: probability that an earthquake of magnitude m at distance r produces a ground motion amplitude A at the site that is greater than a

1.3.2. Area Source Model

The source of most earthquakes is fault except the volcanic earthquakes; however the earthquake fault can't always be found because the fault is sometimes deep and hidden or small and not reached the rupture to the ground surface. The smaller earthquakes are usually not associated with the faults. In probabilistic analysis, the effects of all the earthquakes affecting the study site should be considered. The source model of faults with the location, length, width, depth, magnitude and activity rate is desirable and may bring more accurate result but the faults of most earthquakes are not known.

To cope with this limitation of the data of faults, probabilistic analysis usually introduces the concept of area source model. The earthquakes, which can be associated with the active faults and the necessary parameters are available, are treated as the fault source model and the rest are treated in area source model. The area source model, i.e. the back ground source model is based on the activity in the earthquake catalogue not associated with the fault activities. In this study, the larger events in the magnitude range 8.0 and higher are assumed to occur related to the scenario earthquake faults in Figure 1-2.

The area source model was established based on the earthquake catalogue that was compiled by Prof. Ansary, BUET. The data set includes the event from 1548 to 2007 years including magnitude, depth and epicenter location. The extent of the catalogue is 85.0to 97.0˚E in longitude and 18.0˚ to 30.0˚N in latitude. Figure 1-25 shows the epicenters.

However, the catalogue has been refined by the removal of the dependent earthquakes. The dependent earthquakes such as foreshocks and aftershocks are removed based on the methods by Gardner and Knopoff (1974), which is commonly used in the world. Originally the catalogue included 5,116 seismic events, from which 1,442 dependent earthquakes (32 %) have been removed resulting a number of 3,088 independent seismic events as shown in Figure 1-26.

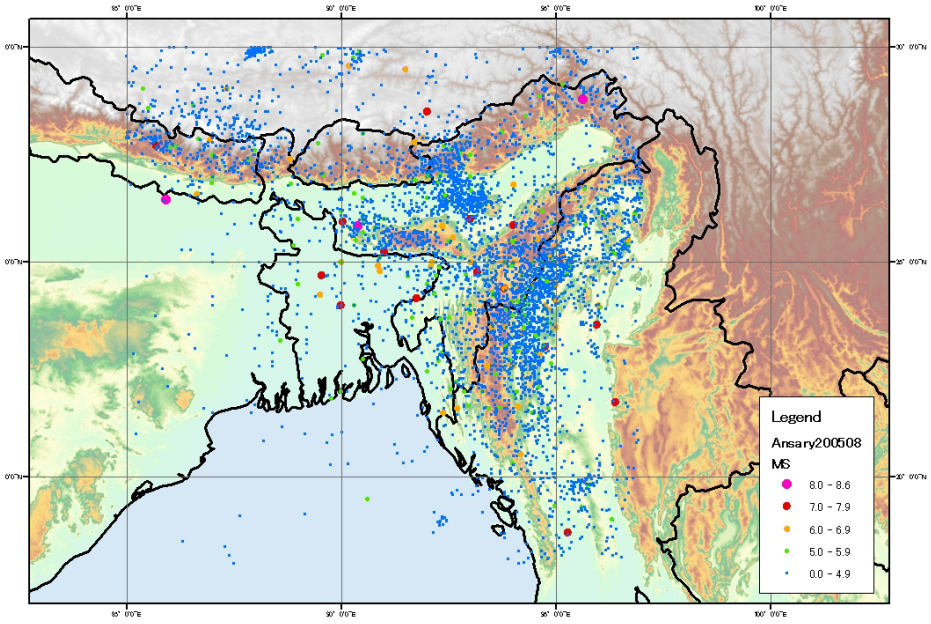

[Earthquake Catalogue: Prepared by Prof. Ansary, BUET]

Figure 1-25 Historical Earthquake Distribution in Magnitude

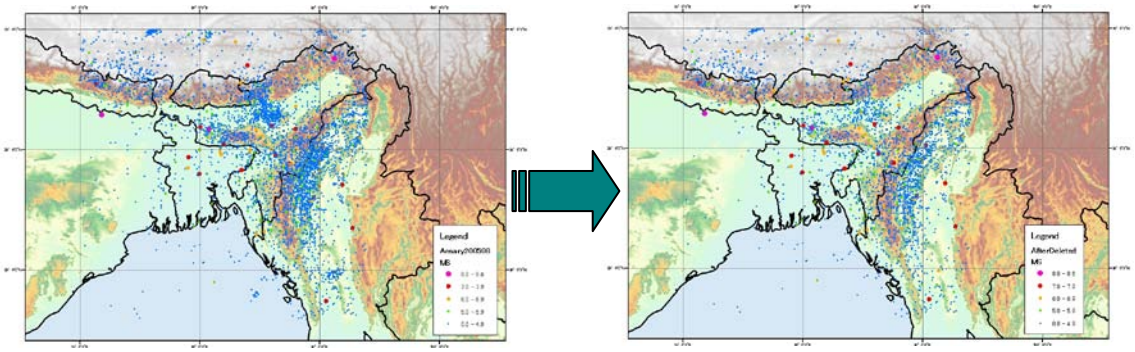

Figure 1-26 Removal of Dependent Earthquakes from All Seismic Events

Then, the completeness of the catalogue along the time with magnitudes is checked by counting the earthquakes by some magnitude ranges and accumulated as Figure 1-27. The black folded lines in Figure 1-26 shows the cumulative number of earthquakes corresponds to

the magnitude ranges shown in the graph. The increasing rate of cumulative number, which is shown by red line, with magnitude equal or larger than 4 seems constant after 1963. If all the earthquakes larger than Mw 4.0 are detected and included in the catalogue currently, it is assumed that this situation has started on 1963. This implies that the catalogue may be complete after 1963 for the earthquake with magnitude equal 4 or larger. The earthquakes equal or larger than magnitude 5 and 7 may be complete after 1920 and 1850 respectively. The area source is divided into four zones of northern and eastern subduction zones and western and eastern shallow crustal zones as shown in Figure 1-28, mainly based on the seismotectonic environment.

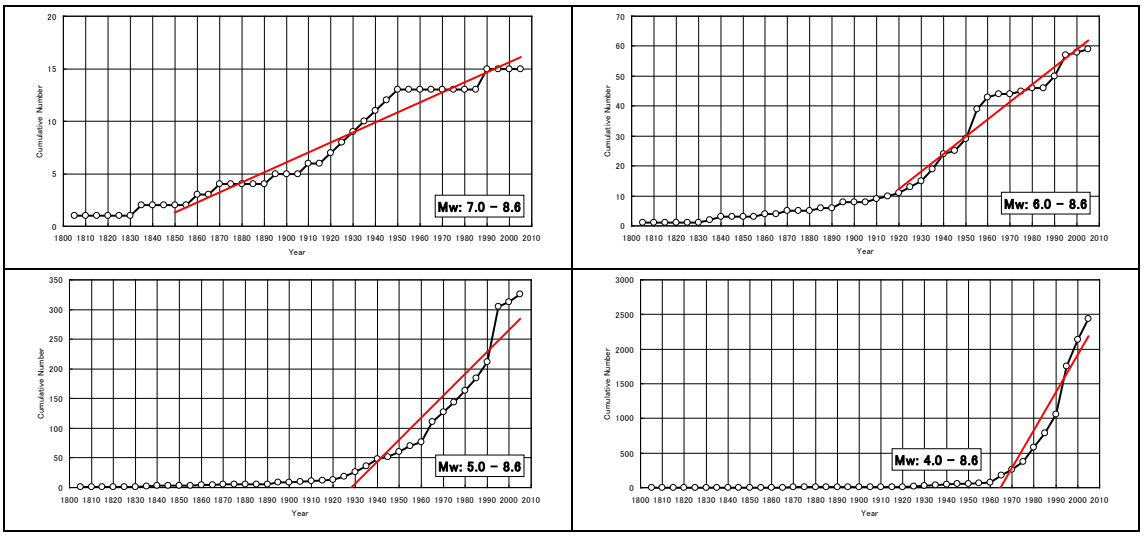

Figure 1-27 Accumulated Number of Events to Check the Completeness of the Catalogue

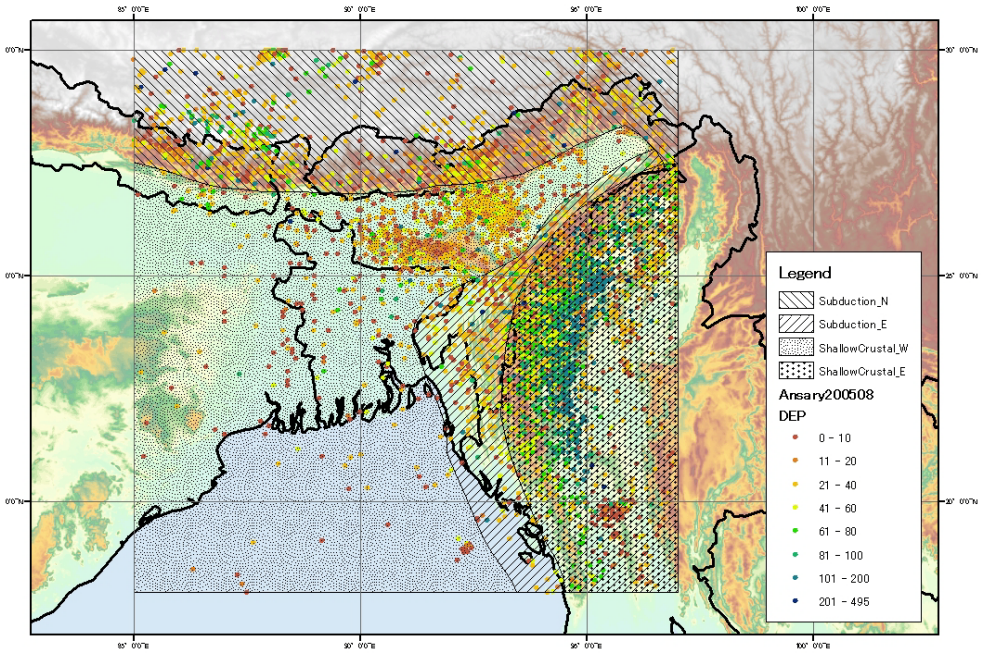

Figure 1-28 Seismic Source Zones in Bangladesh and its Surroundings

Finally, based on the catalogue and the reliability duration for each magnitude range, the Gutenberg-Richter relation parameters are calculated based on Weichert (1980), which employ the modified maximum likelihood method to extend the case of events grouped in magnitude with each group observed over unequal time periods. The results of Gutenberg-Richter figures for source zones are shown in Figure 1-29. In this step, the events equal or larger than 8.0 in magnitude are eliminated from the catalogue except in Subduction-N area because the larger events in the magnitude range 8.0 and higher are assumed to occur related to the scenario earthquake faults. In Subduction-N area, all the events are treated as the area seismic source because Himalaya Main Frontal Thrust is not modeled as scenario earthquake in this study. Also the earthquake in 1885 (M=7.5) is removed because this earthquake might have occurred at Madhupur Fault. The b-values for both shallow crustal zones are 0.83, for the eastern subduction zone is 0.99 and for the northern subduction zone is 0.90, respectively.

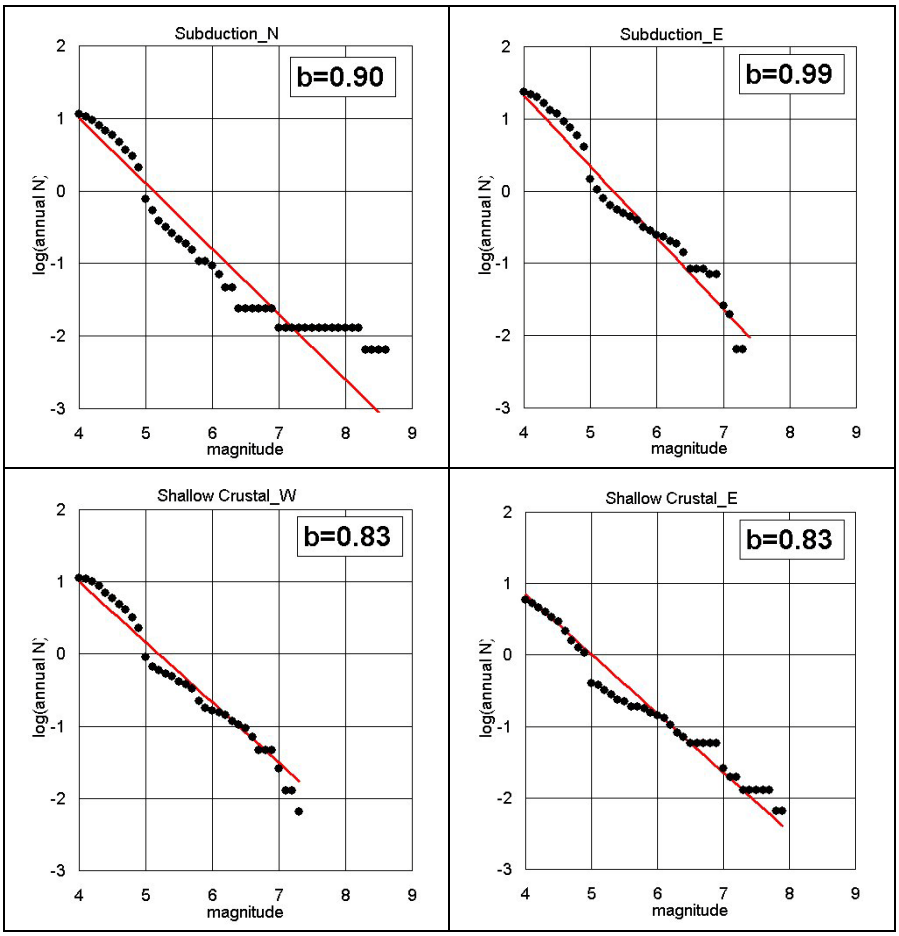

Figure 1-29 b-values for each Seismic Source Zones

The background seismic activities are evaluated for the 3,600 grids of 0.2˚×0.2˚based on the earthquake catalogue for 155 years. The size of grid was decided considering the density of

epicenter and the effect to the analysis. The Gutenberg-Richter exponential magnitude recurrence model is assumed to govern the earthquake activity in these cells. The total number of the earthquakes that are used in the analysis is 2,421 and the number of cells to be evaluated is 3,600 in total. This means each cell of the grid includes only several earthquakes utmost, therefore the overall '*b*' values for the each area sources in Figure 1-29 are used in corresponding cell. Following that, the '*a*' values are calculated for each cell based on the number of earthquakes in the cell and spatially smoothed using two-dimensional Gaussian filter with a decay distance of 50 km.

1.3.3. Fault Source Model

The fault source model will be made based on the time predictable fault model. The activity rate or recurrence interval will be evaluated based on the trenching survey results, GPS measurement results and/or earthquake catalogue.

1.3.4. Probabilistic Seismic Motion

The probabilistic seismic motion at engineering seismic baserock (Vs=760 m/sec) will be calculated for 2% and 10% probability of exceedance in 50 years accounting the contribution of all the area sources and fault sources.

2. Seismic Motion at Ground Surface

2.1. Outline

An empirical method was adopted to evaluate the amplification of sub-surface soil layer. If the velocity layer model at each grid could be made, it is better to conduct response analysis and evaluate the amplification by surface layer in the analytical way. However, currently available and reliable information of the ground, especially the shear wave velocity data is quite limited and the soil model for response analysis was made for only 19 points, where PS loggings were conducted in this project. The empirical method was verified by the response analysis at 19 points.

2.2. Amplification Analysis

The amplification of the seismic motion by sub-surface soil layers was evaluated by the amplification factor which was decided by average S wave velocity from ground surface to 30 m depth (Vs30). In this study, the ground of each grid was classified based on the NEHRP (National Earthquake Reduction Program) Provisions in USA. NEHRP Provisions classify the ground to five classes from A to E based, in part, on Vs30. The Vs30 range of class D is 180 to 360 m/sec and most of the study area is classified as class D. The short period amplification factor of weak motion for class C, D and E is 1.2, 1.6 and 2.5 respectively. Therefore the class D was divided to five sub-classes to make the step of amplification factor is about 0.2, namely D1 to D5 as shown in Table 2-1. The soil amplification factors for short period (0.3 sec) and 1.0 sec acceleration response spectrum (Sa) by NEHRP Provisions are provided in Figure 2-1 for site class A to E. The several colored folded lines in this figure correspond to the different baserock amplitudes. The amplification factor becomes lower in case that Sa at baserock becomes large to approximately express the effect of nonlinearity of soft soils. The amplification factor for class B is 1.0 and this means that class B (760m/sec < Vs30 < 1500m/sec) layer is treated as engineering seismic baserock. The amplification factors for class D1 to D5 were interpolated and shown in Figure 2-2.

Table 2-1 Ground Classification Applied in this Study

Ground Class	Vs30
C	360 - 760 m/sec
D1	300 - 360 m/sec
D2	250 - 300 m/sec
D3	220 - 250 m/sec
D4	200 - 220 m/sec
D5	180 - 200 m/sec
E	- 180 m/sec

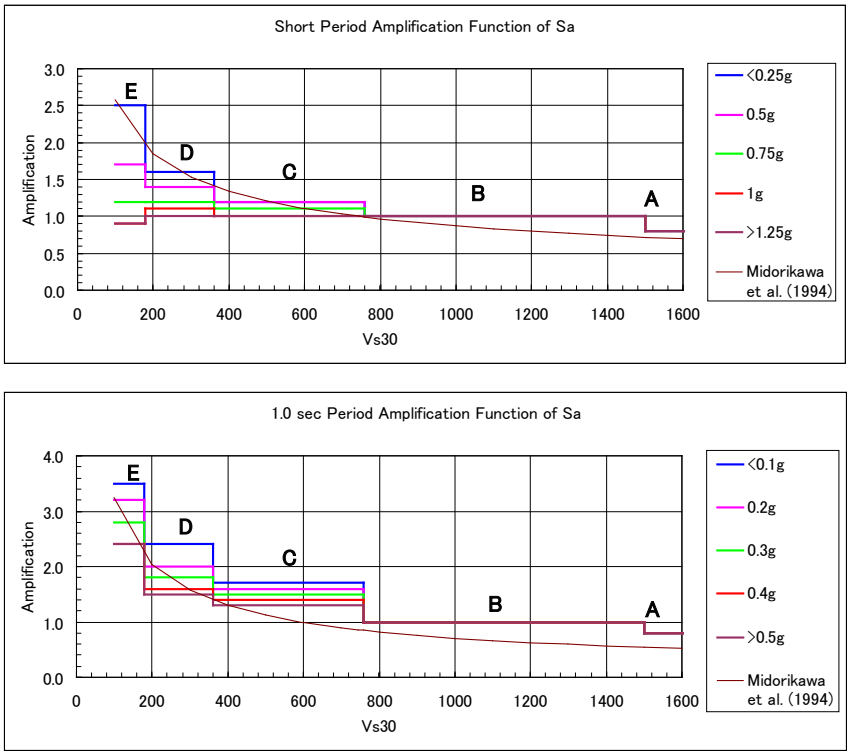

Figure 2-1　Amplification Function from 1997 NEHRP Provisions

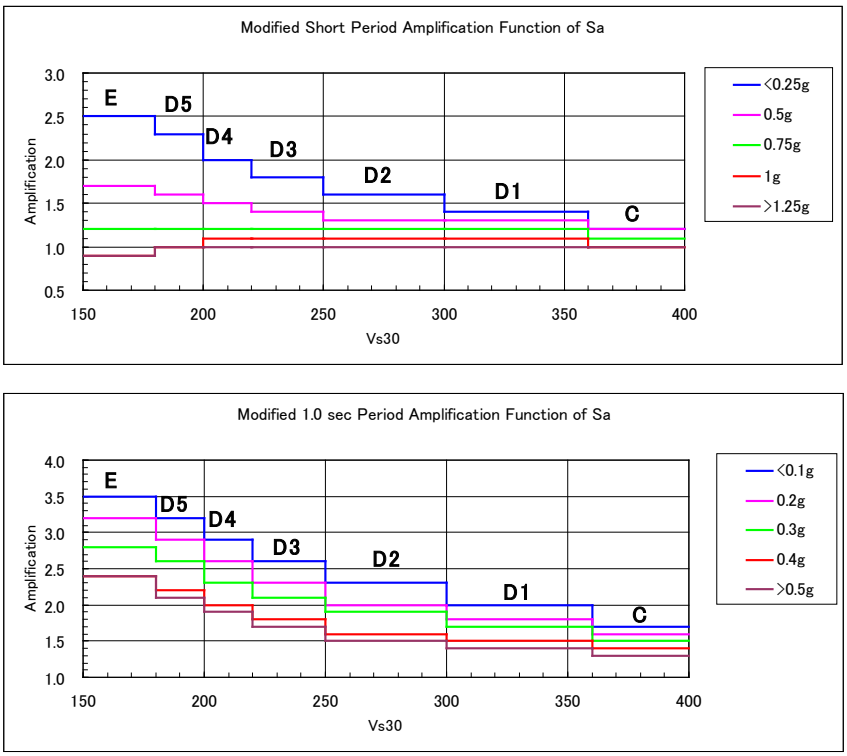

Figure 2-2　Modified Amplification Function

The ground classifications of Dhaka, Chittagong and Sylhet are shown in Figure 2-3. Dhaka is mainly covered by D2 to D3 grounds. In Chittagong, hill area is C to D1 and low land is mostly class E. The lowland of Sylhet is classified as E and hill area is D1 to D4.

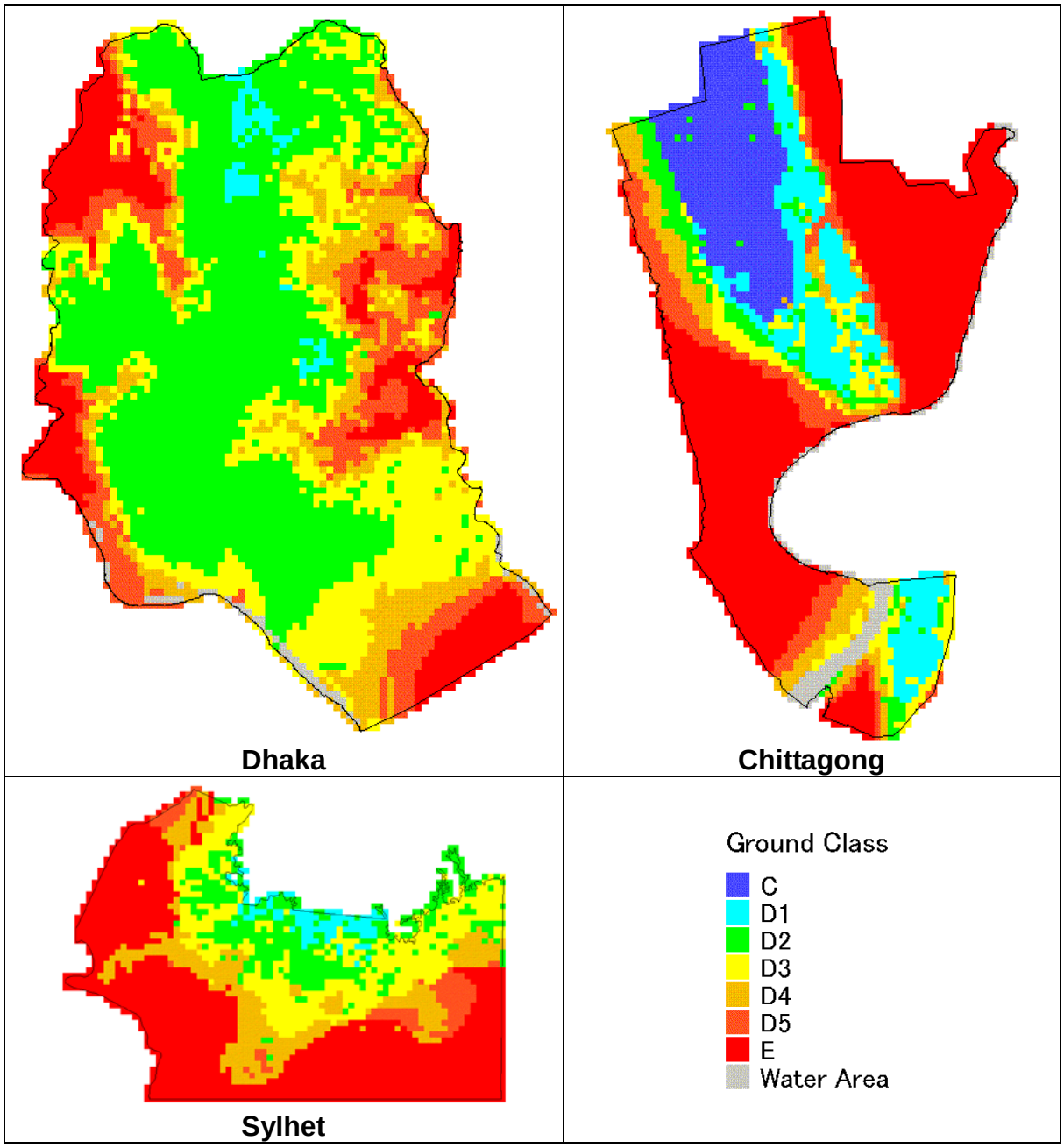

Figure 2-3 Ground Classification based on Vs30

The NEHRP Provisions refer USA and the amplifications of ground classes are derived mainly from the domestic examples. In Figure 2-1, the amplification factor related to Vs30 in Japan by Midorikawa et al. (1994), which is made from examples in Japan, is added. The amplification function based Vs30 in USA and in Japan show good correlation; however the applicability of the amplification by NEHRP to Bangladesh is unsure. To verify the applicability, the response analysis was conducted at 19 PS logging points. The S-wave velocity layer models to around 30 meters depth were made and 1D response analysis (SHAKE 91) was conducted. The S-wave velocity of the base layer for these ground models are around 400 m/sec. The wave forms by stochastic Green's function method (Section 1.2.4) were used as the input waves for the base layer in the analysis. The non linear dynamic properties are considered for soils with Vs<300 m/sec. The non linear dynamic soil properties in Bangladesh are not available; the typical curves in Japan were used. These curves are used in the study by Cabinet Office of Japan (2003) referencing the recent study of non-linear behavior of non-cohesive soils. The curves are shown in Figure 2-4. The dumping coefficient of the layers with Vs>300m/sec was estimated by following formula that is popularly used in Japan.

$$Q = Vs/15$$
$$h = 1/2Q$$

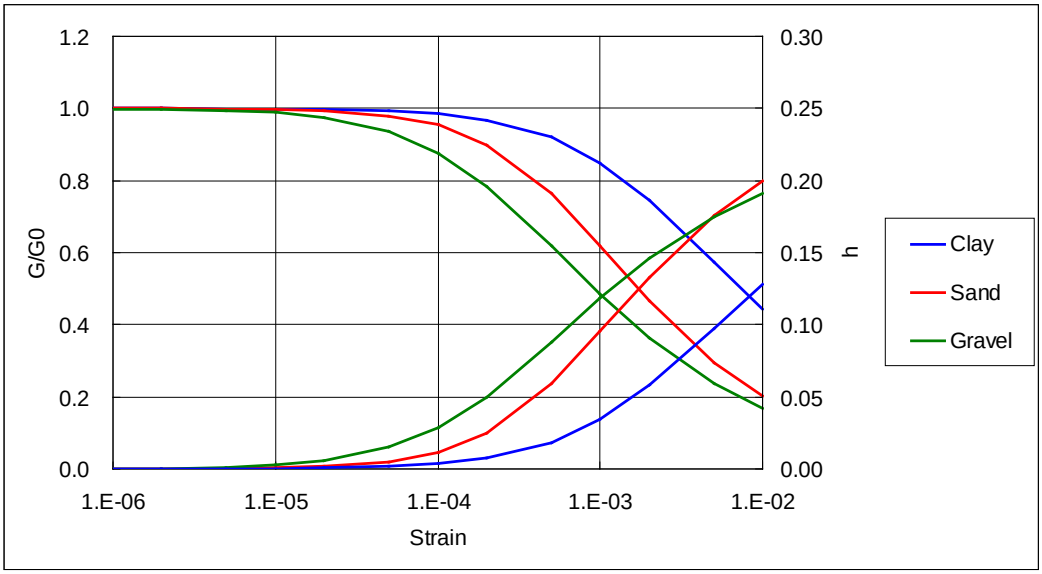

Figure 2-4 Non Linear Properties of Soil

The surface amplification factor for PGA by empirical relation based on Vs30 and the results by response analysis are compared in Figure 2-5. The amplification factors by empirical method show around average of the ones by response analysis, then the applicability of empirical method to study area may be verified.

The NEHRP Provisions do not provide the amplification factors for PGA or PGV, but HAZUS uses the same amplification factor of short period (0.3 sec) spectral acceleration for PGA and amplification factor of 1.0 sec for PGV respectively. In this study, the amplification for PGA and PGV were decided following HAZUS.

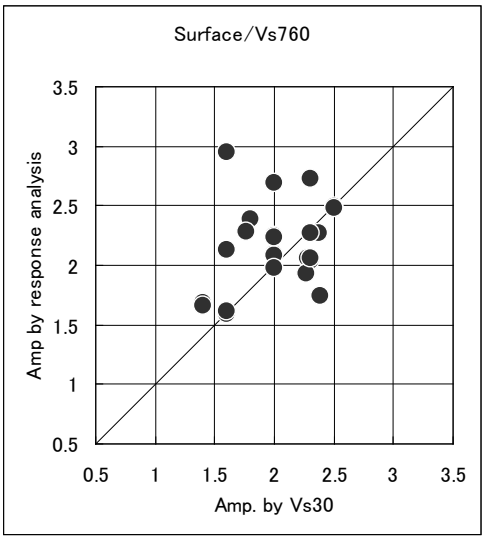

Figure 2-5 Comparison of Amplification Factor by Response Analysis and by Vs30

The amplification factors based on the Vs30 for short and long period Sa in Dhaka are shown in Figure 2-6 and Figure 2-7. The PGA and Sa (0.3sec) amplification factors for MF show lower value than the other scenario because of the effect of non-linearity. The amplification factors of PGV and Sa (1.0 sec) are almost same for all cases.

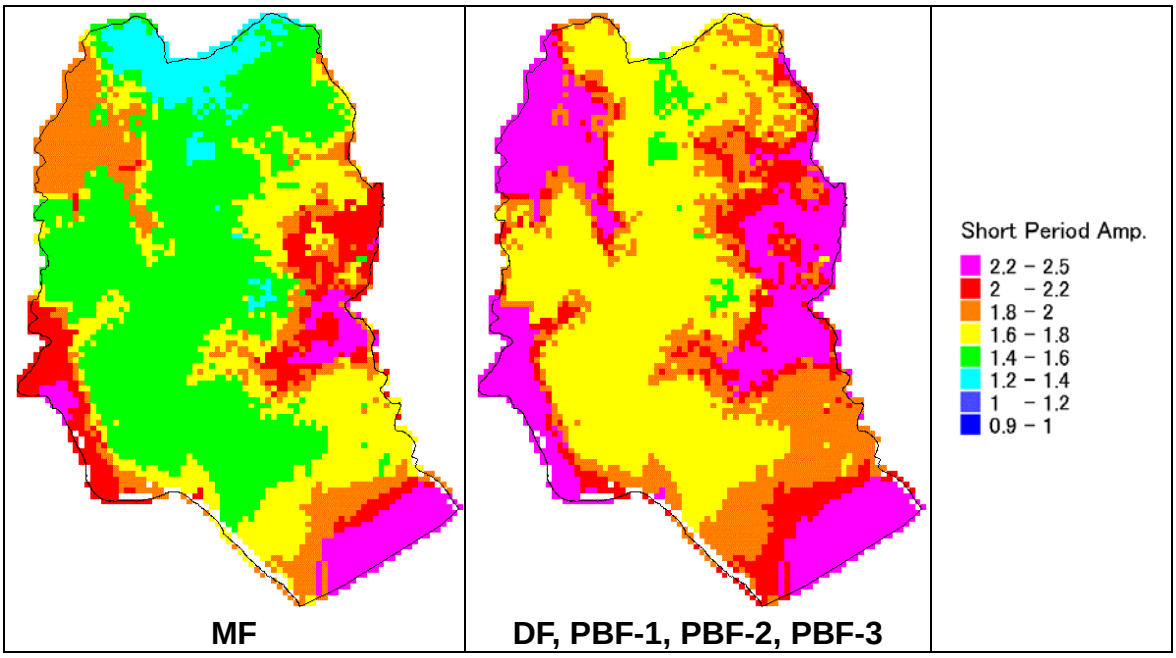

Figure 2-6 Amplification for PGA and Sa(0.3sec) in Dhaka

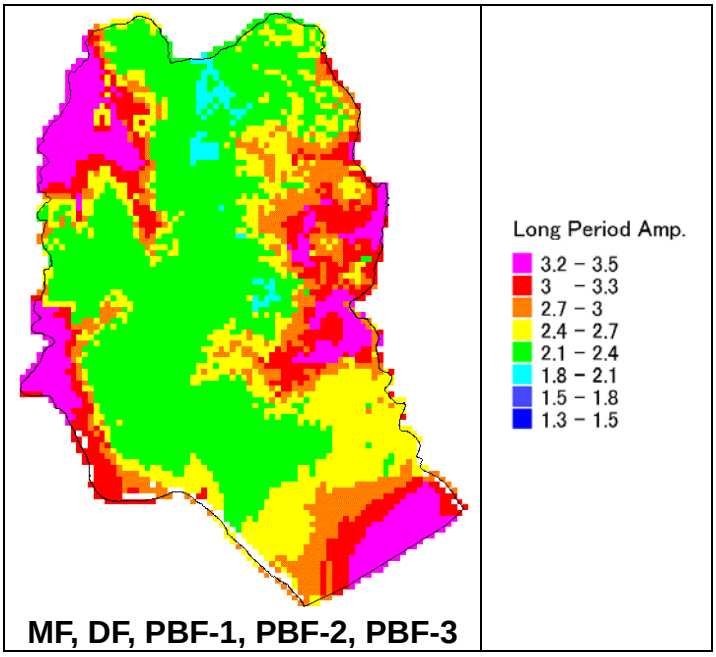

Figure 2-7 Amplification for PGV and Sa(1.0sec) in Dhaka

Figure 2-8 and Figure 2-9 show the amplification factors for Chittagong. The amplification factors for PBF-1 show lower value comparing to the other cases. It is notable that the factors for PGA and Sa (0.3 sec) show de-amplification phenomena at ground class E.

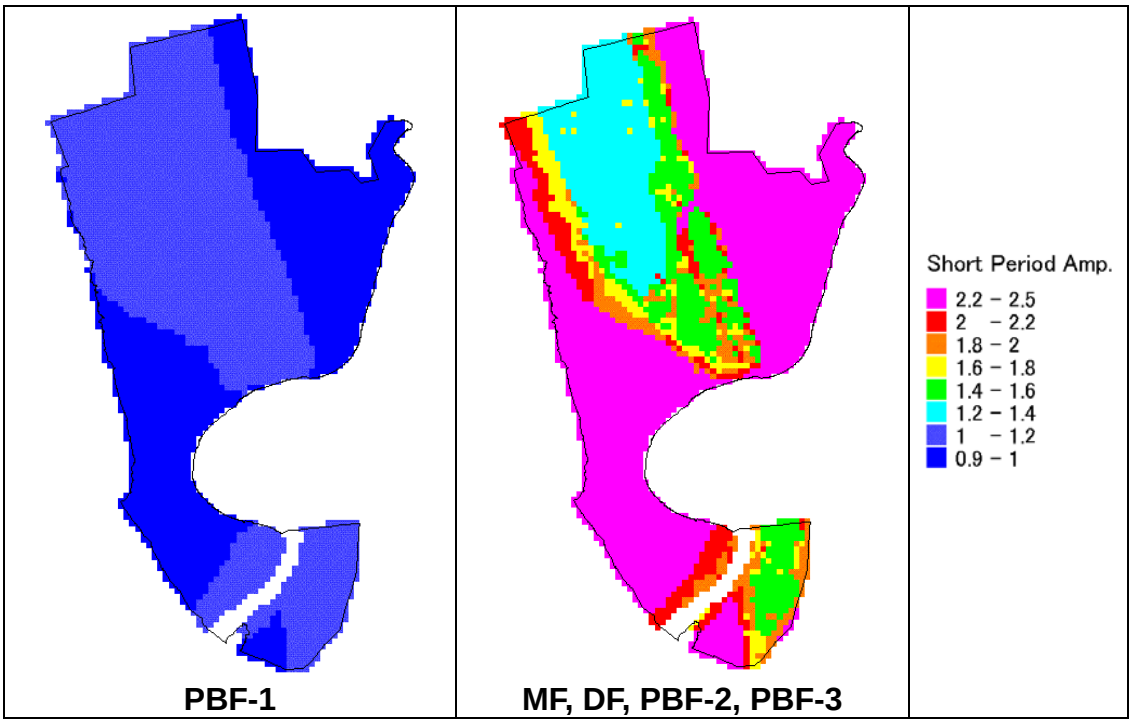

Figure 2-8 Amplification for PGA and Sa (0.3 sec) in Chittagong

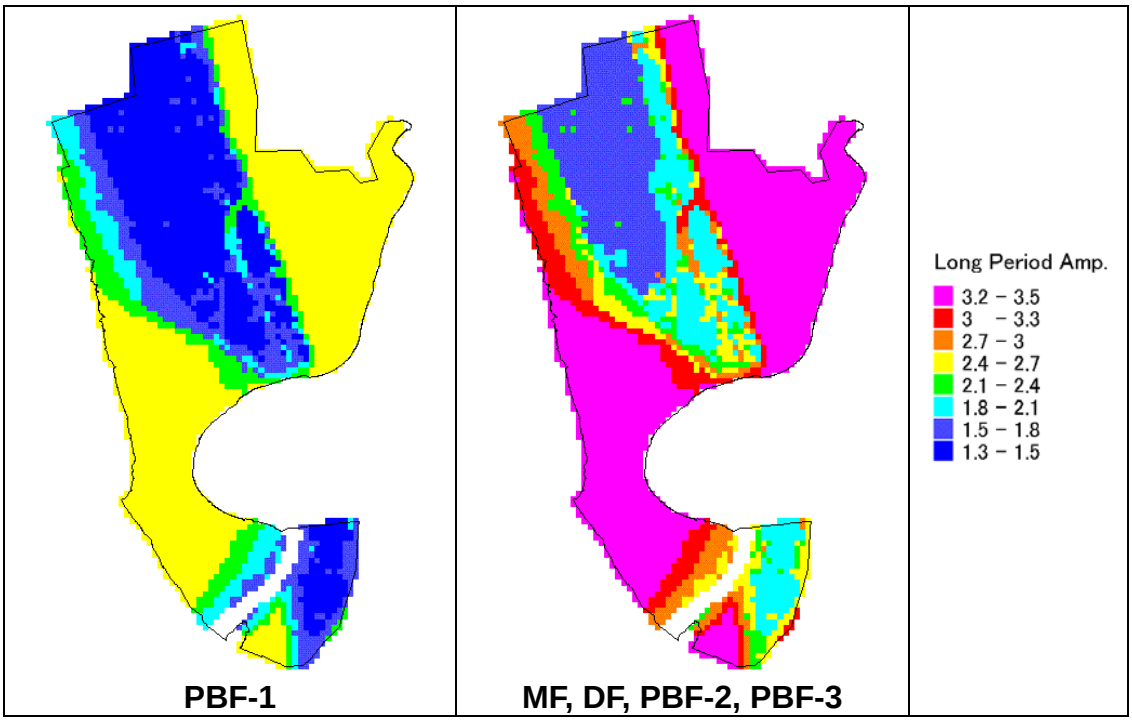

Figure 2-9 Amplification for PGV and Sa (1.0 sec) in Chittagong

The amplification factors for Sylhet are shown in Figure 2-10 and Figure 2-11. In case of DF and PBF-2, the non-linear effect to the amplification is observed.

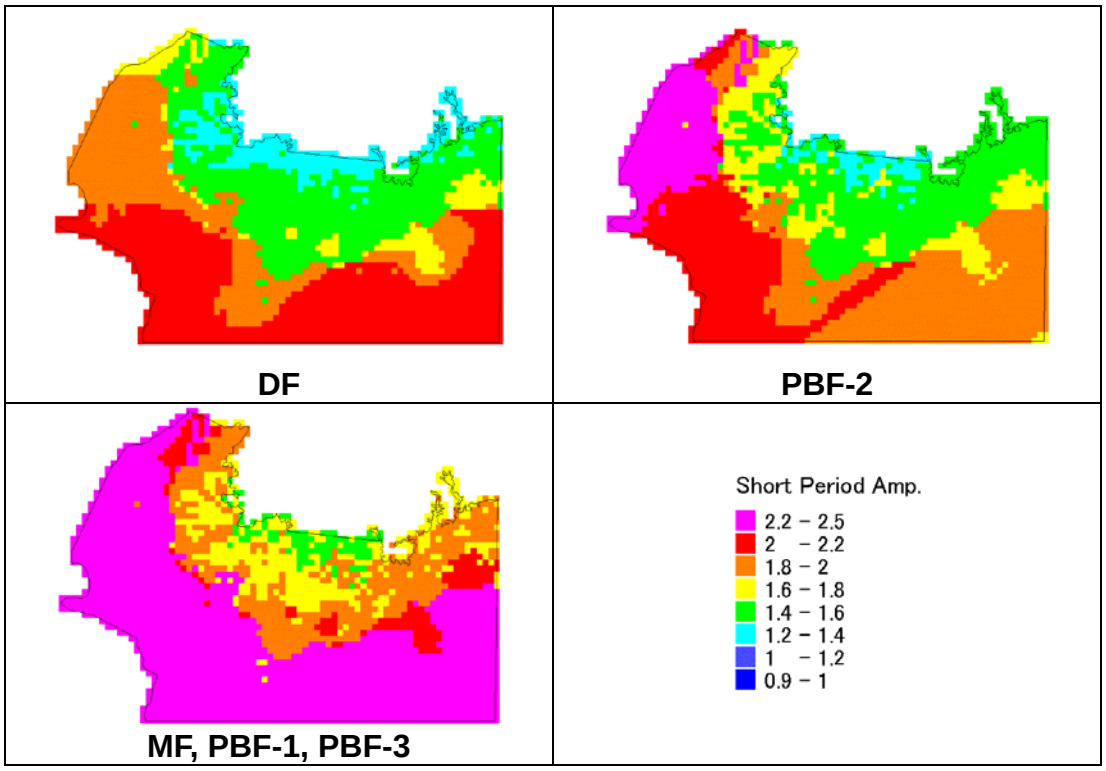

Figure 2-10 Amplification for PGA and Sa(0.3sec) in Sylhet

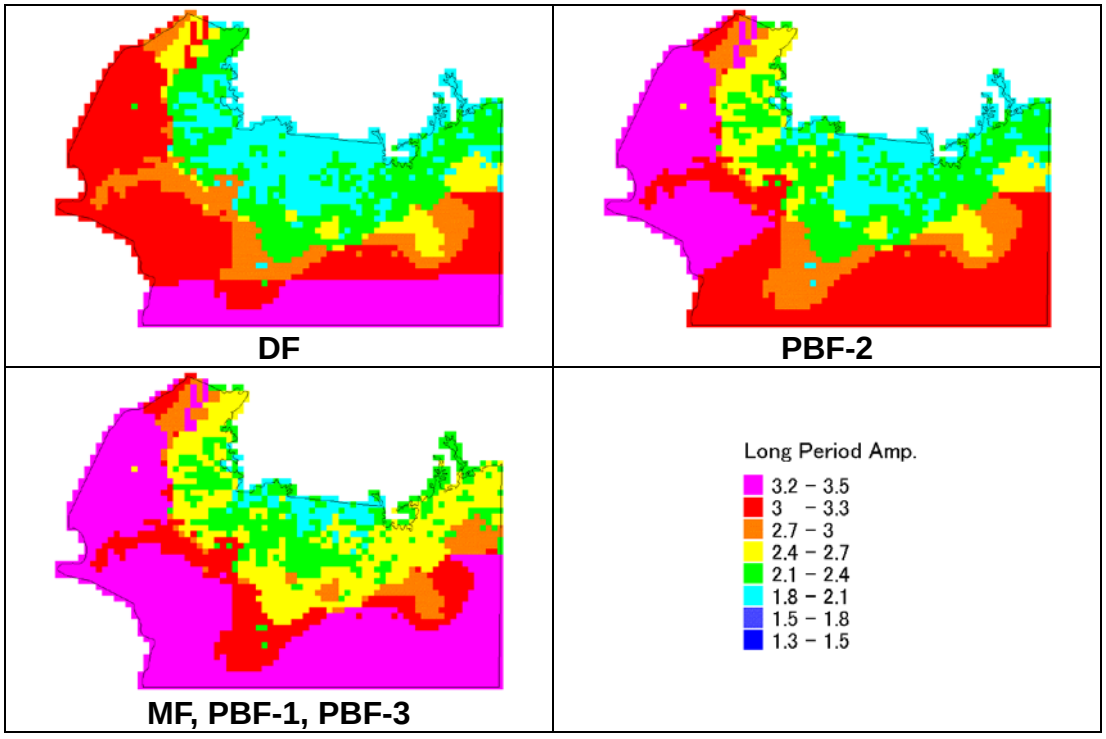

Figure 2-11 Amplification for PGV and Sa(1.0sec) in Sylhet

2.3. Surface Ground Motion

The PGA, PGV and Sa (h=5%, T=0.3 and 1.0 sec) at ground surface were calculated for five scenario earthquakes. In this analysis, the effects of non linearity of soils were considered.

The maps for Dhaka are shown in Figure 2-12 to Figure 2-15. The most important earthquake is MF and the PGA in Dhaka is 220 to 410 gal.

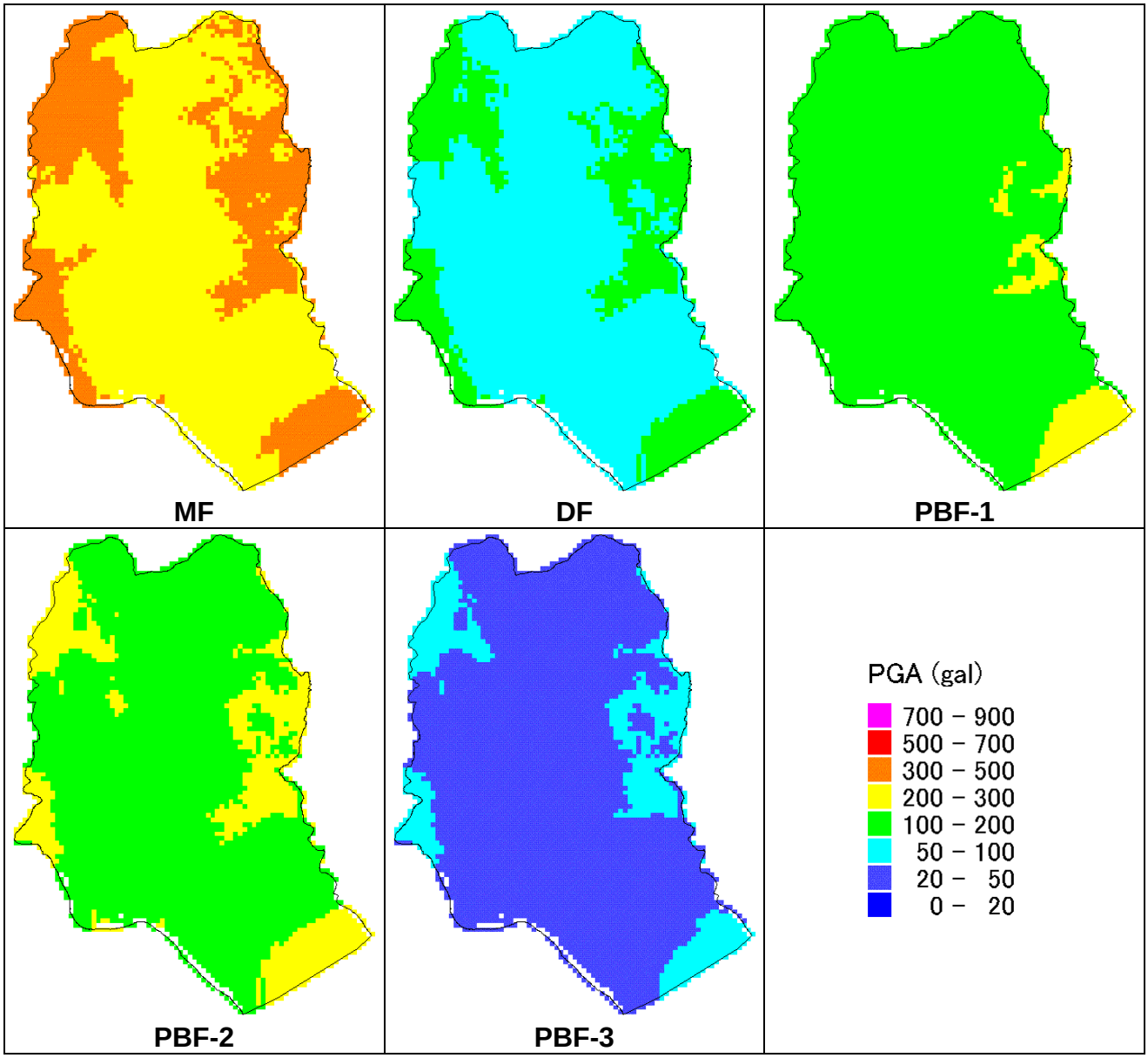

Figure 2-12 PGA at Ground Surface in Dhaka

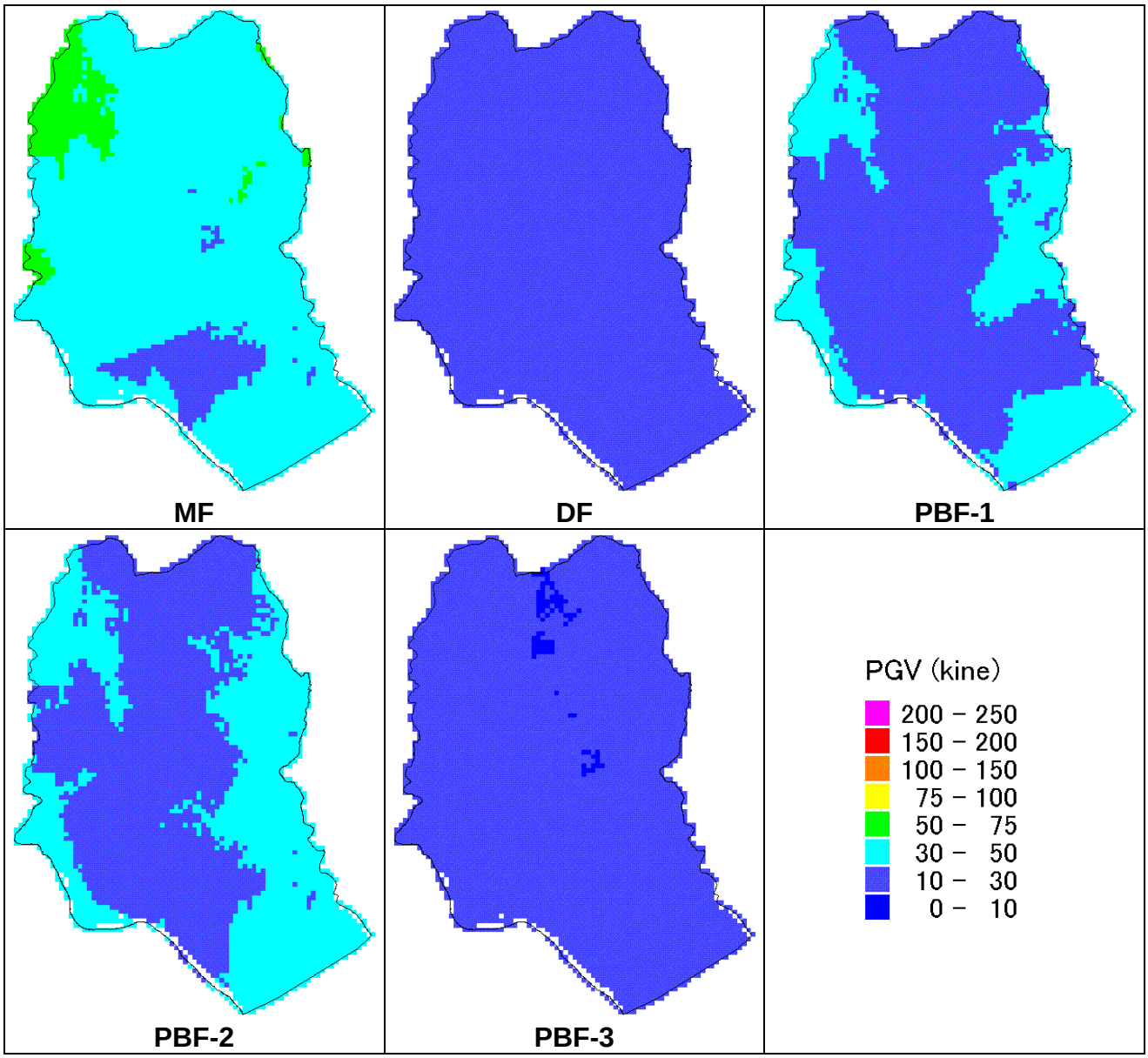

Figure 2-13 PGV at Ground Surface in Dhaka

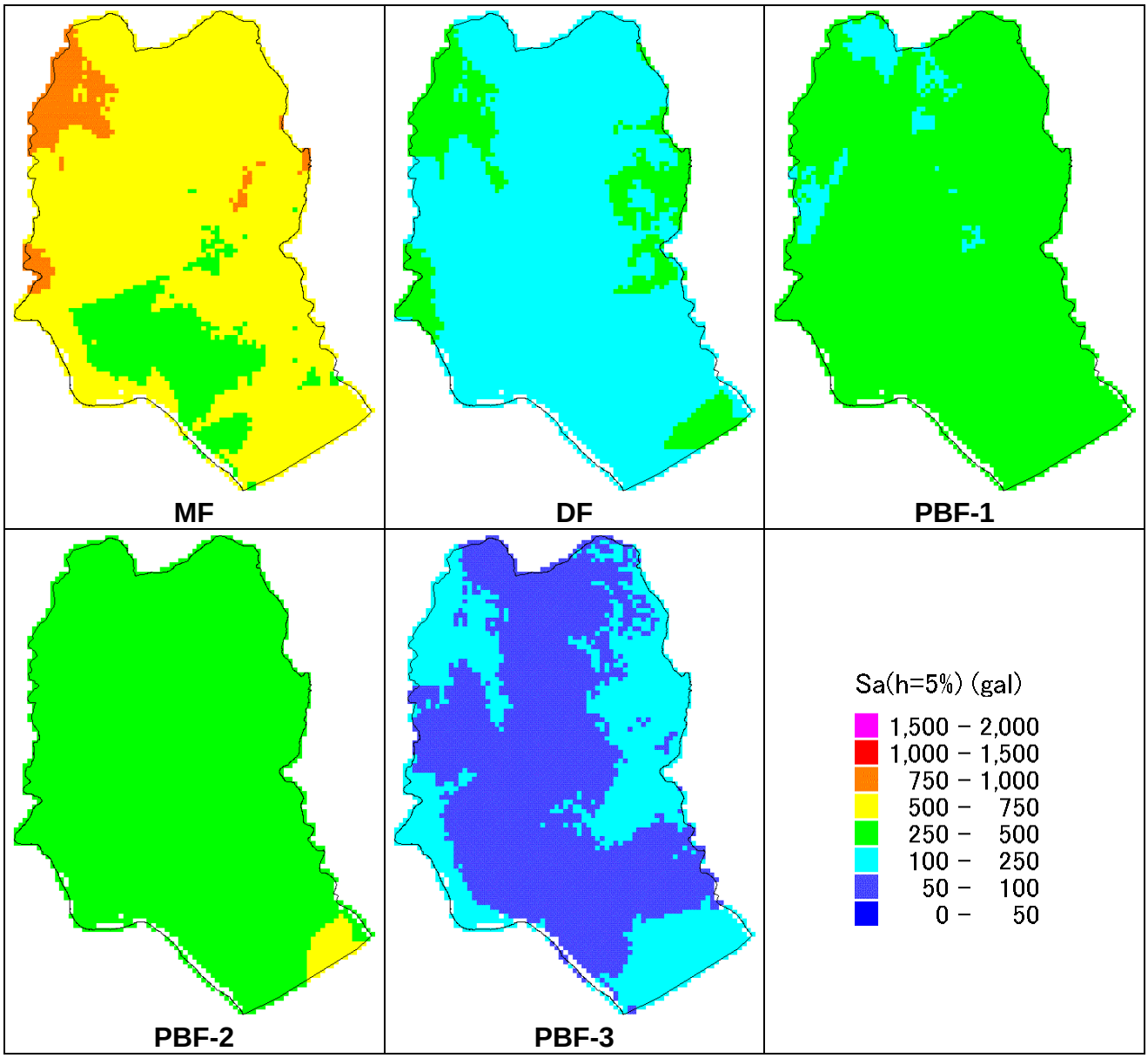

Figure 2-14 Sa (h=5%) for T=0.3 sec at Ground Surface in Dhaka

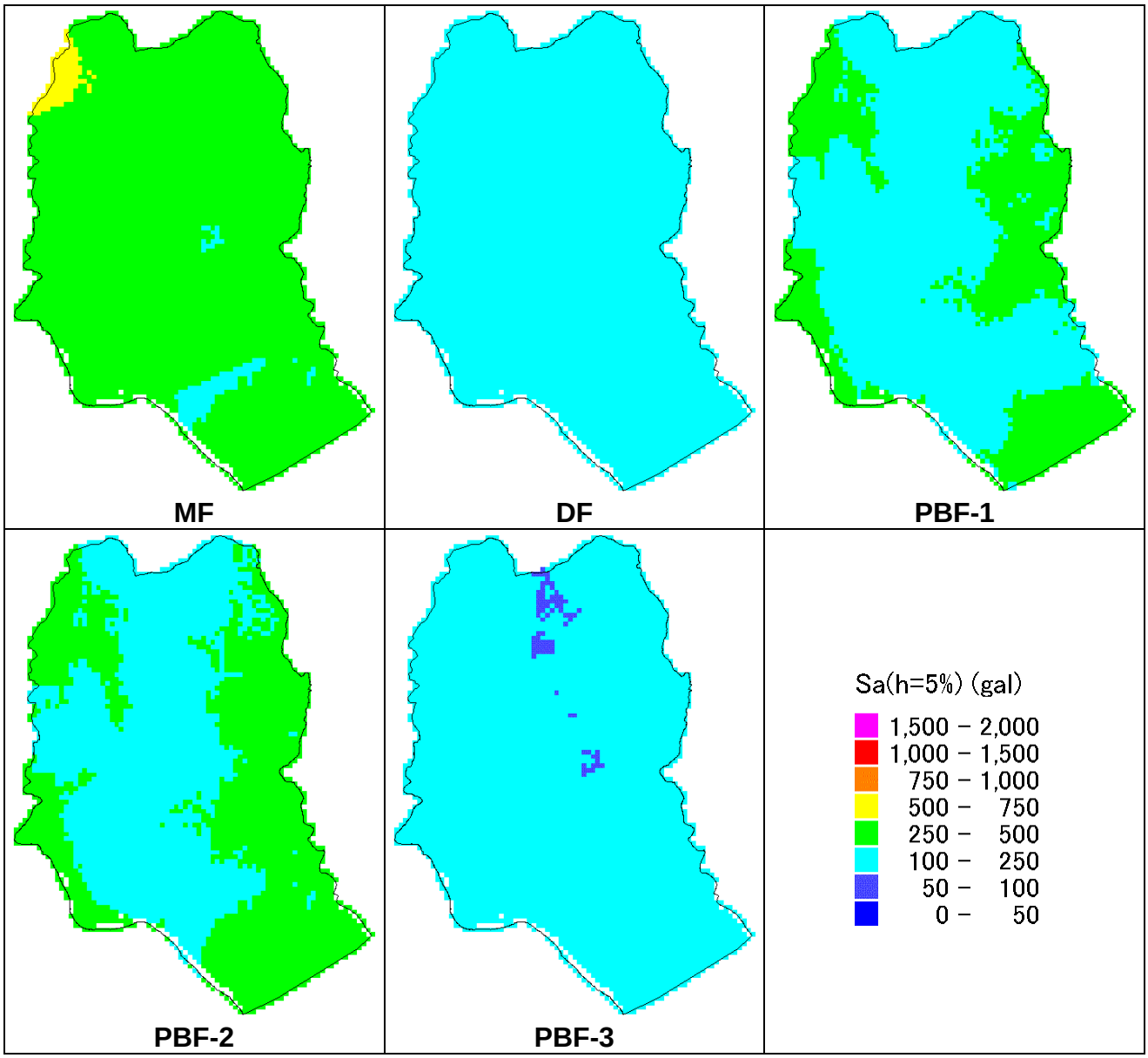

Figure 2-15 Sa (h=5%) for T=1.0 sec at Ground Surface in Dhaka

The maps for Chittagong are shown in Figure 2-16 to Figure 2-19. The most important earthquake is PBF-1 and the PGA in Chittagong reaches 600 to 770 gal, however the amplification by surface soil layer is very little or de-amplified because of the nonlinearity of soils. The nonlinearity effect is larger in lowland (class E) and PGA at lowland is smaller than hill area; but in other scenario earthquakes, the PGA at lowland is larger than hill area because nonlinear effect is not observed in other smaller cases. Similar situation is also observed for Sa (T=0.3 sec). For PGV or Sa (T=1.0 sec), surface ground motion at lowland is always larger than hill area.

As per PGA at Chittagong caused by PBF-1, it is reasonable even 600 to 770 gals, because the distance from fault plane is only several kilometers with magnitude more than 8. This is verified by recent strong ground motion observation in the world. For example, the PGA at JMA Kobe Station at the 1995 Kobe earthquake (M 7.3) was 818 gals at ground surface.

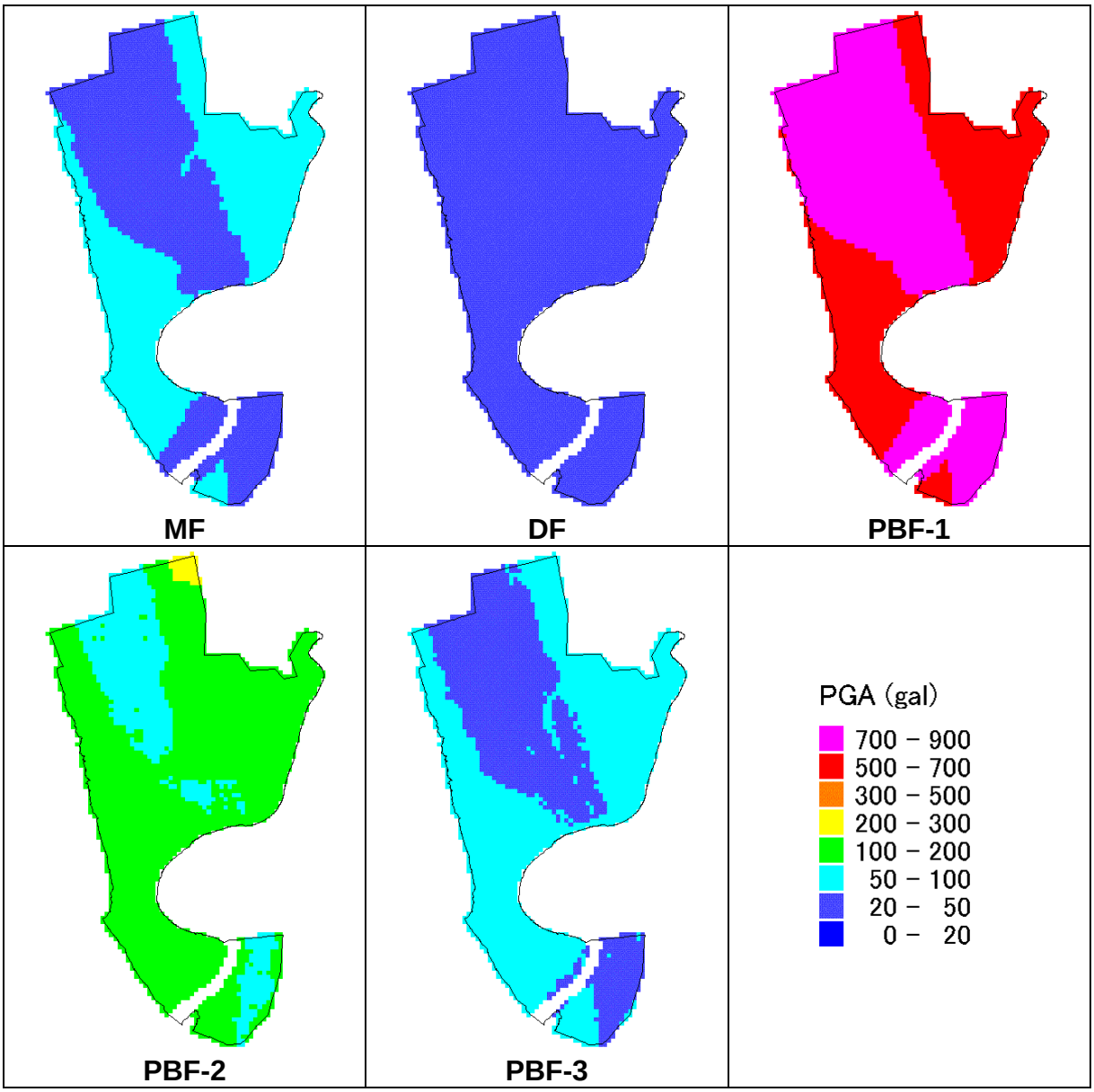

Figure 2-16 PGA at Ground Surface in Chittagong

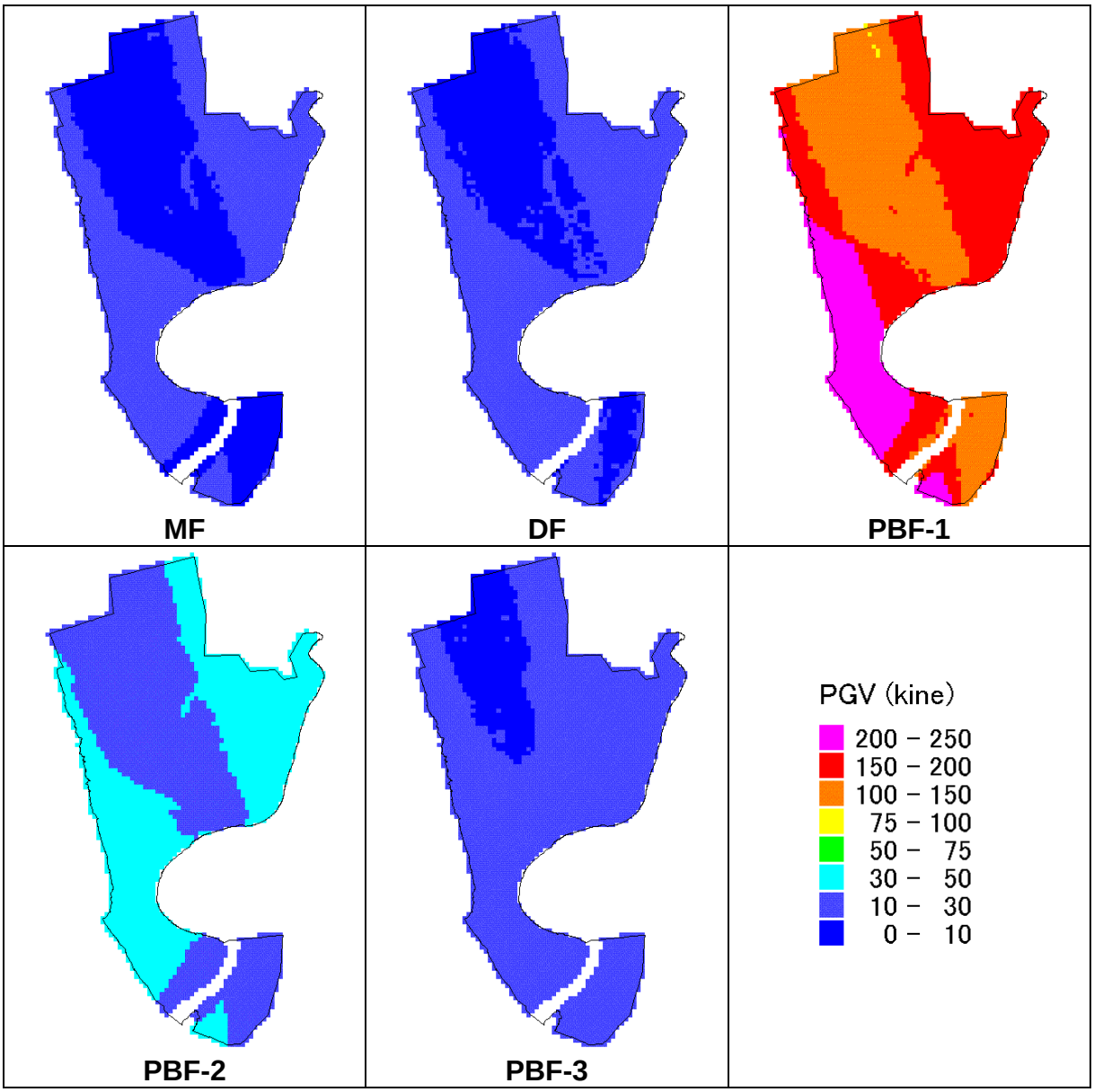

Figure 2-17 PGV at Ground Surface in Chittagong

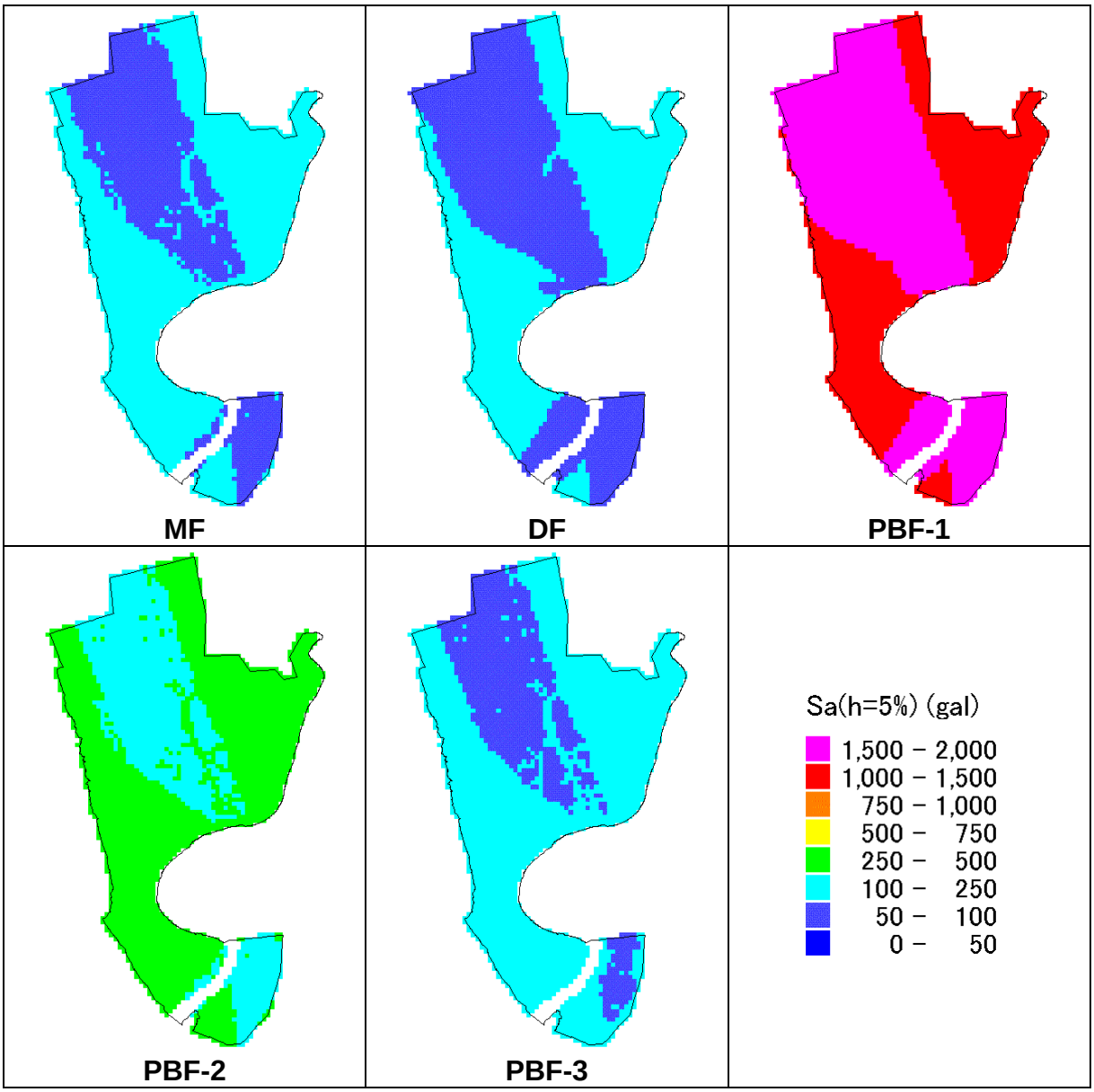

Figure 2-18 Sa (h=5%) for T=0.3 sec at Ground Surface in Chittagong

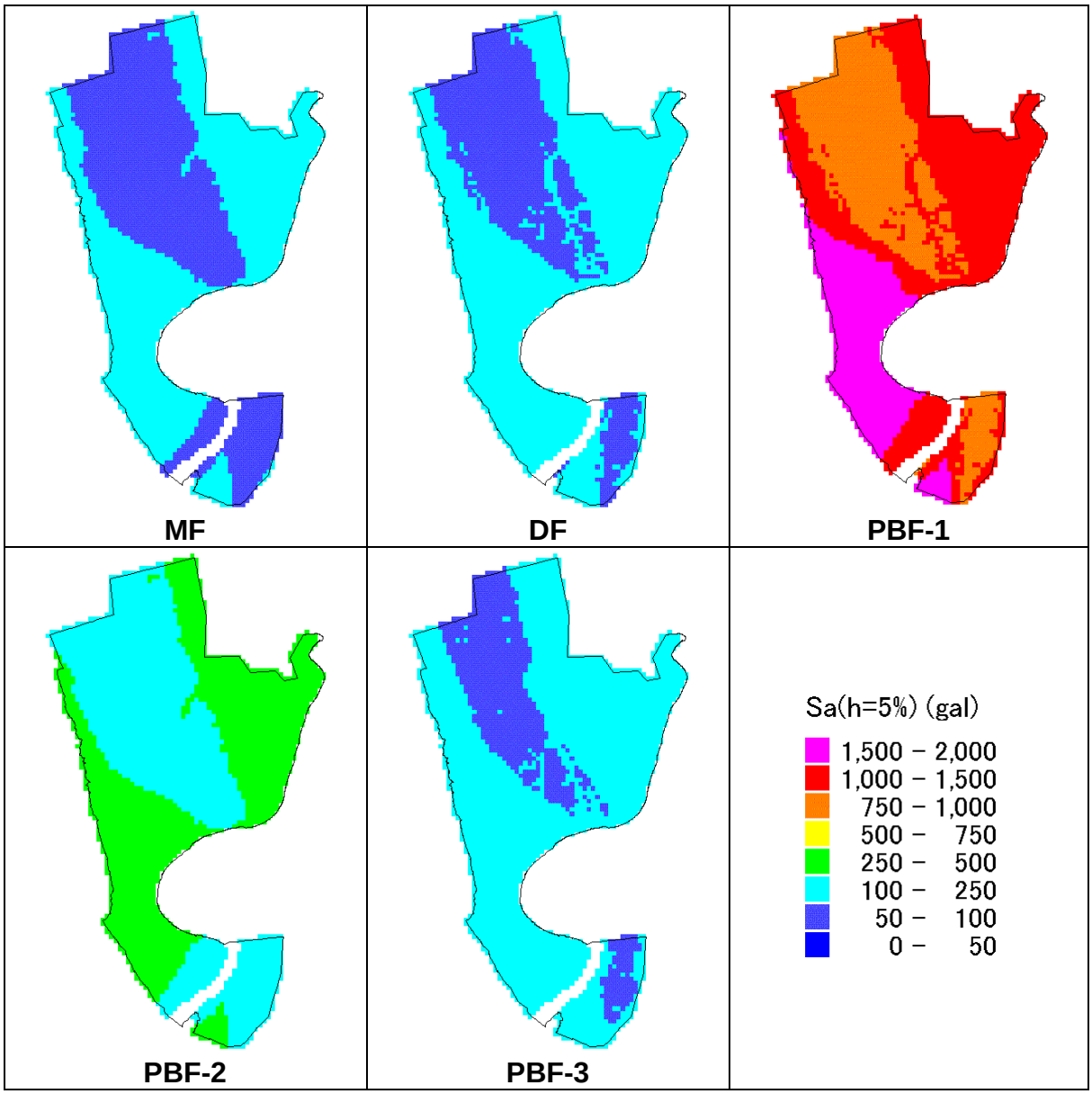

Figure 2-19 Sa (h=5%) for T=1.0 sec at Ground Surface in Chittagong

The maps for Sylhet are shown in Figure 2-20 to Figure 2-23. The most important earthquakes are DF and PBF-2. PGA by DF is 270 to 420 gal and 230 to 420 gal by PBF-2.

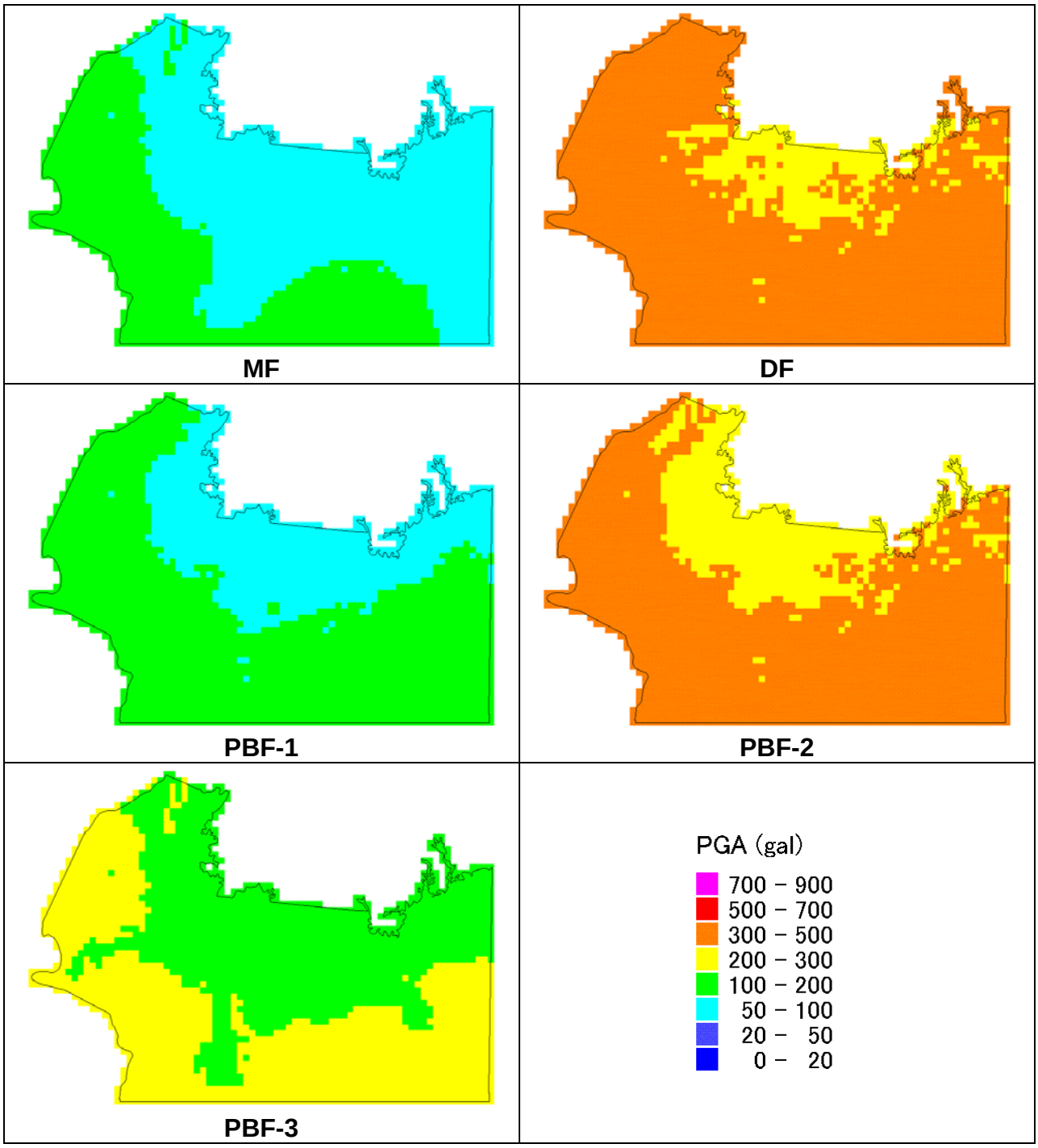

Figure 2-20 PGA at Ground Surface in Sylhet

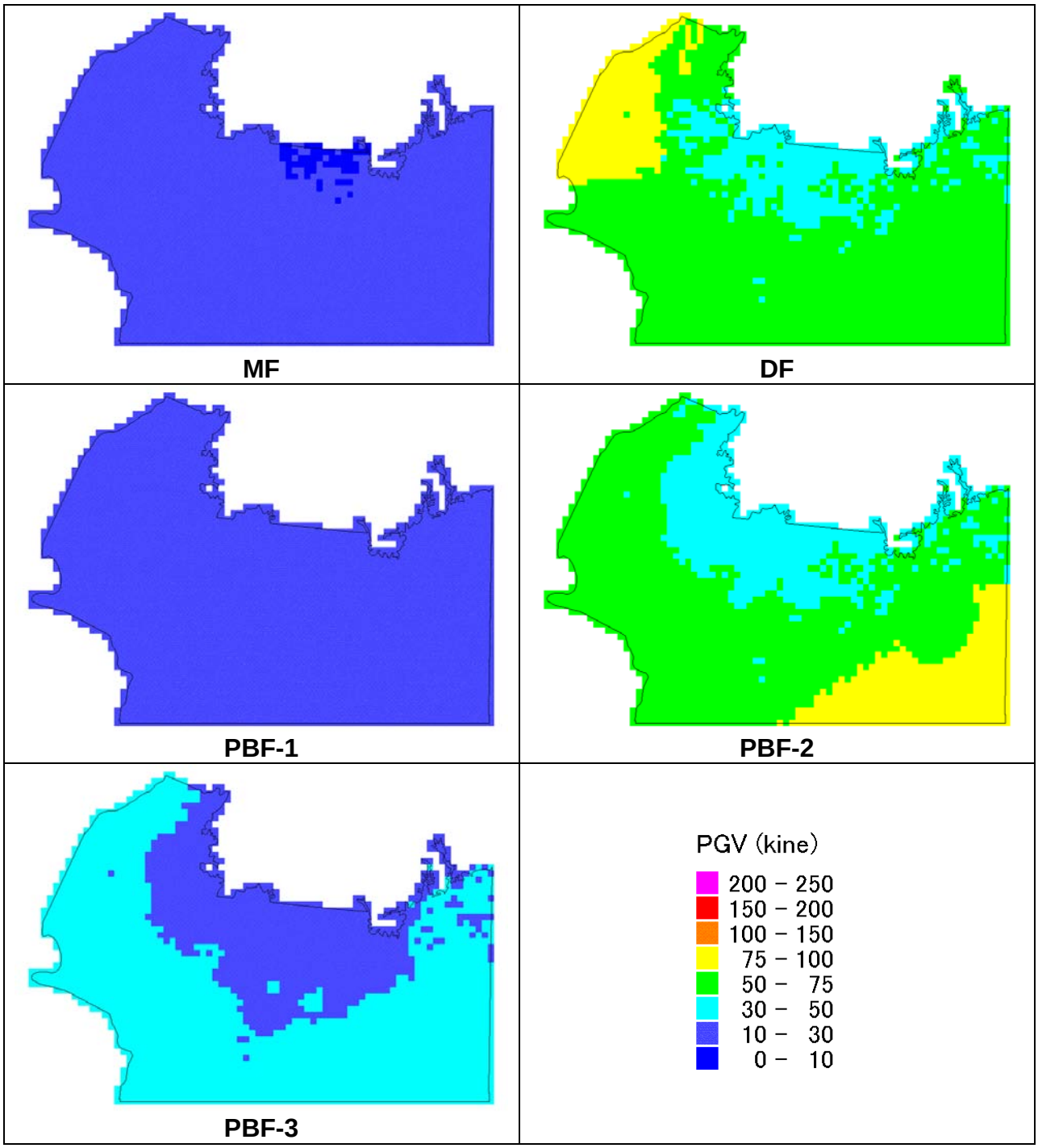

Figure 2-21 PGV at Ground Surface in Sylhet

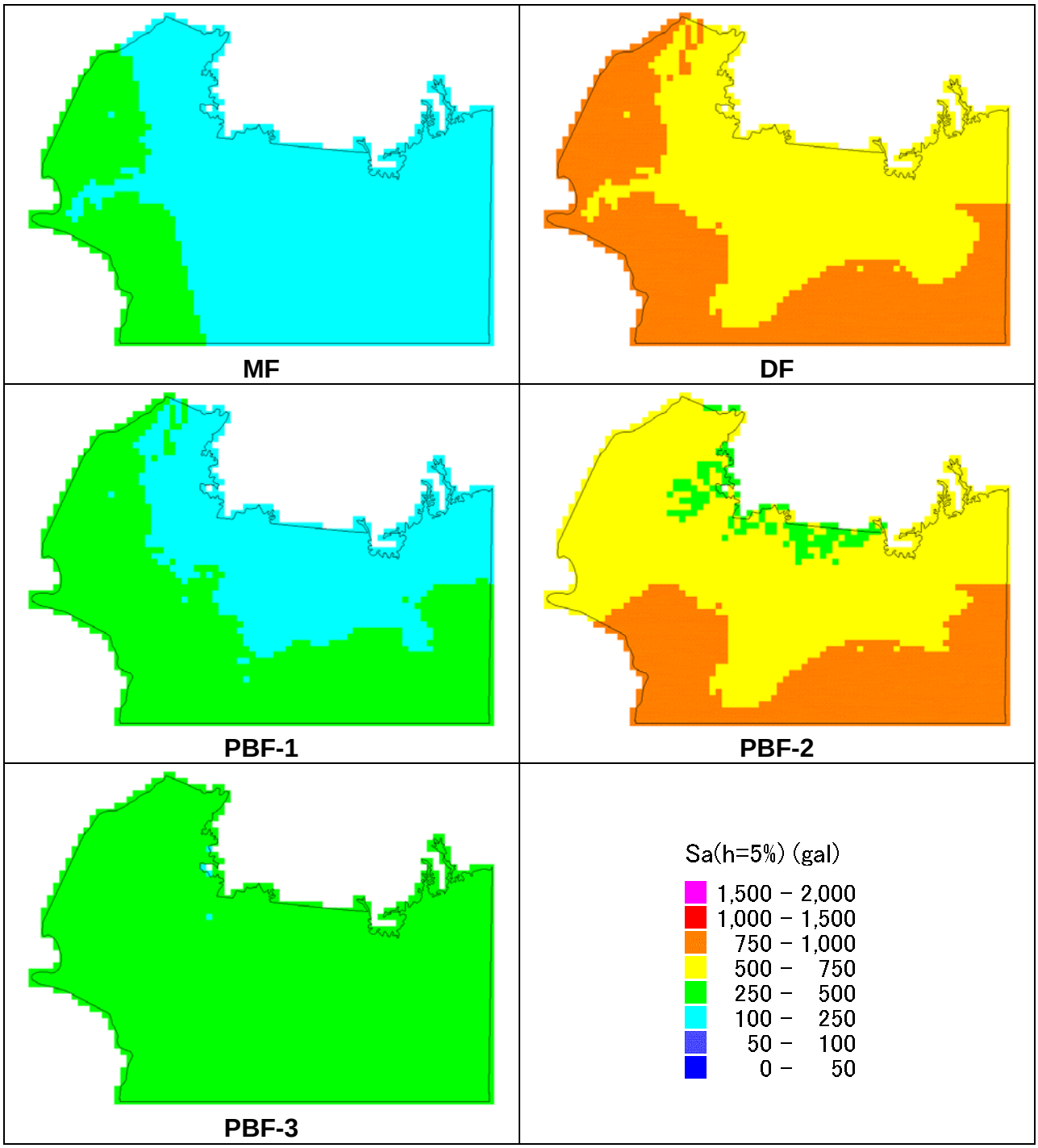

Figure 2-22 Sa (h=5%) for T=0.3 sec at Ground Surface in Sylhet

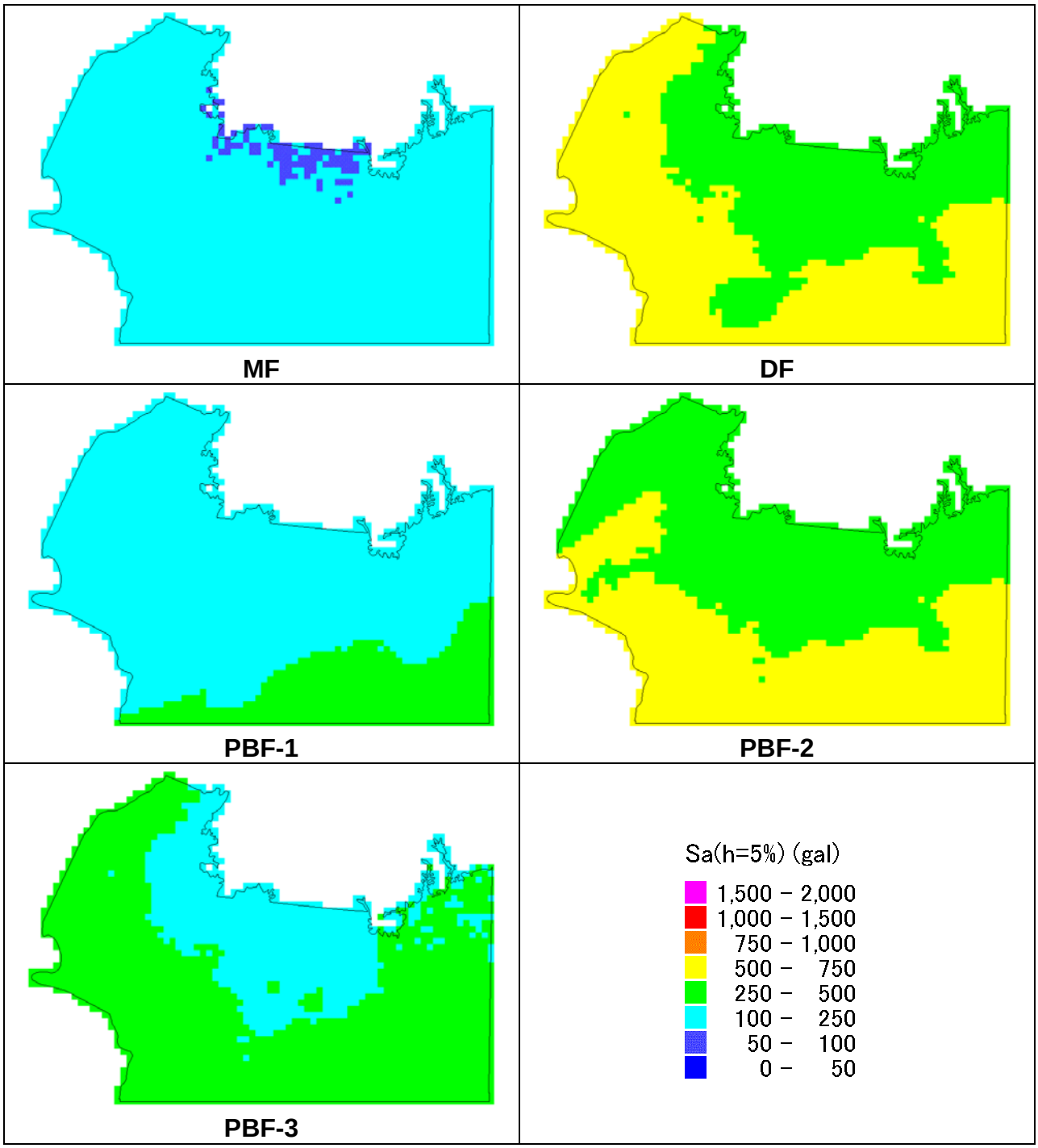

Figure 2-23 Sa (h=5%) for T=1.0 sec at Ground Surface in Sylhet

3. Seismic Hazard Analysis

3.1. Liquefaction Analysis

3.1.1. Outline

To evaluate liquefaction potential computationally, the liquefaction resistance of soil is estimated by results of dynamic test, SPT, etc. and compared with the shear stress in the soil due to cyclic shaking and high excess pore water pressure during an earthquake. When this procedure is adopted, accumulated database related with the above mentioned properties are required and it can not possibly be achievement overnight. These investigations / studies are fairly under way in Bangladesh, thus empirical procedure, HAZUS that geologic / geomorphologic data, PGA (peak ground acceleration) at ground surface, M_w (moment magnitude) of a scenario earthquake and groundwater depth is used, for area-wide evaluating liquefaction susceptibility / probability are suitable in this study.

There are 2 steps for the liquefaction analysis in accordance with HAZUS. At first, liquefaction susceptibility is evaluated by geologic / geomorphologic data and information of geological age. Secondary, liquefaction probability is estimated by inputting PGA, Mw and groundwater level into the above evaluated liquefaction susceptibility map.

3.1.2. Liquefaction Susceptibility

Youd and Perkins (1978) presented relationship between liquefaction susceptibility and geological deposit type / geological age as shown in Table 3-1.

Table 3-1 Liquefaction Susceptibility evaluated by Geological Information

Type of Deposit	General Distribution of Cohesionless Sediments in Deposits	Likelihood that Cohesionless Sediments when Saturated would be Susceptible to Liquefaction (by Age of Deposit)			
		< 500 yr Modern	Holocene < 11 ka	Pleistocene 11 ka – 2 Ma	Pre-Pleistocene > 2 Ma
(a) Continental Deposits					
River channel	Locally variable	Very High	High	Low	Very Low
Flood plain	Locally variable	High	Moderate	Low	Very Low
Alluvial fan and plain	Widespread	Moderate	Low	Low	Very Low
Marine terraces and plains	Widespread	---	Low	Very Low	Very Low
Delta and fan-delta	Widespread	High	Moderate	Low	Very Low
Lacustrine and playa	Variable	High	Moderate	Low	Very Low
Colluvium	Variable	High	Moderate	Low	Very Low
Talus	Widespread	Low	Low	Very Low	Very Low
Dunes	Widespread	High	Moderate	Low	Very Low

Type of Deposit	General Distribution of Cohesionless Sediments in Deposits	Likelihood that Cohesionless Sediments when Saturated would be Susceptible to Liquefaction (by Age of Deposit)			
		< 500 yr Modern	Holocene < 11 ka	Pleistocene 11 ka – 2 Ma	Pre-Pleistocene > 2 Ma
Loess	Variable	High	High	High	Unknown
Glacial till	Variable	Low	Low	Very Low	Very Low
Tuff	Rare	Low	Low	Very Low	Very Low
Tephra	Widespread	High	High	?	?
Residual soils	Rare	Low	Low	Very Low	Very Low
Sebka	Locally variable	High	Moderate	Low	Very Low
(b) Coastal Zone					
Delta	Widespread	Very High	High	Low	Very Low
Estuarine	Locally variable	High	Moderate	Low	Very Low
Beach					
High Wave Energy	Widespread	Moderate	Low	Very Low	Very Low
Low Wave Energy	Widespread	High	Moderate	Low	Very Low
Lagoonal	Locally variable	High	Moderate	Low	Very Low
Fore shore	Locally variable	High	Moderate	Low	Very Low
(c) Artificial					
Uncompacted Fill	Variable	Very High	---	---	---
Compacted Fill	Variable	Low	---	---	---

Geomorphic map edited by GSB (2008) is used for this method. Moreover, it is required that artificial fill area is incorporated in the geomorphic map (refer to Figure 3-1), because these areas are high risk for the liquefaction hazard due to distribution of loose sand caused by uncompacted work and high groundwater level. These geomorphic units are corresponded with the deposit type and the geological age of Table 3-1 judged by results of the boring, AVS 30 conditions and so on, as shown in Table 3-2, and Figure 3-1 shows liquefaction susceptibility map in each city.

Table 3-2 Susceptibility for each Geomorphic Unit

[Dhaka]

Geomorphic Unit	Type of Deposit	Geological Age	Susceptibility
Meander Channel	River channel	Modern	Very High
Back Swamp	Flood plain	Holocene	Moderate
Swamp / Depression	Flood plain	Holocene	Moderate
Flood Plain	Flood plain	Holocene	Moderate
Shallow Alluvial Gully	Colluvium	Holocene	Moderate
Deep Alluvial Gully	Colluvium	Holocene	Moderate
Gully Head	Talus	Holocene	Low
Valley Fill	Colluvium	Holocene	Moderate
Channel Bar	Dunes / Delta and fan-delta	Modern	High
Point Bar	Dunes / Delta and fan-delta	Modern	High
Natural Levee	Dunes / Delta and fan-delta	Modern	High

Geomorphic Unit	Type of Deposit	Geological Age	Susceptibility
Lateral Bar	Dunes / Delta and fan-delta	Modern	High
Lower Modhupur Terrace	Residual soils	Pleistocene	Very Low
Upper Modhupur Terrace	Residual soils	Pleistocene	Very Low
Modhupur Slope	Talus	Modern	Low

[Chittagong]

Geomorphic Unit	Type of Deposit	Geological Age	Susceptibility
Depression	Flood plain	Holocene	Moderate
Sandy Beach	Beach - Low Wave Energy	Modern	High
Clayey Beach	Beach - High Wave Energy	Modern	Moderate
Lower Tidal Flat	Beach - Low Wave Energy	Holocene	Moderate
Estuarine Tidal Flat	Estuarine	Holocene	Moderate
Inter Tidal Flat	Beach - Low Wave Energy	Holocene	Moderate
Supra Tidal Flat	Beach - Low Wave Energy	Holocene	Moderate
Younger Point Bar	Dunes / Delta and fan-delta	Modern	High
Ancient Point Bar	Dunes / Delta and fan-delta	Holocene	Moderate
Natural Levee	Dunes / Delta and fan-delta	Modern	High
Sand Dune	Dunes	Modern	High
Gully Fill	Colluvium	Holocene	Moderate
Deep Valley Fill	Colluvium	Holocene	Moderate
Isolated Valley	Colluvium	Holocene	Moderate
River Tidal Flat	Flood plain	Holocene	Moderate
Fluvio Tidal Plain	Flood plain	Holocene	Moderate
Alluvial Fan	Flood plain	Holocene	Moderate
Piedmont Plain	Flood plain	Holocene	Moderate
Hill Slope	Talus	Holocene	Low
Level Hill	No liquefiable soil deposit	-	None
Rounded Top Highly Dissected Hill	No liquefiable soil deposit	-	None
Sharp Crest Highly Dissected Hill	No liquefiable soil deposit	-	None
Sharp Crest Slightly Dissected Hill	No liquefiable soil deposit	-	None

[Sylhet]

Geomorphic Unit	Type of Deposit	Geological Age	Susceptibility
Abandoned Channel	River channel	Holocene	High
Meander Scar	River channel	Holocene	High
Back Swamp	Flood plain	Holocene	Moderate
Swamp / Depression	Flood plain	Holocene	Moderate
Floodplain	Flood plain	Holocene	Moderate
Point Bar	Dunes / Delta and fan-delta	Modern	High
Natural Levee	Dunes / Delta and fan-delta	Modern	High
Lateral Bar	Dunes / Delta and fan-delta	Modern	High
Alluvial Fan	Flood plain	Holocene	Moderate
Gully Fill	Colluvium	Holocene	Moderate
Valley	Colluvium	Holocene	Moderate
Piedmont Plain	Flood plain	Holocene	Moderate
Level Hill	No liquefiable soil deposit	-	None
Ridge	No liquefiable soil deposit	-	None
Isolated Hills	No liquefiable soil deposit	-	None

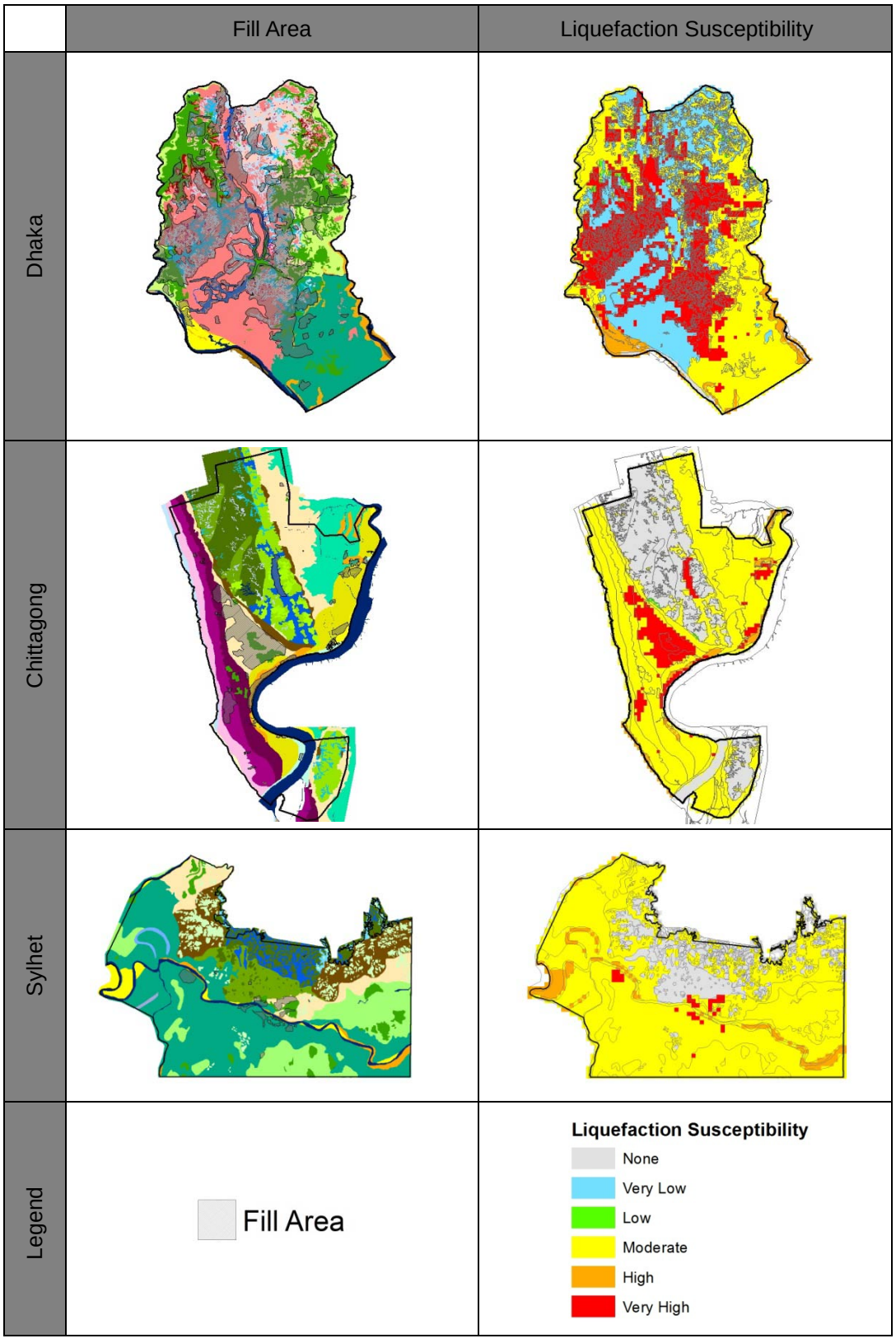

Figure 3-1 Geomorphic Map with Fill Area and Liquefaction Susceptibility in each City

3.1.3. Liquefaction Probability

(1) Procedure of Liquefaction Probability

Liquefaction probability is significantly influenced by ground shaking amplitude, such as PGA, an earthquake Mw, and groundwater depth. Thus, the probability of liquefaction for a given susceptibility category can be determined by the following equation.

$$P[Liquefactionx_{SC}] = \frac{P[Liquefaction_{SC}|PGA = a]}{K_M \cdot K_W} \cdot P_{ml}$$

Where,

$P[Liquefaction_{SC}|PGA=a]$: Conditional liquefaction probability for a given susceptibility category at a specified level of PGA (refer to Table-A and Figure-A)

Table-A Conditional Probability Relationship for Liquefaction Susceptibility Categories

Susceptibility Category	$P[Liquefaction_{SC}\|PGA=a]$
Very High	0 ≤ 9.09a – 0.82 ≤ 1.0
High	0 ≤ 7.67a – 0.92 ≤ 1.0
Moderate	0 ≤ 6.67a – 1.00 ≤ 1.0
Low	0 ≤ 5.57a – 1.18 ≤ 1.0
Very Low	0 ≤ 4.16a – 1.08 ≤ 1.0
None	0.0

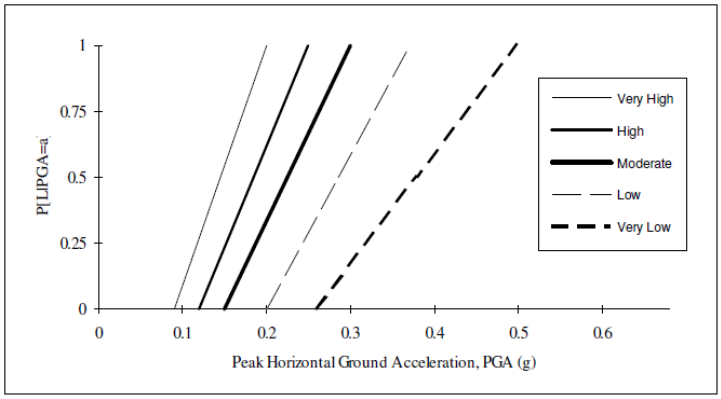

Figure-A Conditional Liquefaction Probability Relationships for Liquefaction Susceptibility Categories

(after Liao, et. al., 1988)

K_M: M_W correction factor other than M_W = 7.5 calculated by the following equation (refer to Figure-B)

$$K_M = 0.0027M_W^3 - 0.0267M_W^2 - 0.2055M_W + 2.9188$$

where

M_W: Moment magnitude of the seismic event

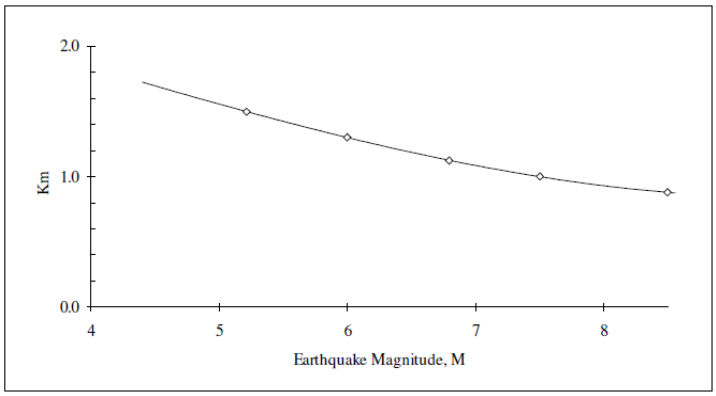

Figure-B Moment Magnitude (M) Correction Factor for Liquefaction Probability Relationships

(after Seed and Idriss, 1982)

K_W: Groundwater depth correction factor other than 5 feet calculated by the following equation (refer to Figure-C)

$$K_W = 0.022d_W + 0.93$$

where

d_w: Groundwater depth in feet

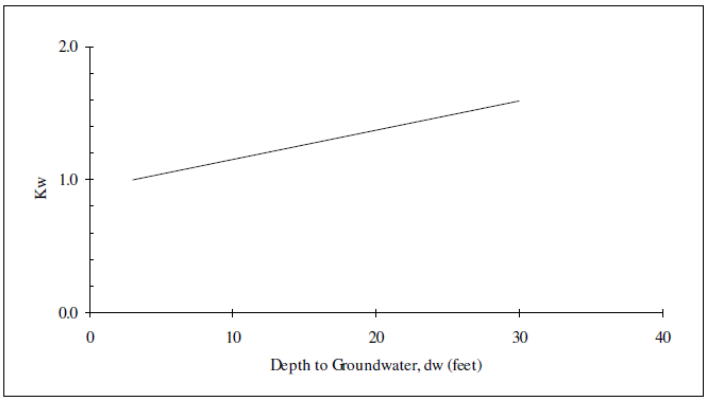

Figure-C Ground Water Depth Correction Factor for Liquefaction Probability Relationships

P_{ml}: Proportion of map unit susceptible to liquefaction (refer to Table-B)

Table-B Proportion of Map Unit Susceptible to Liquefaction

(after Power, et. al., 1982)

Mapped Relative Susceptibility	Proportion of Map Unit
Very High	0.25
High	0.20
Moderate	0.10
Low	0.05
Very Low	0.02
None	0.00

(2) Analysis Conditions

1) PGA

Estimated PGA based on 5 scenario earthquakes (refer to Section 2.3) is used for the calculation of the conditional liquefaction probability.

2) M_W

M_W of each scenario earthquake is estimated in this study (refer to the report of "Time-predictable Fault Modeling"), as shown in Table 3-3.

Table 3-3 Estimated Moment Magnitude of 5 Scenario Earthquakes

Segment	Estimated Moment Magnitude: M_W
Modhupur Fault (MF)	7.5
Dauki Fault (DF	8.0
Plate Boundary Fault 1 (PBF-1)	8.5
Plate Boundary Fault 2 (PBF-2)	8.0
Plate Boundary Fault 3 (PBF-3)	8.3

3) Groundwater Depth

Surface groundwater level (mostly unconfined groundwater level) is required for the liquefaction potential analysis. However, almost existing groundwater observation wells in each city have monitored water level / quality of the deep aquifer such as Dupitila formation. Therefore, it is difficult to get the required groundwater level so far, and a qualitative estimation of the level is adopted in this analysis.

Normal groundwater level for the correction factor is 5 feet. In rainy season, groundwater depth of subsurface ground (Fill or Holocene soil) is basically close to ground surface in wide area of plane site in 3 cities, and this conditions lead to be high risk of liquefaction. Thus, groundwater depth is set on 5 feet in this study on viewpoint from risky side of liquefaction occurrence.

(3) Liquefaction Probability

Based on the above analysis conditions, liquefaction probability is estimated in each city as shown in Figure 3-2 to Figure 3-4.

Generally, adopted method needs to be verified by historical liquefaction record. However, evidently compiled materials / documents including M_w of an earthquake, PGA and groundwater conditions has not been presented in 3 cities so far. It is noted

that this results / calculated value should not be treated as an absolute judgment. Therefore, the calculated value makes demarcations according to rank, from 1 (very low) to 5 (very high) and none (no distribution of saturated soft soil), as a relative evaluation. Threshold of each rank from 1 to 5 are set as less than 0.05, 0.10, 0.15, 0.20 and equal to / more than 0.20, respectively.

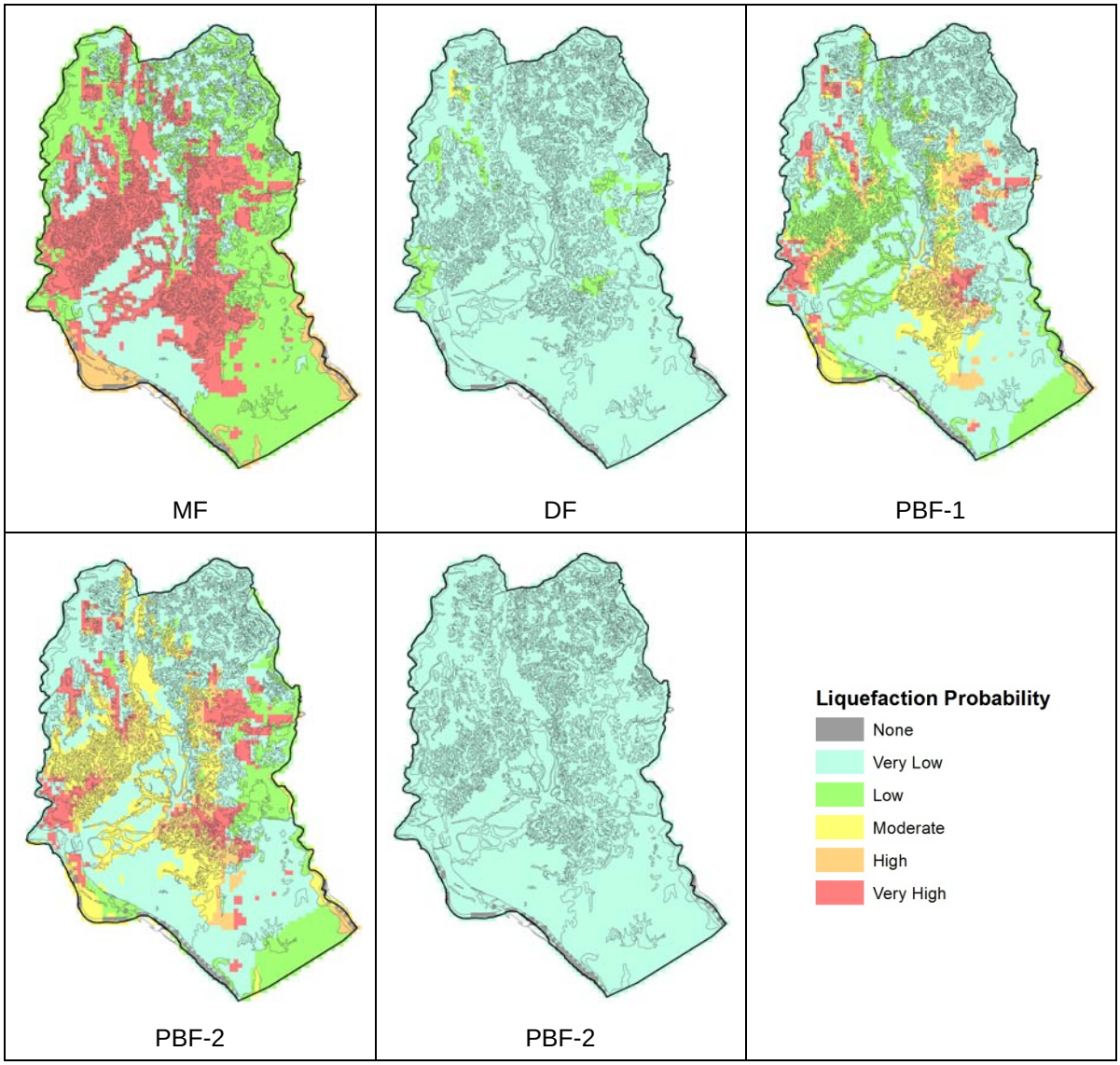

Figure 3-2 Liquefaction Probability for 5 Scenario Earthquakes in Dhaka

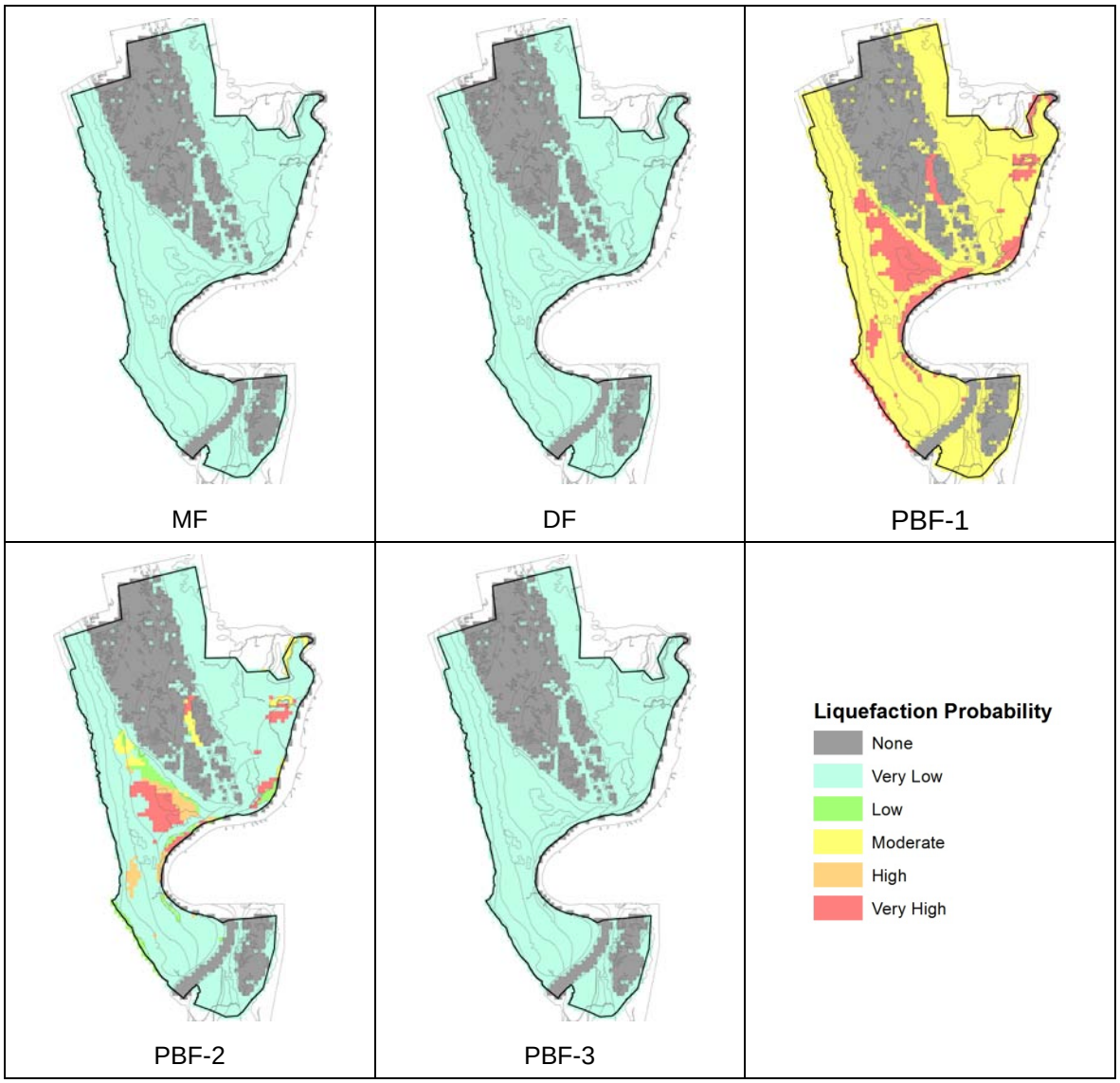

Figure 3-3 Liquefaction Probability for 5 Scenario Earthquakes in Chittagong

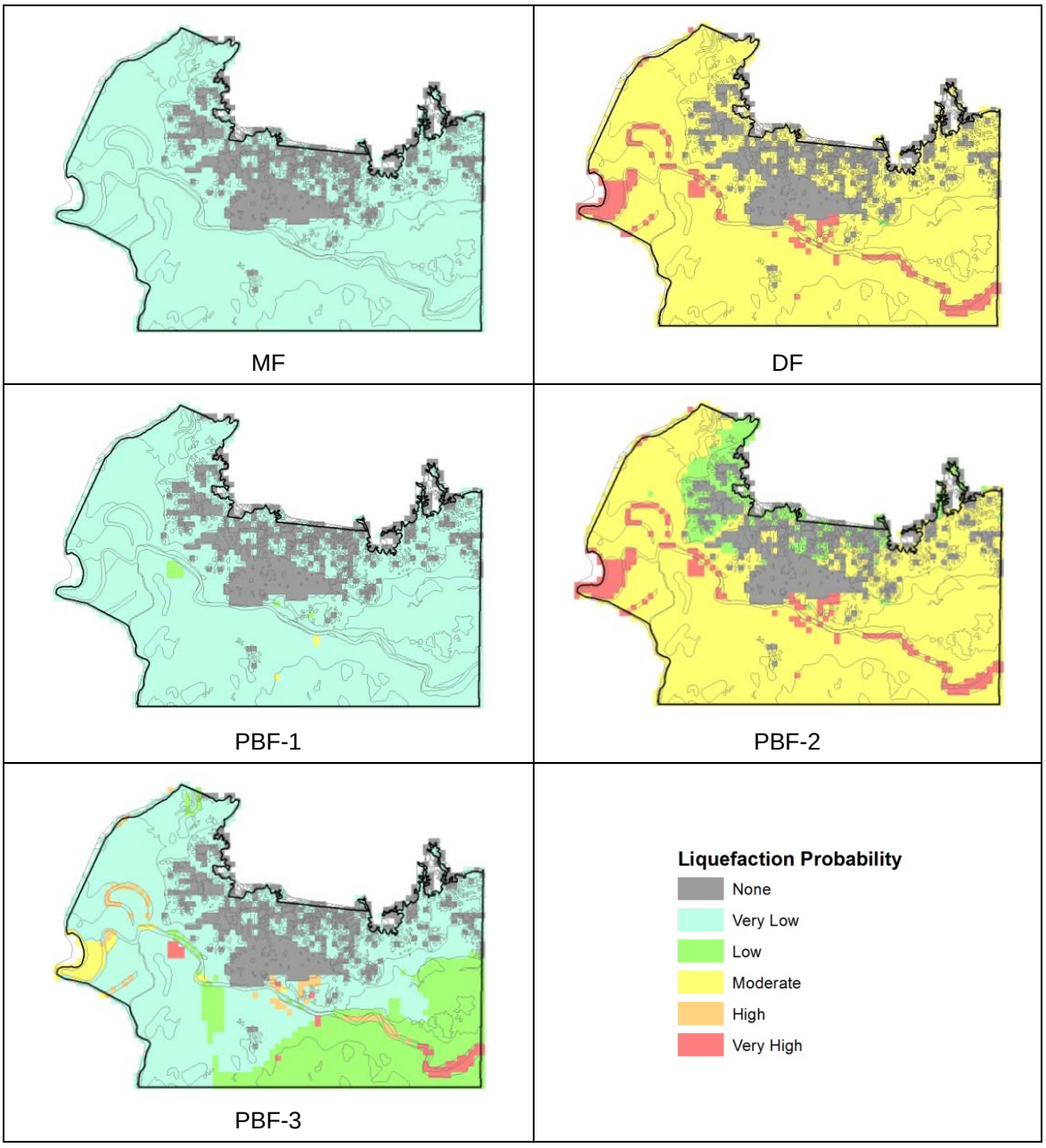

Figure 3-4 Liquefaction Probability for 5 Scenario Earthquakes in Sylhet

3.2. Slope Failure Analysis

3.2.1. Outline

Considering slope failure during the scenario earthquakes, the following four steps are carried out.

(1) The slope angle distribution was analyzed from 50m spacing DEM (Digital Elevation Model) produced in this project. Considering more than 30 degrees of slope angle as high risk, the distribution maps of frequency of such angles per one grid is adopted as susceptibility map.

(2) The properties of weathered rock were estimated by the laboratory tests of this project.

(3) To estimate the slope hazards following earthquakes such as slope failure, two different methods are applied for the evaluation. One is Wilson et al. (1979) and the other is Koppula (1984).

3.2.2. Methodology

Considering the situations in the target area regarding to slope failures, the Wilson's method is applied to mainly surface failure which usually occurs at steep slopes of the sandy layers, and the Koppula's method is applied to creep type slope failure which may occur even in the gentle slope for the clayey layers.

(1) Method by Wilson et al. (1979)

Wilson et al. (1979) assumed that in a surface thin layer, as shown in Figure 3-5, sliding occurs due to inertial loading. Equation of sliding and resisting forces is given as follows:

$$ac = g\left[\frac{C}{\gamma h} + (\cos\theta\tan\phi - \sin\theta)\right] \quad \text{.....(3.1)}$$

where

ac: critical horizontal acceleration including the slide
g: acceleration of gravity
C: cohesion of soil
γ: unit weight of soil
h: thickness of the sliding layer
θ: angle of slope
ϕ: internal friction angle of the layer

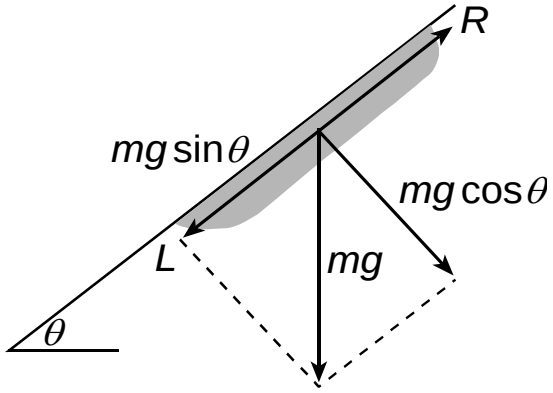

[after Tanaka, 1982]

Figure 3-5 Model of Potential Landslide Mass for Wilson Method

Given the distribution of slope angle (θ), the strength parameter C, ϕ, and horizontal acceleration, the estimation of the distribution of slope vulnerability can be made.

(2) Method by Koppula (1984)

The method originally proposed by Kioppula (1984) was a pseudo-static evaluation of slope stability utilizing a seismic coefficient A to account for the earthquake induced horizontal forces. The variation in shear strength (C) with depth is assumed to be linear, and the potential failure surface is taken as a circular arc (radius: R) as shown in Figure 3-6.

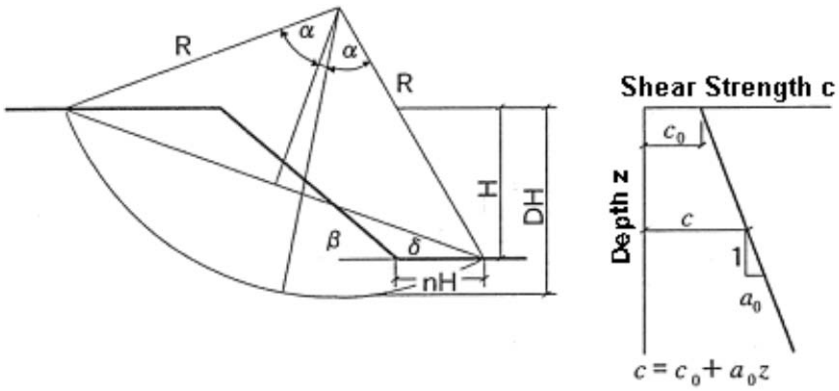

(after Koppula, 1984)

Figure 3-6 Typical Profile of Slope for Koppula Method

Parameters α, β, δ, and n are related to the geometry of the slope and the configuration of the sliding surface. As given below, the safety factor, Fs, can be defined:

$$Fs = \frac{a_0}{\gamma} N_1 + \frac{C_0}{\gamma H} N_2 \quad \text{.....(3.2)}$$

where,

$$a_0 = \gamma \tan \phi$$

$$N_1 = \frac{3(\alpha + \cot\delta - \alpha \cot\alpha \cot\delta)}{\sin^2\alpha \cdot \sin^2\delta (D_1 + D_2)}$$

$$N_2 = \frac{6\alpha}{\sin^2\alpha \cdot \sin^2\delta (D_1 + D_2)}$$

$$D_1 = 1 - 2\cot^2\beta - 3\cot\alpha\cot\beta + 3\cot\beta\cot\delta + 3\cot\delta\cot\alpha - 6n\cot\beta - 6n^2 - 6n\cot\alpha + 6n\cot\delta$$

$$D_2 = A(\cot\beta + \cot^3\delta + 3\cot\alpha\cot^2\delta - 3\cot\alpha\cot\beta\cot\delta - 6n\cot\alpha\cot\delta)$$

A (seismic coefficient) = *PGA* (peak ground acceleration)/ *g* (acceleration of gravity)/3.0

In this report, a linear variation with depth is assumed regarding the shear strength (C) of normally consolidated soils as the following:

$$C = a_0 \cdot z + C_0 \quad \text{.....(3.3)}$$

To simplify the slope, H defined as the slope height (see Figure 3-7)

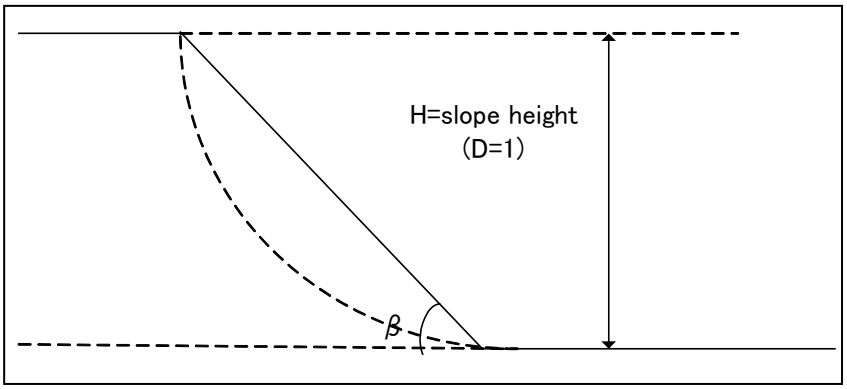

Figure 3-7 Definition of *H*

Generally, for sandy soil, its cohesion coefficient *C* is small and usually nearly 0, and friction angle ϕ has exact value and ϕ is usually around 30 degrees. On the other hand for clayey soil, its property *C* has exact value, and ϕ is usually very small, nearly 0 degree.

Then, in case of pure sandy soil, the equation (3.2) is estimated as $Fs = \frac{a_0}{\gamma} N_1$

In case of pure clayey soil, the equation (3.2) is estimated as $Fs = \frac{C_0}{\gamma H} N_2$

Thus, the safety factor depends on friction angle ϕ, shear strength C and stability numbers N_1, N_2, representing the configuration of the slope and failure surface. The minimum values of the stability numbers are determined by carrying out a parametric study in terms of α, δ and n (see Figure 3-6) to find the most critical failure surface. The variation of minimum N_1, N_2 can be expressed as a function of β (slope angle) and A (seismic coefficient). It becomes possible at this stage to calculate the minimum safety factor Fs using Figure 3-8 and Figure 3-9, if ϕ and C_0 can be determined.

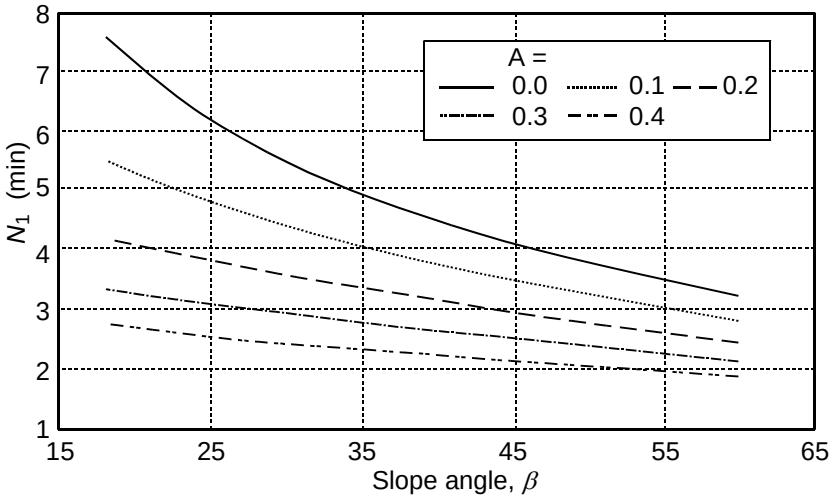

(after Koppula, 1984)

Figure 3-8 Variation of N_1 (min)

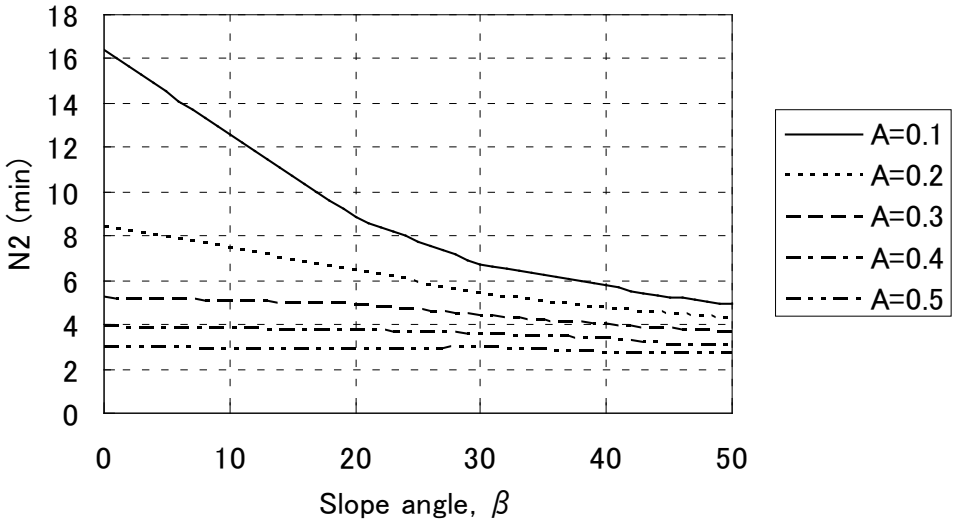

(after Koppula,1984)

Figure 3-9 Variation of N_2 (min)

3.2.3. Slope Hazard Susceptibility

(1) Distribution of Slope Angles

In order to examine slope angle distribution in the area, 50m spacing DEM (Digital Elevation Model) was produced using published maps (Dhaka: 1/2,000 topographic map, Chittagong: 10,000 topographic map) and satellite images (Sylhet) in this project. The slope angle was calculated as the maximum value which is surrounded in the eight directions. Since this slope angles may have the possibility of being gentler than real slope angle, they are converted to the one with using half distant unit space, i.e. 25 m.

Figure 3-10 to Figure 3-12 shows the slope angle distribution in each city. And Table 3-4 shows the average and maximum angles. 15 degrees in Dhaka, 64 degrees in Chittagong and 58 degrees in Sylhet are the maximum.

Table 3-4 Data of Slope Angle

City	Average Slope Angle (degrees)	Maximum Slope Angle (degrees)	Calculated Data Number
Dhaka	0.42	14.92	199,060
Chittagong	2.40	64.39	180,236
Sylhet	2.57	57.98	116,624

(2) Slope hazard susceptibility estimation

Each grid of 250 m square has 25 values of angles. Then, Figure 3-13 to Figure 3-15 show the frequency of more than 30 degrees of the slope angle per one grid in each city. There are no such steep angles in Dhaka, but about 1 % is steep and susceptible in both Chittagong and Sylhet.

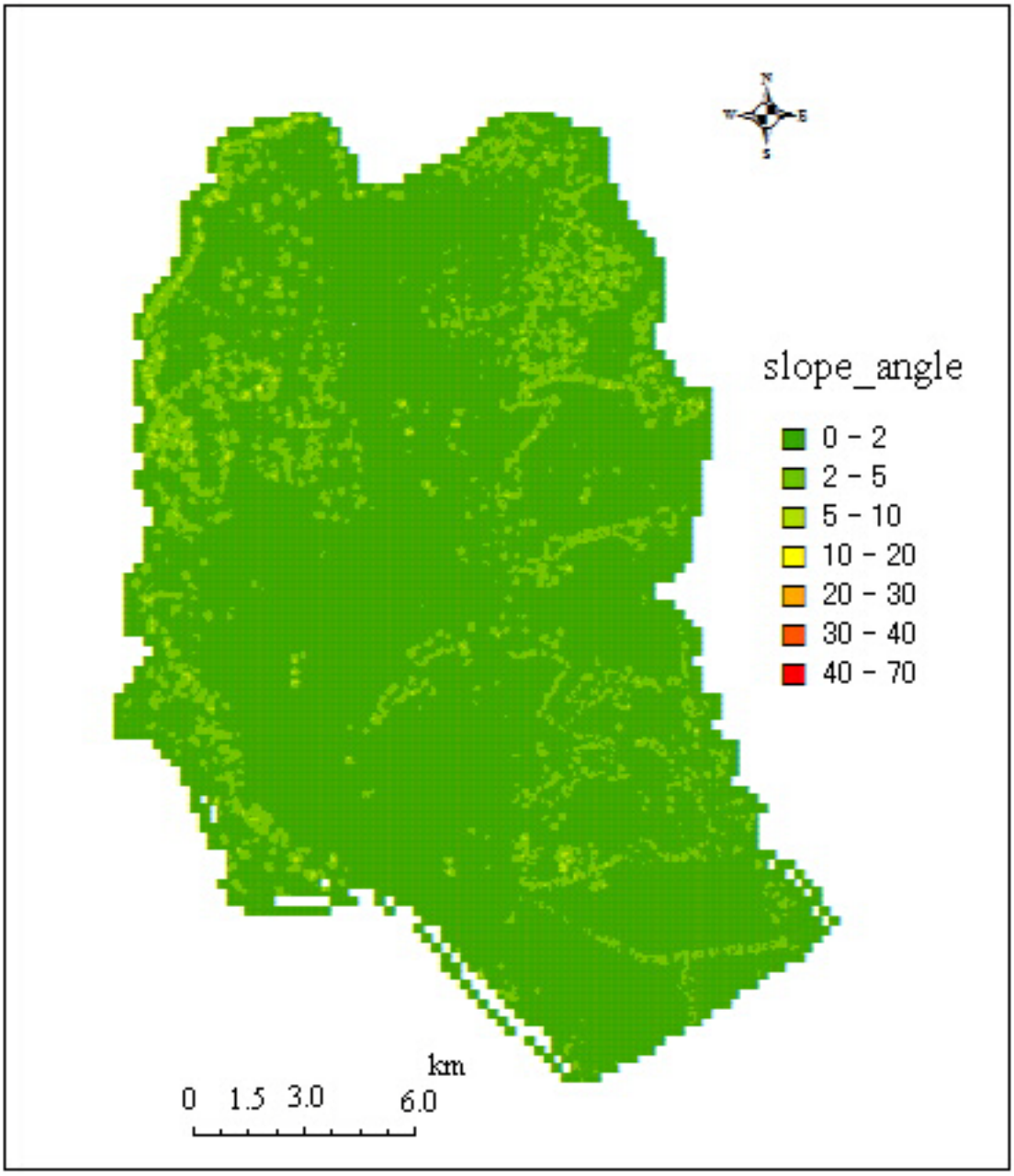

Figure 3-10 Distribution of Slope Angle in Dhaka City

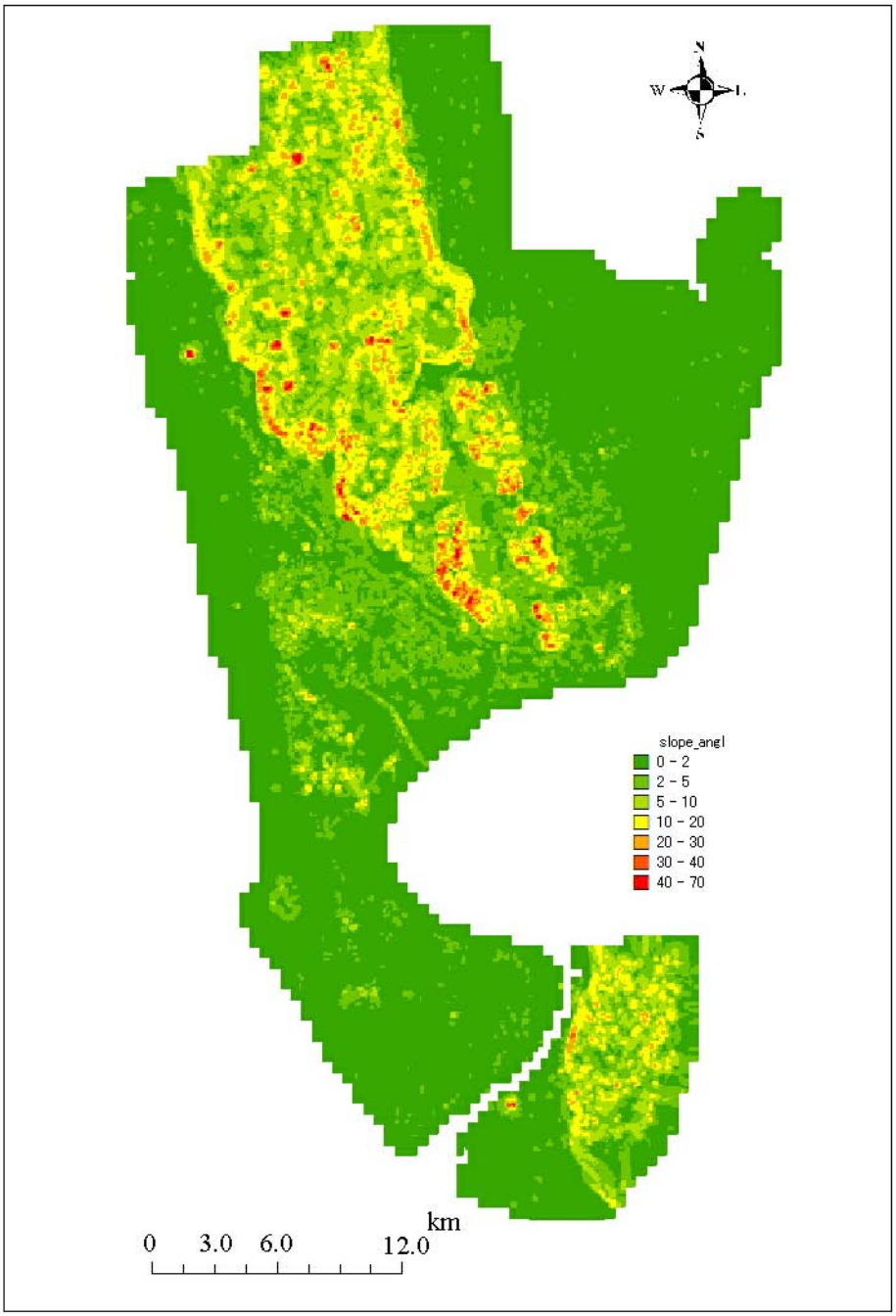

Figure 3-11 Distribution of Slope Angle in Chittagong City

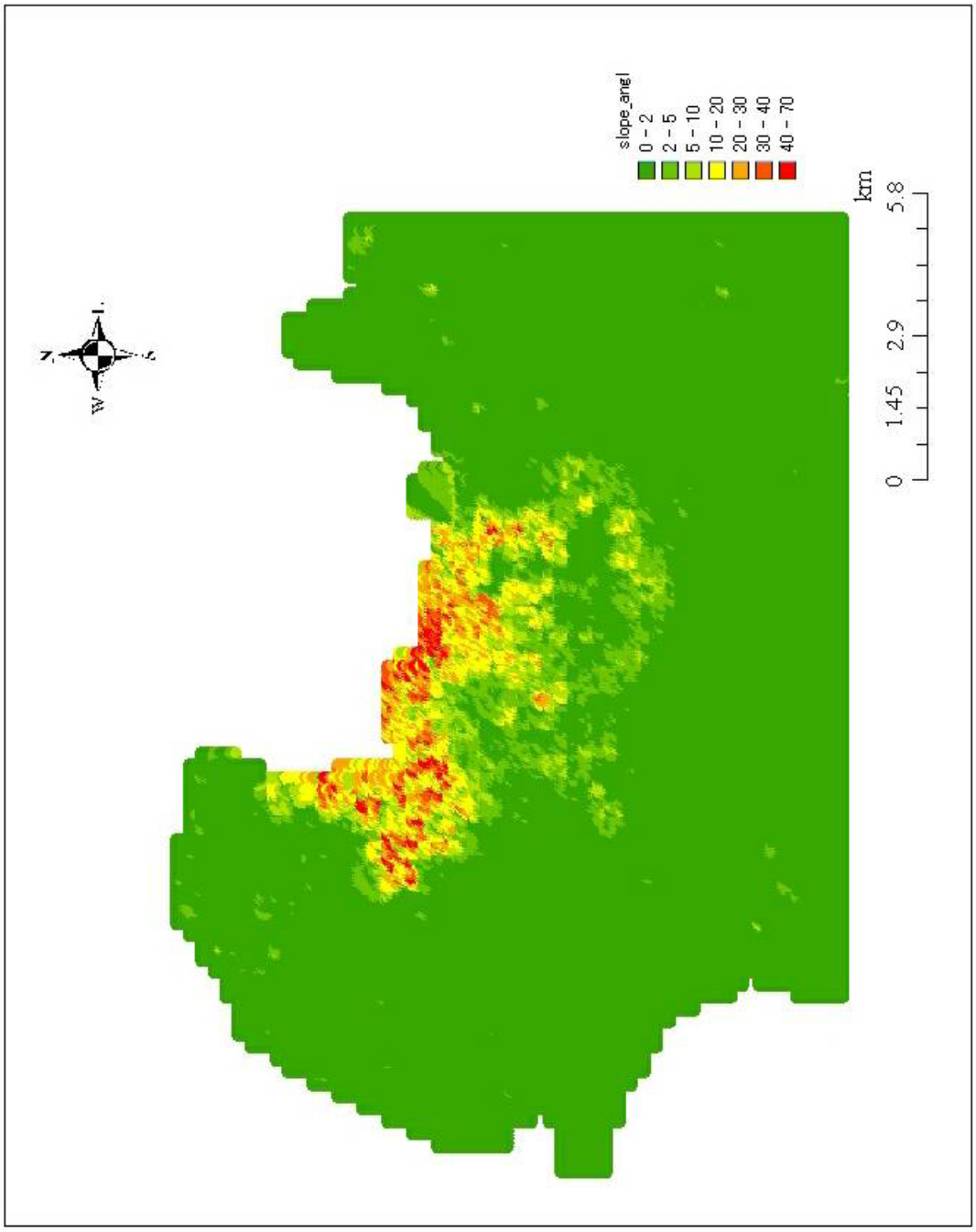

Figure 3-12 Distribution of Slope Angle in Sylhet City

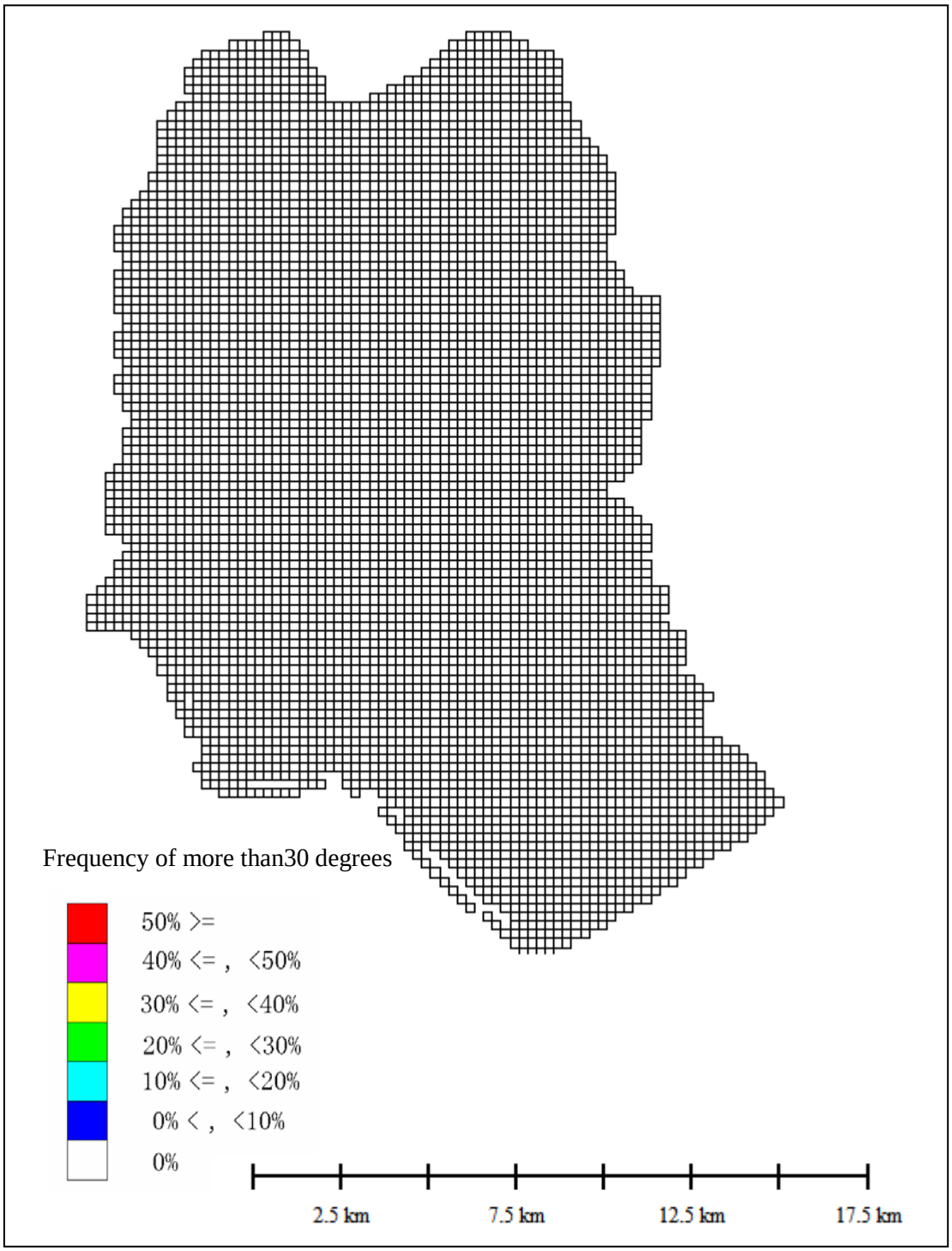

Figure 3-13 Frequency of more than 30 Degrees of the Slope Angle per One Grid in Dhaka

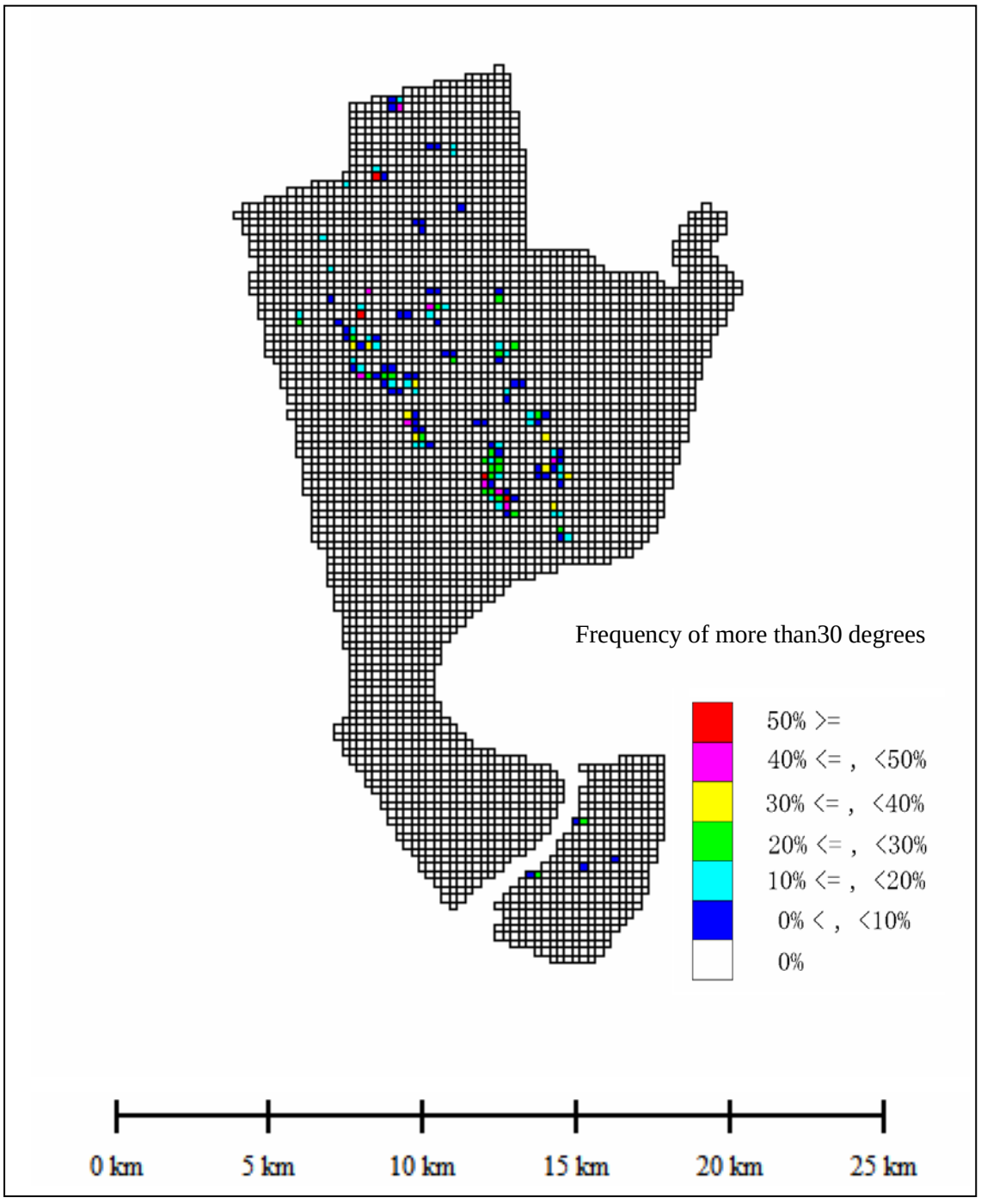

Figure 3-14 Frequency of more than 30 Degrees of the Slope Angle per One Grid in Chittagong

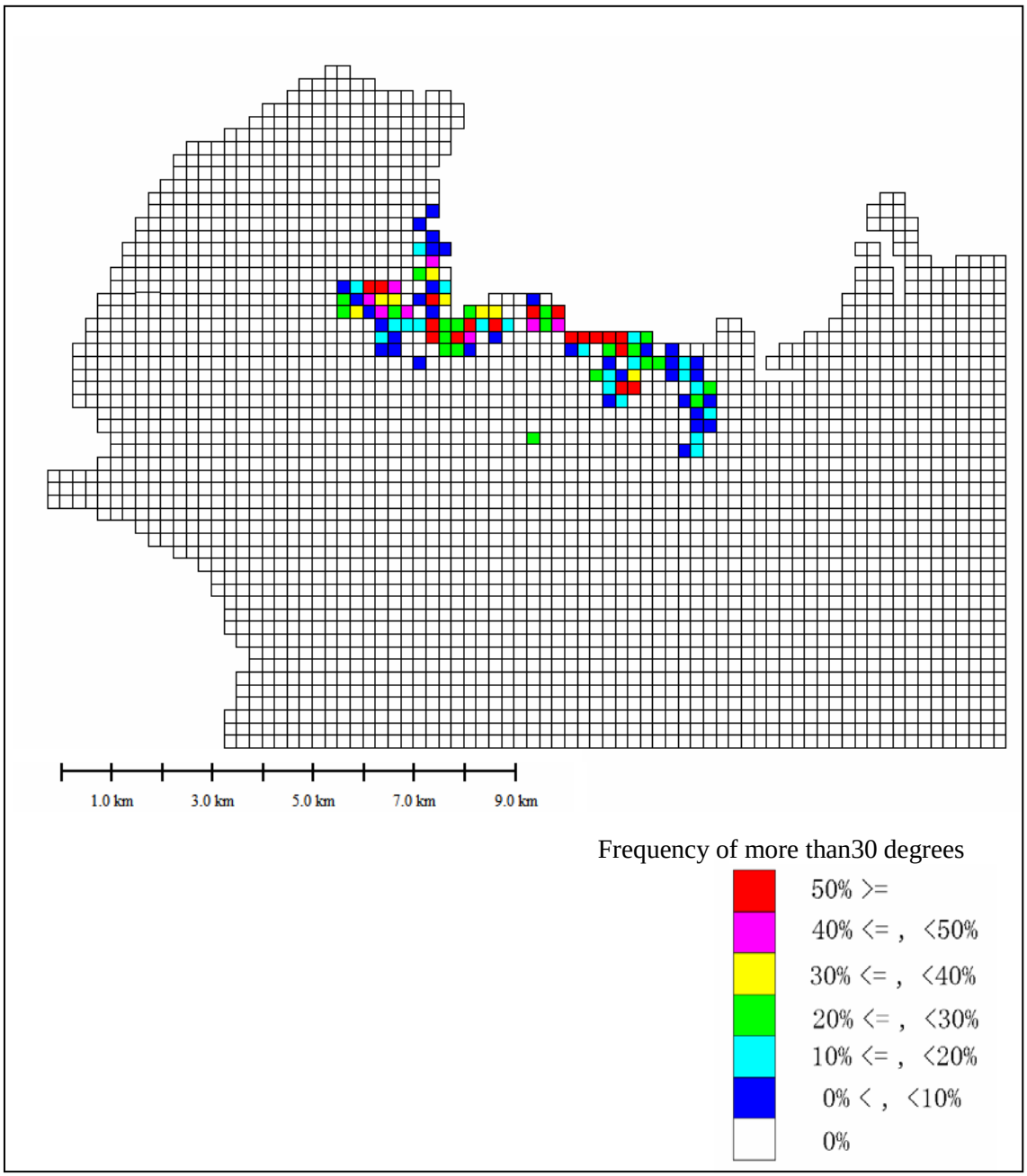

Figure 3-15 Frequency of more than 30 Degrees of the Slope Angle per One Grid in Sylhet

3.2.4. Slope Hazard Probability

(1) *C* and ϕ (Soil Properties)

The soil properties of *C* (cohesion coefficient: shear strength) and ϕ (friction angle) are necessary parameters for conduction of the slope stability analysis. In this project, several laboratory tests were carried out to estimate *C* and ϕ. In Table 3-5, the reliable laboratory test results for surface soils such as shallower depth less than 7m were shown. In general, the shallow layer is weak and soft, and these kinds of soils will likely be collapsed following earthquakes. Since these data are in the range of typical properties of soil, the selection from them will be reasonable. Thus the representative values are adopted c=0.25 kgf/cm^2 and ϕ = 12.5, as the round value of the average. These data are the similar to the data of Dhk_30. Then, for density value, 1.94 g/cm^3 is adopted considering the vulnerability of stability.

Table 3-5 Summary of the selected Laboratory Test Results for *C*, ϕ and Density

BH	From	To	GC	N	C		Ø	density
No	(m)	(m)	symbol		Psi	kgf/cm2		g / cm3
Ctg_29	4.5	4.95	H-C	8	4.05	0.28	12.02	1.94
Ctg_32	6	6.45	H-C	4	4.12	0.29	9.54	1.93
Dhk_30	6	6.45	H-C	3	3.6	0.25	12.59	1.7
Dhk_31	4.5	4.95	H-C	4	4.2	0.3	12.02	
Dhk_34	4.5	4.95	H-C	2	4	0.28	20.26	1.8
Dhk_37	6	6.45	H-C	14	3.99	0.28	8.09	
Syl_37	4	4.4	H-S	10	1.94	0.14	11.29	
Syl_38	3	3.65	H-S	9	2.06	0.14	14.61	

(2) Estimation of Slope Hazard Probability

Slope failures are examined by both Wilson's method and Koppula's method. The two methods require the parameter of soil properties (*C*, ϕ and density) and *PGA*. *PGA* distributions due to the 5 scenario earthquakes were estimated in the section 2.3.

By the way, if the above soil parameters are applied, stability factor (*Fs)* becomes less than 1.0, when slope angle exceeds more than 45 degrees. And when Fs = 1.2, the critical slope angle is 60 degrees. This is reasonable for the current existing situation of slope angles in the three target cities. Thus, *Fs=1.2* is adopted for the following estimation.

Figure 3-16 and Figure 3-17 show the slope failure probability in Dhaka. Figure 3-18 and Figure 3-19 show the slope failure probability in Chittagong. Figure 3-20 and Figure 3-21 show the slope failure probability in Sylhet. In other word, Figure 3-16, Figure 3-18 and Figure 3-20 are examined by Wilson's method. Figure 3-17, Figure 3-19 and Figure 3-21 are examined by Koppula's method.

According to these figures, the results by Koppla's method show similar to potential or susceptibility. Therefore, more detailed study for each slope for landslide is necessary in the future. On the other hand the results by Wilson's method show the probability variation reasonably according to the *PGA's* variation. The probabilities of slope failures are expected in the hilly or mountainous area in Chittagong and in Sylhet. It is clear when the *PGA* is larger, the *Fs* is smaller, and the slope angle is steeper, the slope failure is expected even if *PGA* is smaller. For Dhaka, no probability, but in Chittagong, PBF-1 earthquake is the highest, and for Sylhet, DF and PBF-2 are higher probability.

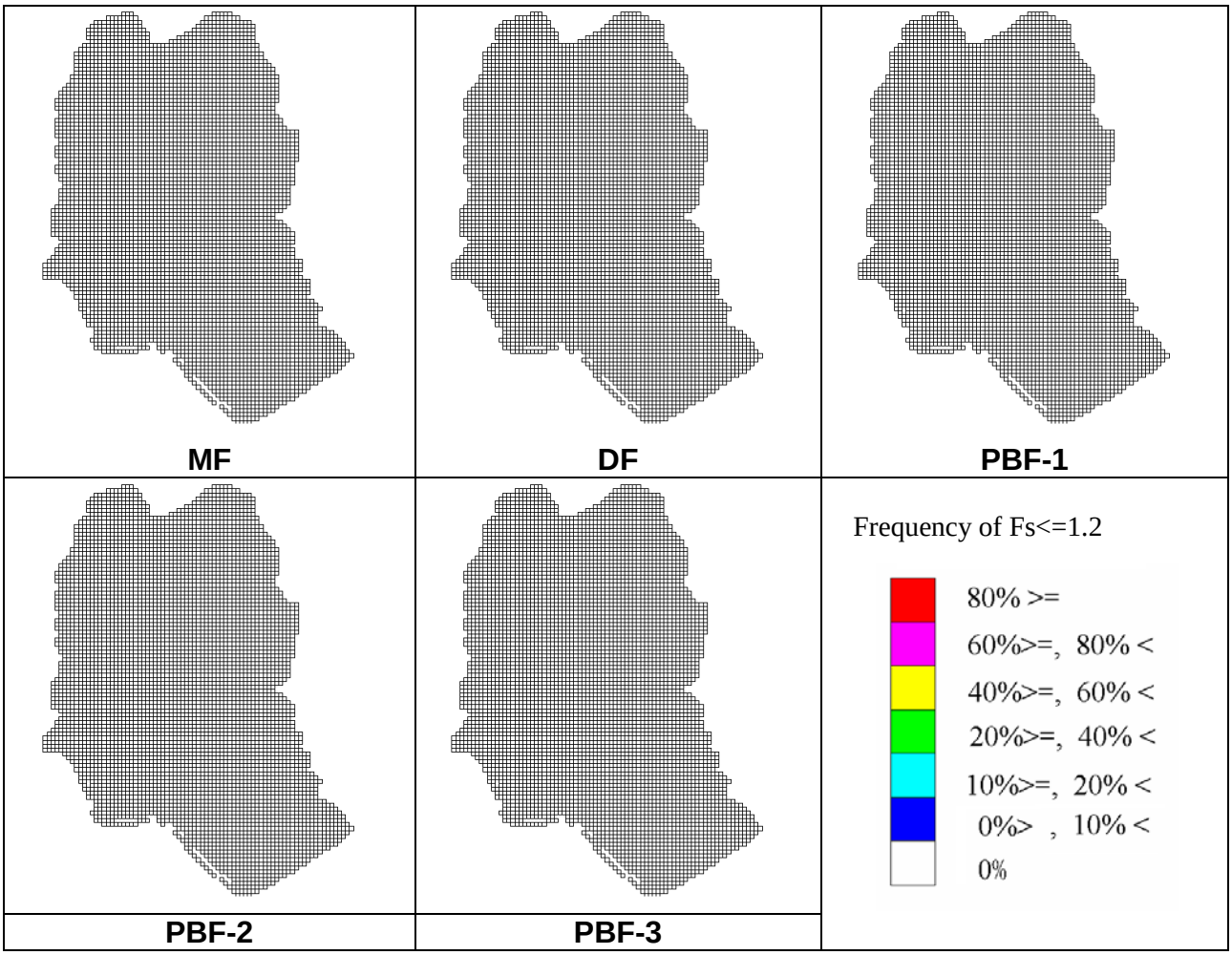

Figure 3-16 The Frequency of Fs<=1.2 by Wilson's Method in Dhaka

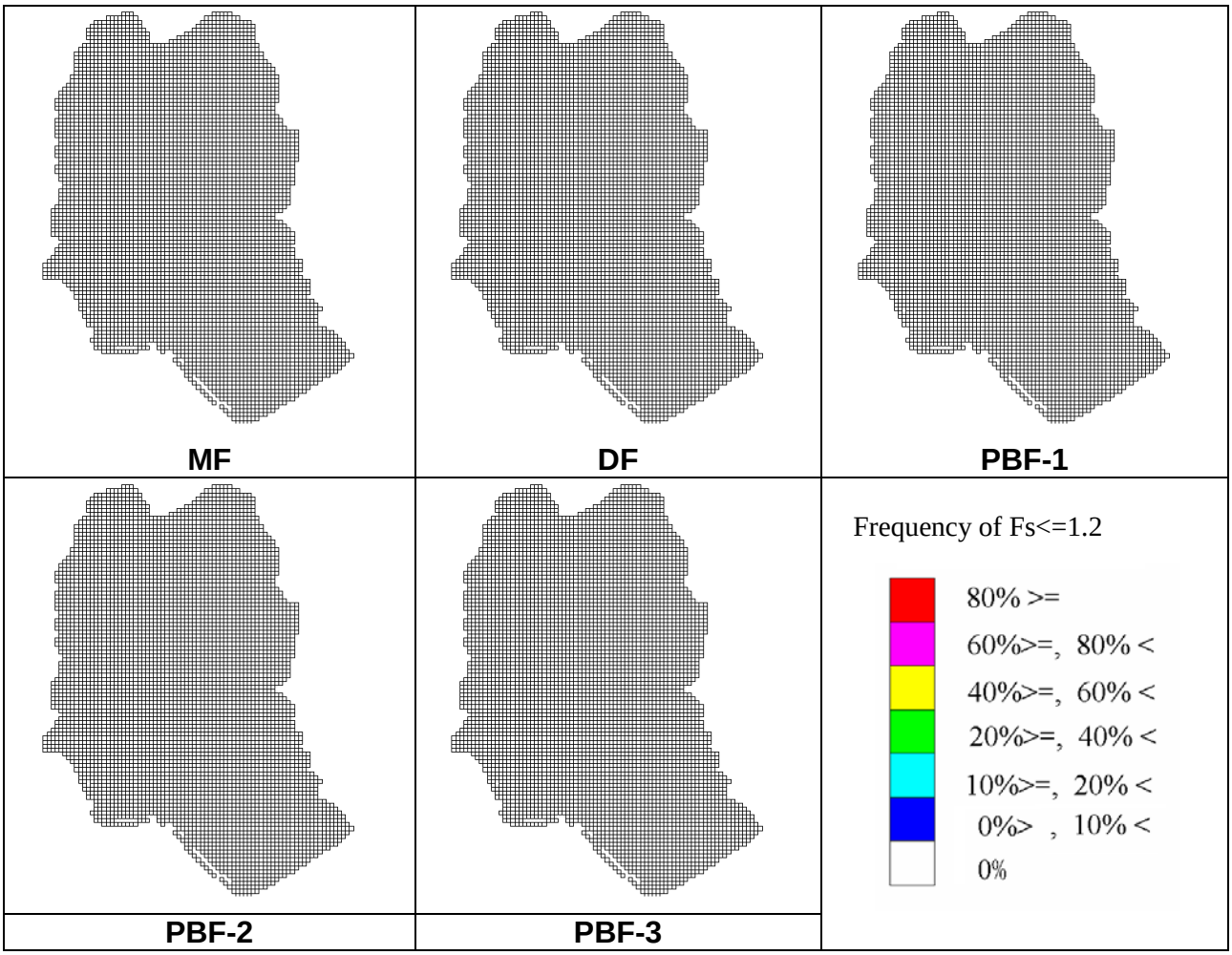

Figure 3-17 The Frequency of Fs<=1.2 by Koppula's Method in Dhaka

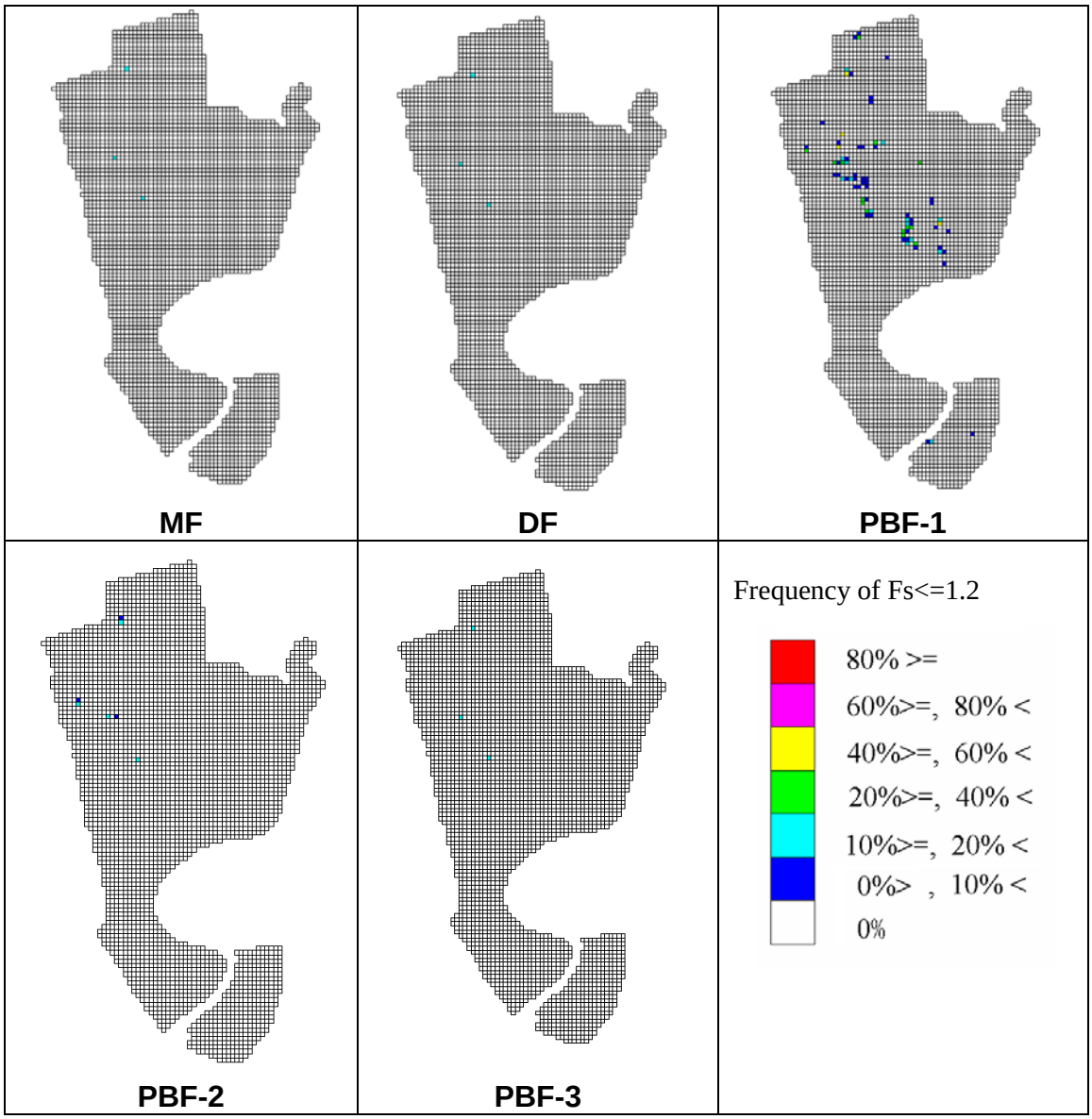

Figure 3-18 The Frequency of Fs<=1.2 by Wilson's Method in Chittagong

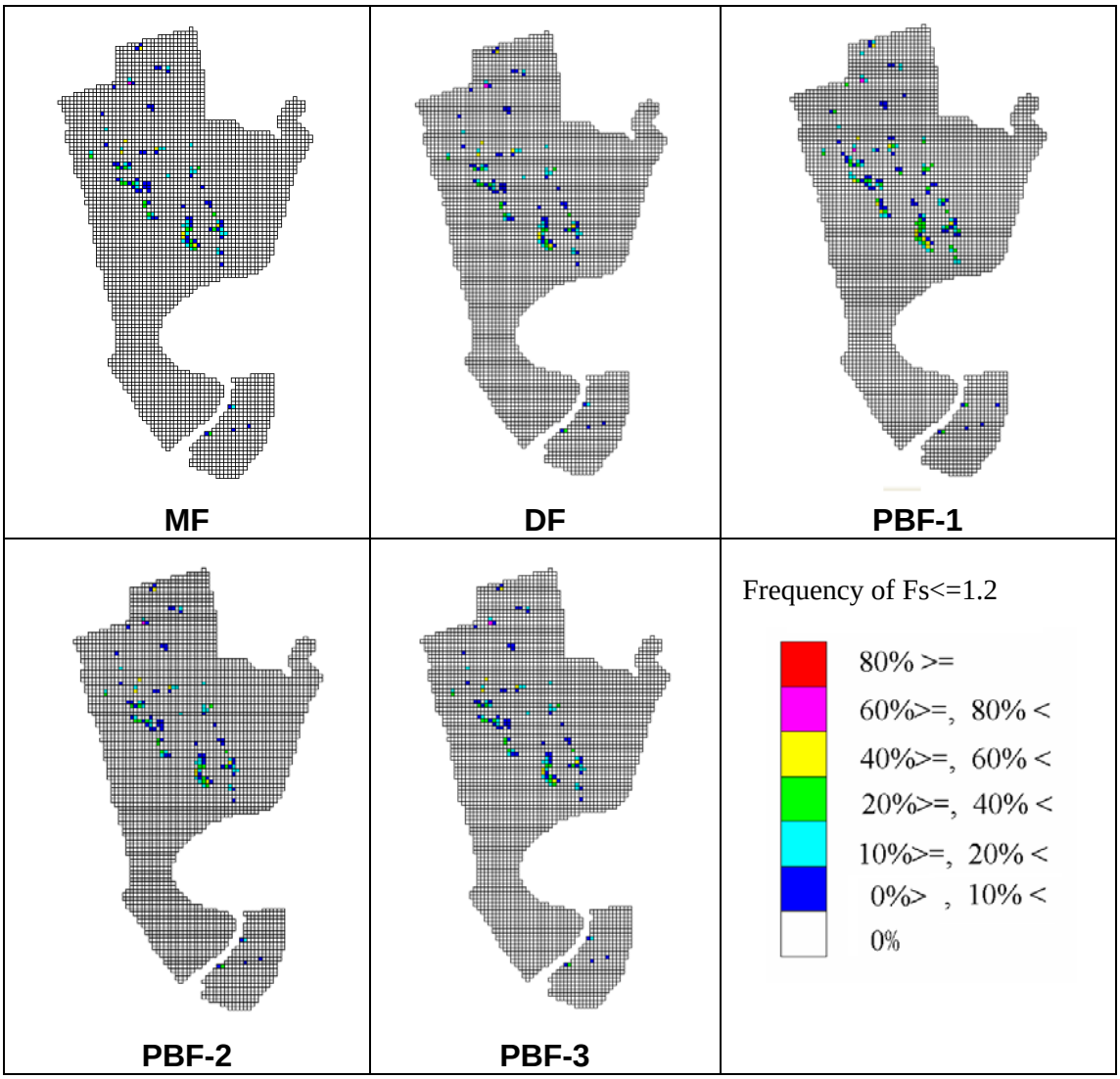

Figure 3-19 The Frequency of Fs<=1.2 by Koppula's Method in Chittagong

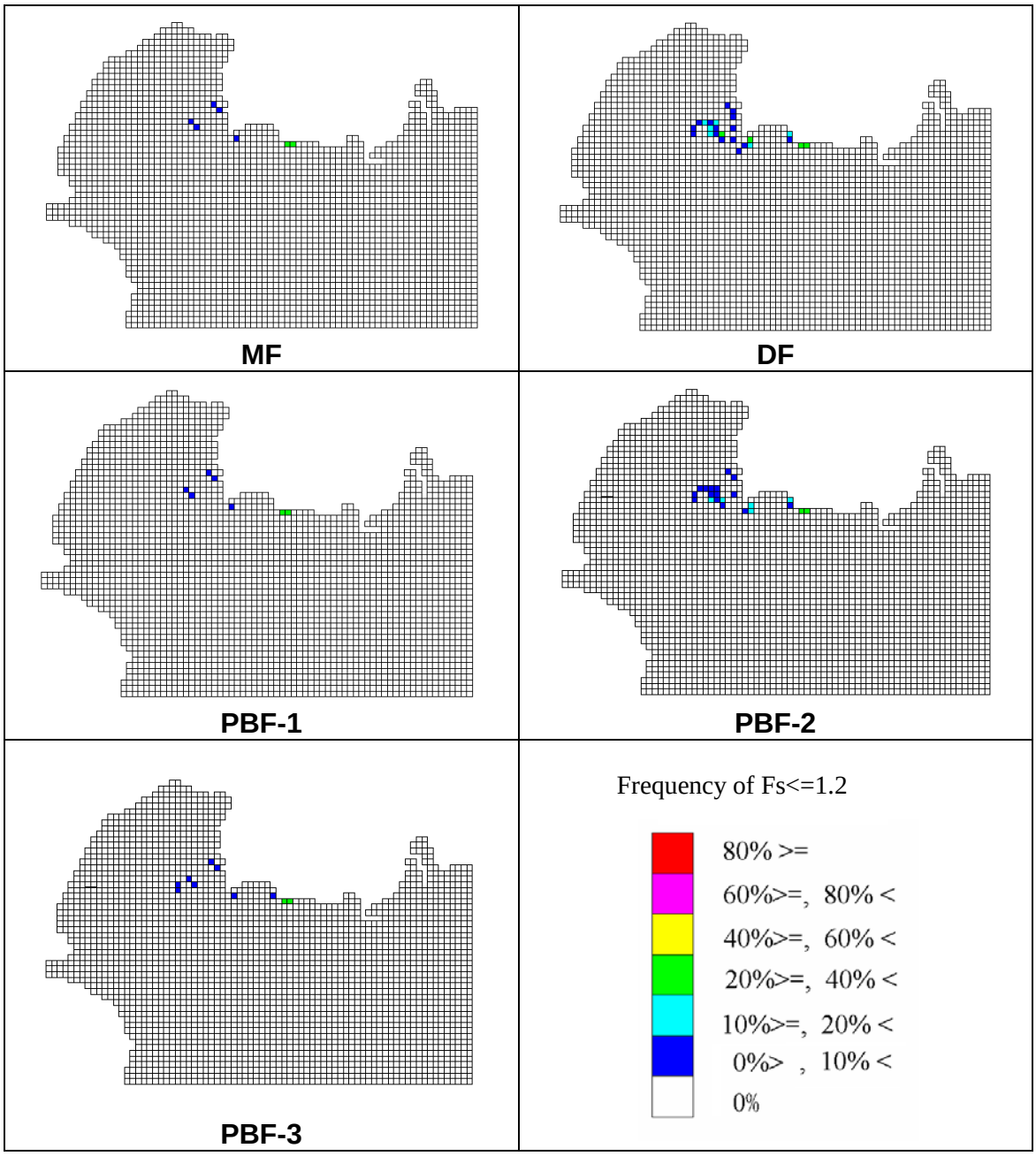

Figure 3-20 The Frequency of Fs<=1.2 by Wilson's Method in Sylhet

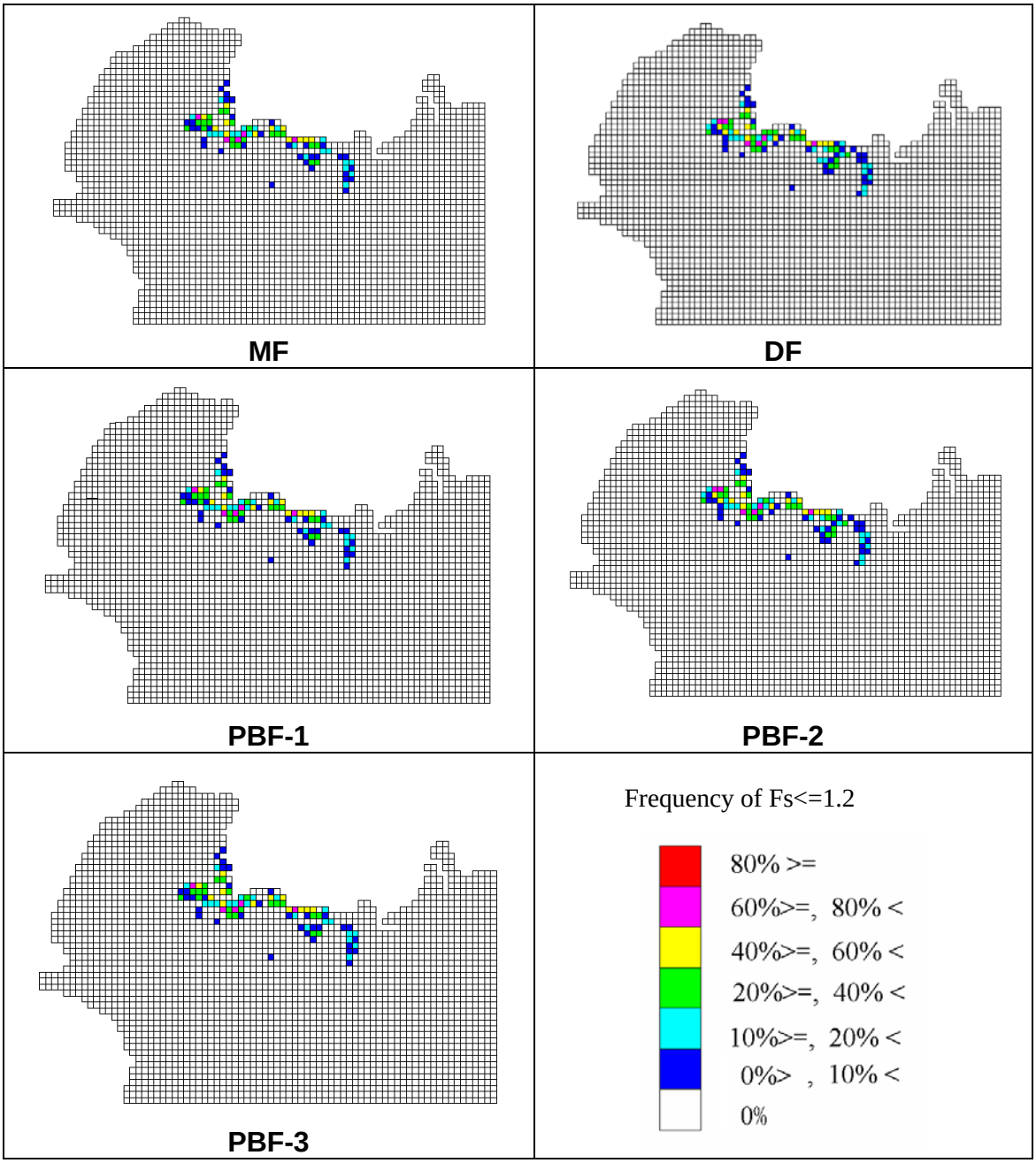

Figure 3-21 The Frequency of Fs<=1.2 by Koppula's Method in Sylhet

References

[Chapter 1]

Abrahamson N. and W. Silva, 2008, Summary of the Abrahamson & Silva NGA Ground-Motion Relations, Earthquake Spectra, Vol. 24, Issue 1, pp. 67-97.

Atkinson G. M. and D. M. Boore, 2003, Empirical Ground-Motion Relations for Subduction-Zone Earthquakes and Their Application to Cascadia and Other Regions, Bull. Seism. Soc. Amer., Vol. 93, No. 4, 1703-1729.

Boore D. M. and G. M. Atkinson, 2008, Ground-Motion Prediction Equations for the Average Horizontal Component of PGA, PGV, and 5%-Damped PSA at Spectral Periods between 0.01 s and 10.0 s, Earthquake Spectra, Vol. 24, Issue 1, pp. 99-138.

Boore, D. M., 1983, Stochastic simulation of high-frequency ground motions based on seismological models of the radiated spectra, Bull. Seism. Soc. Amer., Vol. 73, No. 6, 1865-1894.

Campbell K. W. and Y. Bozorgnia, 2008, NGA Ground Motion Model for the Geometric Mean Horizontal Component of PGA, PGV, PGD and 5% Damped Linear Elastic Response Spectra for Periods Ranging from 0.01 to 10 s, Earthquake Spectra, Vol. 24, Issue 1, pp. 139-171.

Chiou B. S.-J. and R. R. Youngs, 2008, An NGA Model for the Average Horizontal Component of Peak Ground Motion and Response Spectra, Earthquake Spectra, Vol. 24, Issue 1, pp. 173-215.

Gardner, J. K. and L. Knopoff, 1974, Is the sequence of earthquake in Southern California, with aftershocks removed, Poissonian, Bull. Seism. Soc. Amer., 64, 1363 - 1367.

Irikura, K., 1986, Prediction of Strong Acceleration Motion Using Empirical Green's Function, Proc. 7th Japan Earthq. Symp., 151-156.

Kamae, K., K. Irikura and Y. Fukuchi, 1991, Strong Motion Prediction during Large Earthquake based on the Scaling Law of the Earthquake, J. Struct. Constr. Eng., AIJ, No. 430, 1-9.

Parvez, I. A., F. Vaccan and G. F. Panza,2003, A Deterministic Seismic Hazard map of India and Adjacent areas, Geophysical Journal International, Vol. 155, pp. 489-508.

Weichert, D.H., 1980, Estimation of the earthquake recurrence parameters for unequal observation periods for different magnitudes, Bull. Seism. Soc. Amer., Vol. 70, No. 4, 1337-1346.

[Chapter 2]

Cabinet Office of Japan, 2003, http://www.cao.go.jp/.

Midorikawa S., M. Matsuoka and K. Sakugawa, 1994, Site Effects on Strong-Motion Records Observed During the 1987 Chhiba-Ken-Toho-Oki, Japan Earthquake, Proc. 9th Japan Earthq. Eng. Symp., E-085 - E-090.

[Chapter 3]

- Section 3.1

Liao, S. S., Veneziao, D., and R. V. Whitman, 1988. Regression Models for Evaluationg Liquefaction Probability, Journal of Geotechnical Engineering, vol. 114, No. 4, April.

Power, M. S., A. W. Dawson, D. W. Streiff, R. G. Perman, and S. C. Haley, 1982. Evaluation of Liquefactin Susceptibility in the San Diego, Clfornia Urban Area. Proceedings 3rd International Conference on Microzonation, II, pp. 957-968.

Seed, H. B., and Idriss, I. M. 1982. Ground Motions and Soil Liquefaction During Earthquakes, Earthquake Engineering Research Institute, Oakland, Calfornia, Monograph Series, P. 13.

Youd, T.L., and Perkins, D. M., 1978. Mapping of Liquefaction Induced Ground Failure Potential, Journal of the Geotechnical Engineering Division, American Society of Civil Engineers, vol. 104, no. 4, pp. 433-446

- Section 3.2

Koppula, S.D. (1984) Pseudo-static analysis of clay slopes to earthquakes, Geotechnique, 34, 71-79.

Tanaka, K.(1982) Seismic Slope Stability Map (Present situation and several mooted points), Journal of Japan Landslide Society, 19-2, 12-19. (in Japanese)

Wilson, R.C., Wieczorek, G.F., and Horp, E.L. (1979) Development of Criteria for regional Mapping of Seismic Slope Stability, Abstract, 1979 Annual Meeting of the Geological Society of America.

Appendix: Hazard Analysis for the Magnitude 6 Earthquake occurring directly Underneath

Following the “Comments on Seismic Hazard Mapping” from TAG dated May 04, 2009, additional scenario earthquake is considered. The moment magnitude of the scenario earthquake is 6.0 and the earthquake is supposed to occur directly underneath the three cities and the distance from source to every grid center is 10 km.

The seismic motion at engineering seismic baserock (Vs30=760m/sec) is uniform at all grids in three cities and the calculated value is as follows.

- PGA: 245 gal
- PGV: 12.7 kine
- Sa(0.3sec): 455 gal
- Sa(1.0sec): 111 gal

The seismic motion at ground surface is shown in Figure A-1 to Figure A-4.

The amplification factor is shown in Figure A-5 to Figure A-6.

The liquefaction probability and the slope hazard probability are shown in Figure A-7 and Figure A-8, respectively.

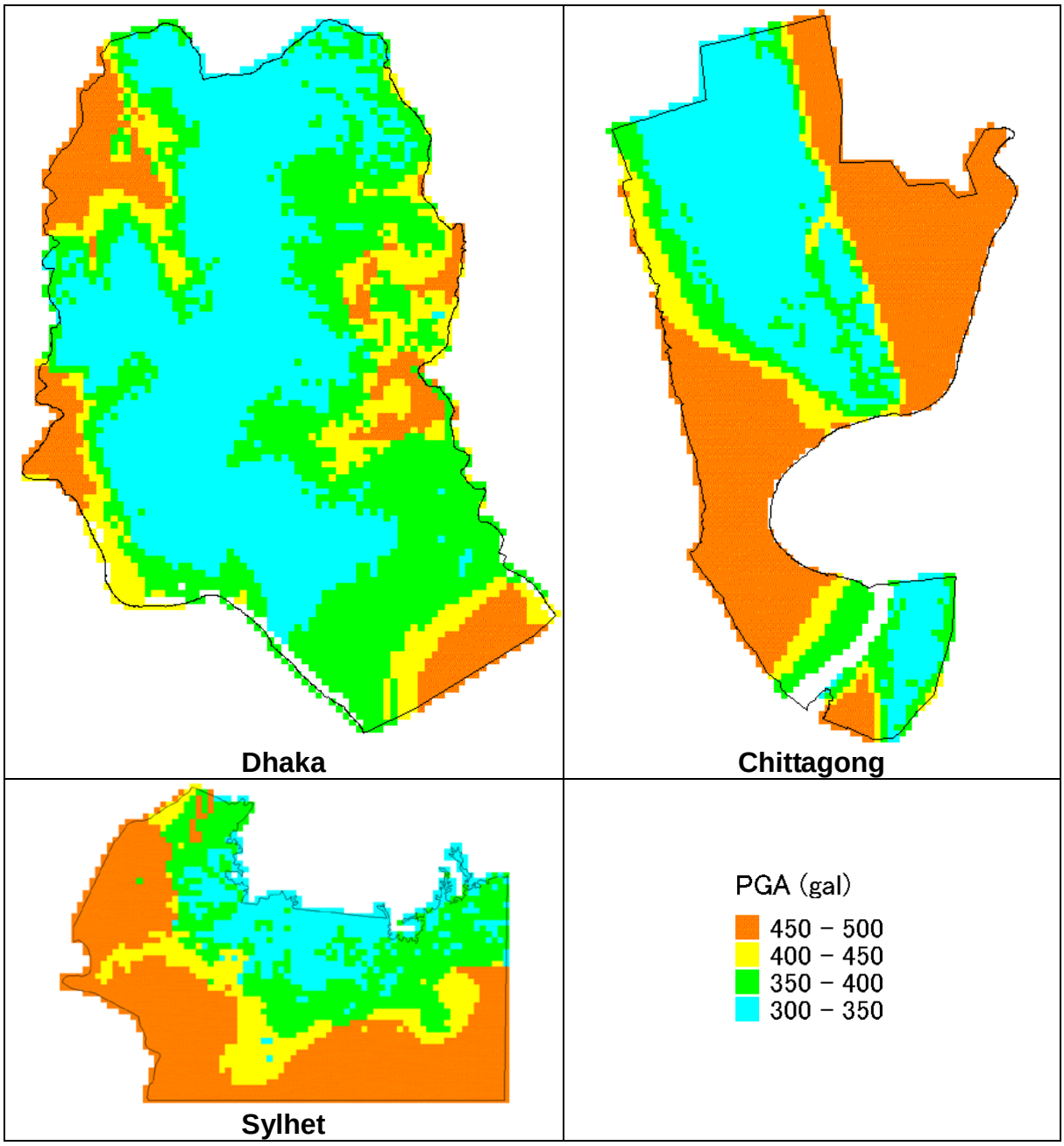

Figure A-1 PGA at Ground Surface for M6 Earthquake occurring directly Underneath

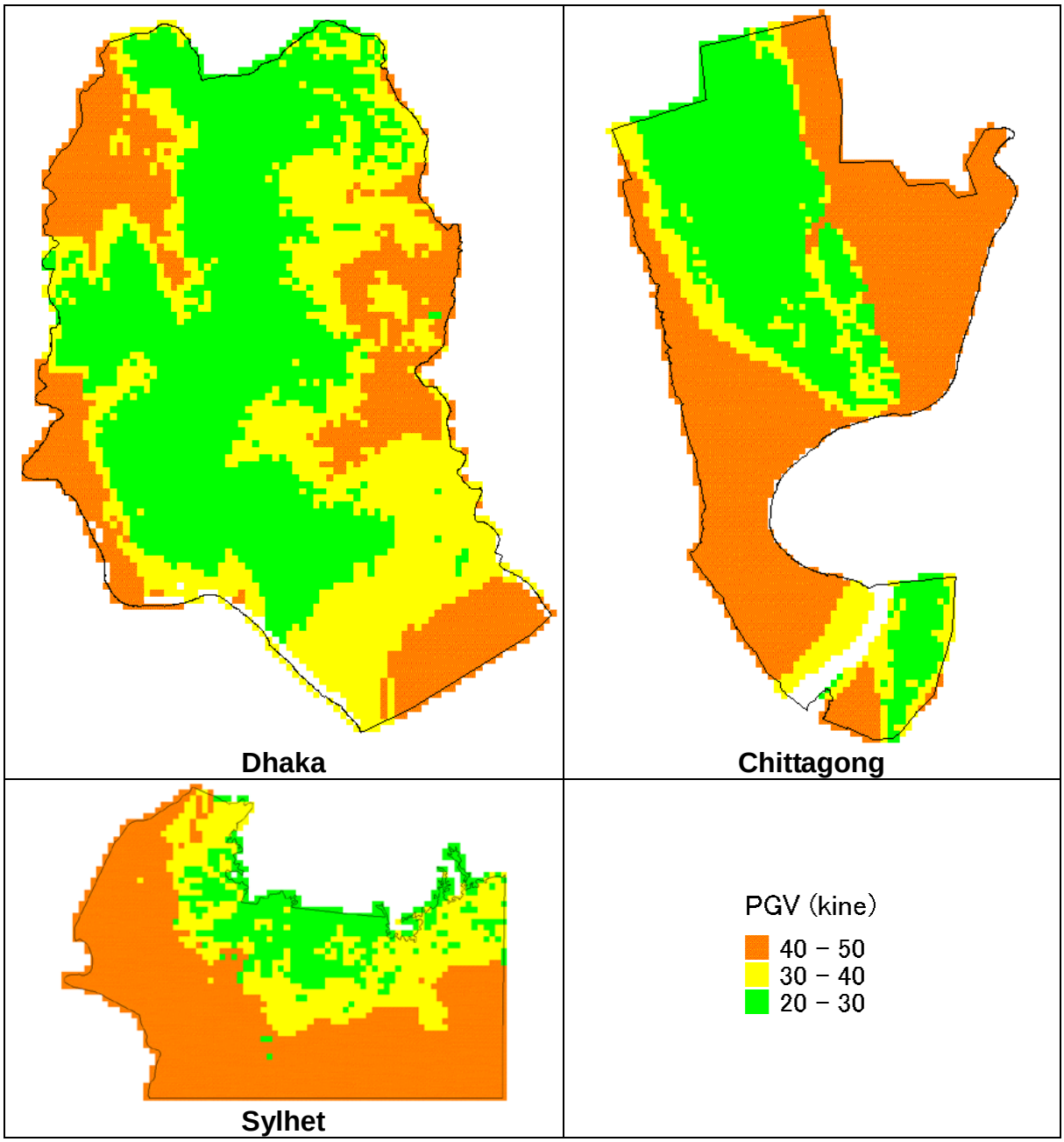

Figure A-2 PGV at Ground Surface for M6 Earthquake occurring directly Underneath

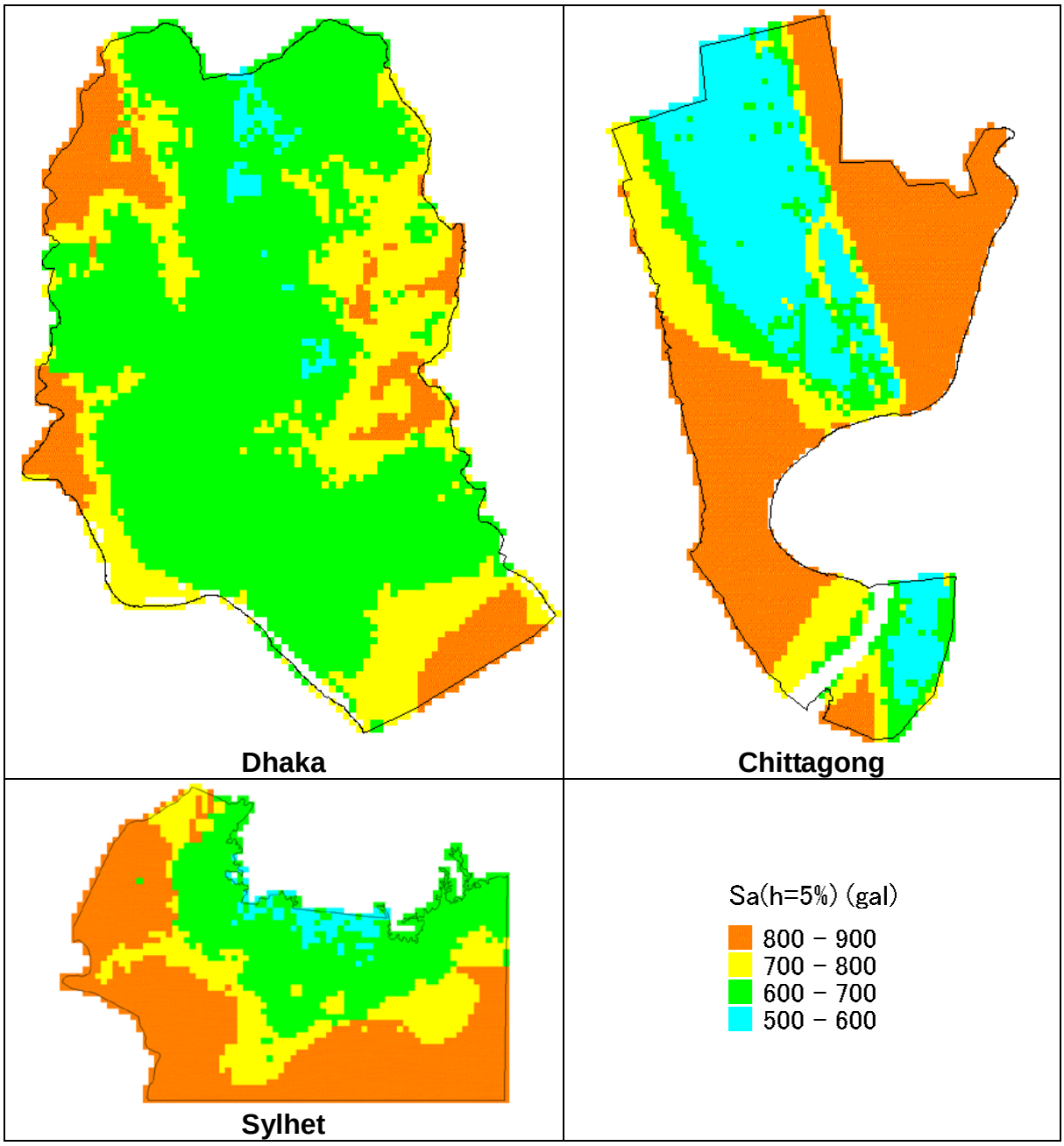

Figure A-3 Sa(h=5%) for T=0.3 sec at Ground Surface for M6 Earthquake occurring directly Underneath

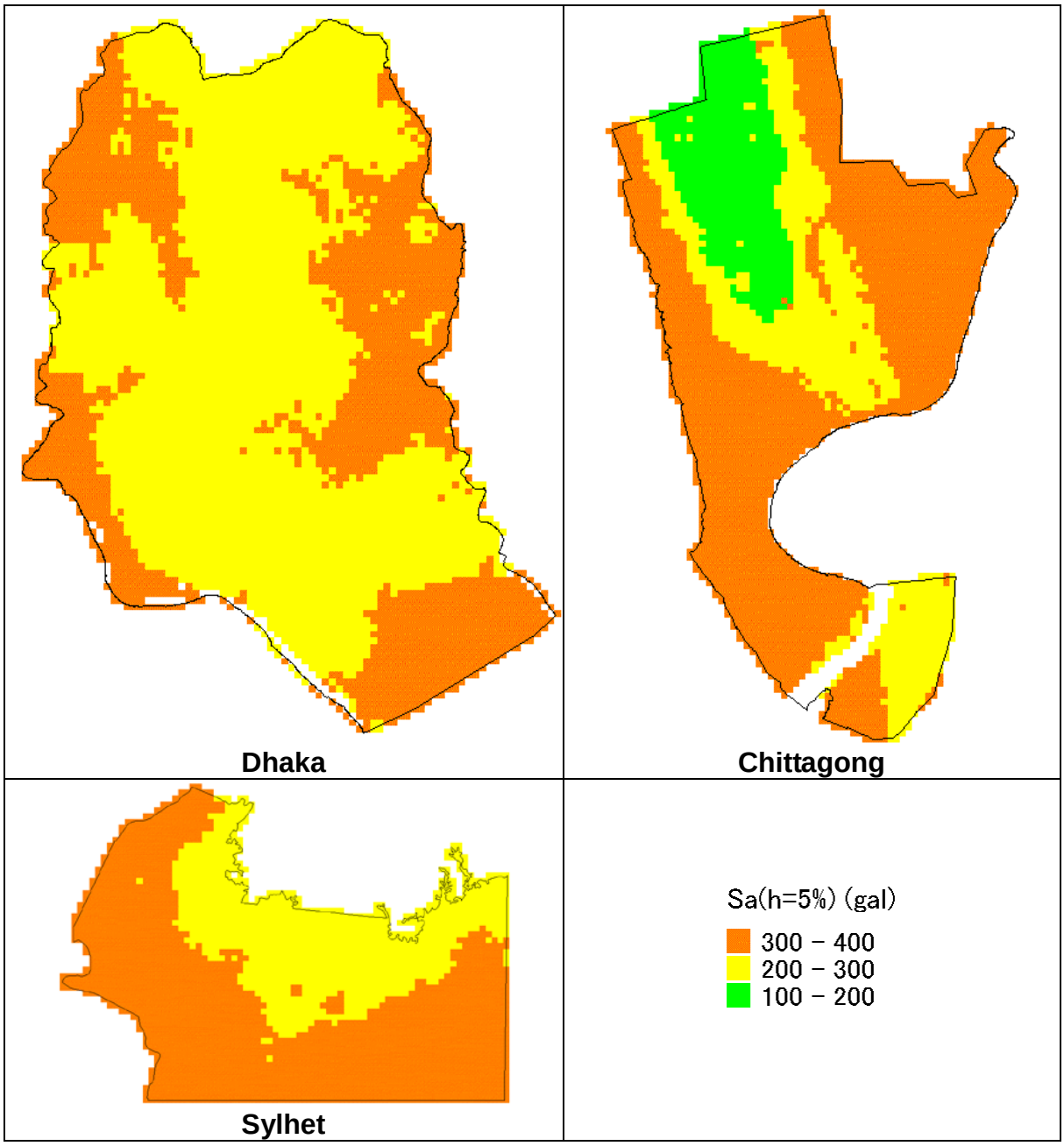

Figure A-4 Sa(h=5%) for T=1.0 sec at Ground Surface for M6 Earthquake occurring directly Underneath

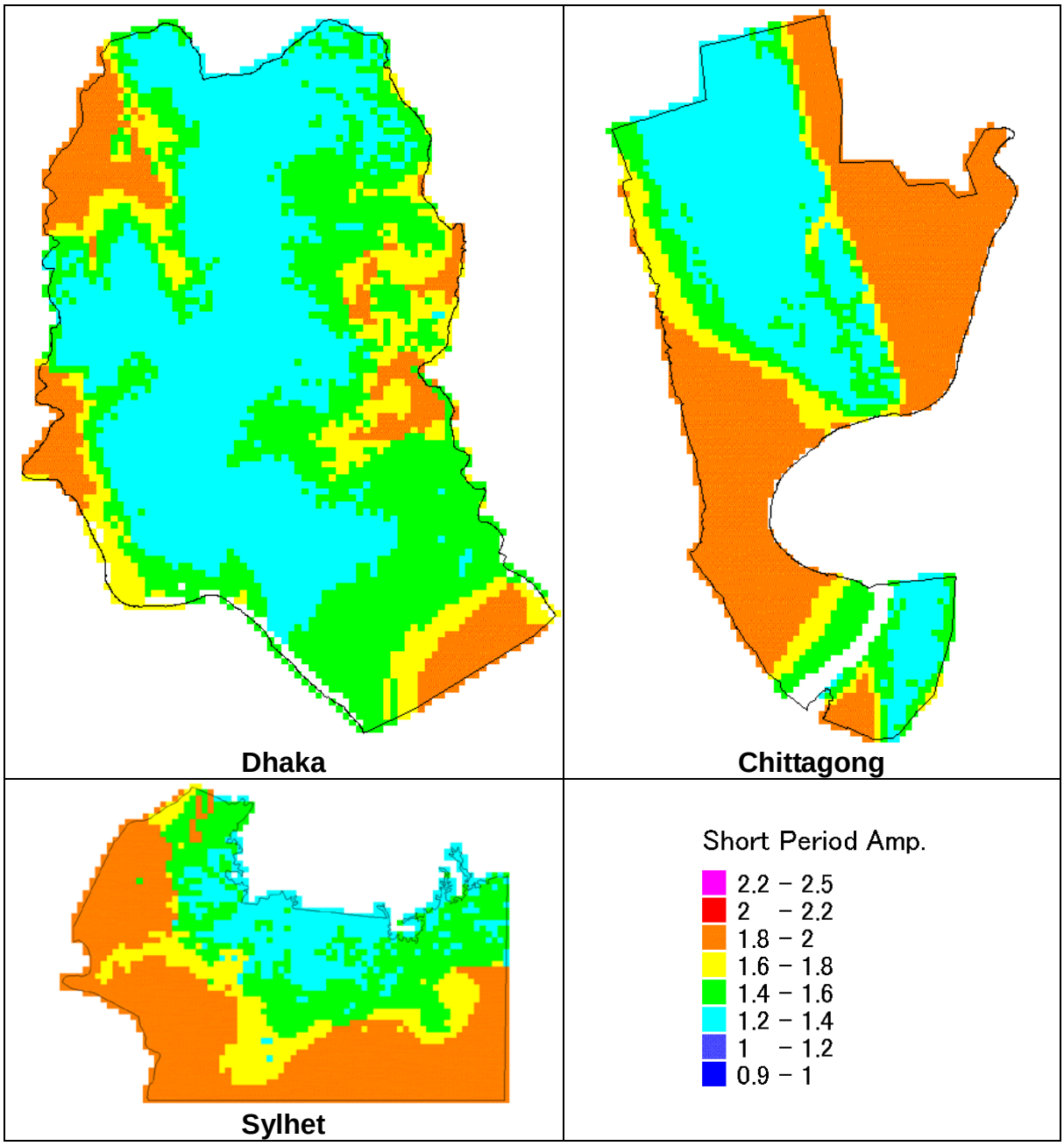

Figure A-5 PGA and Sa(0.3 sec) Amplification for M6 Earthquake occurring directly Underneath

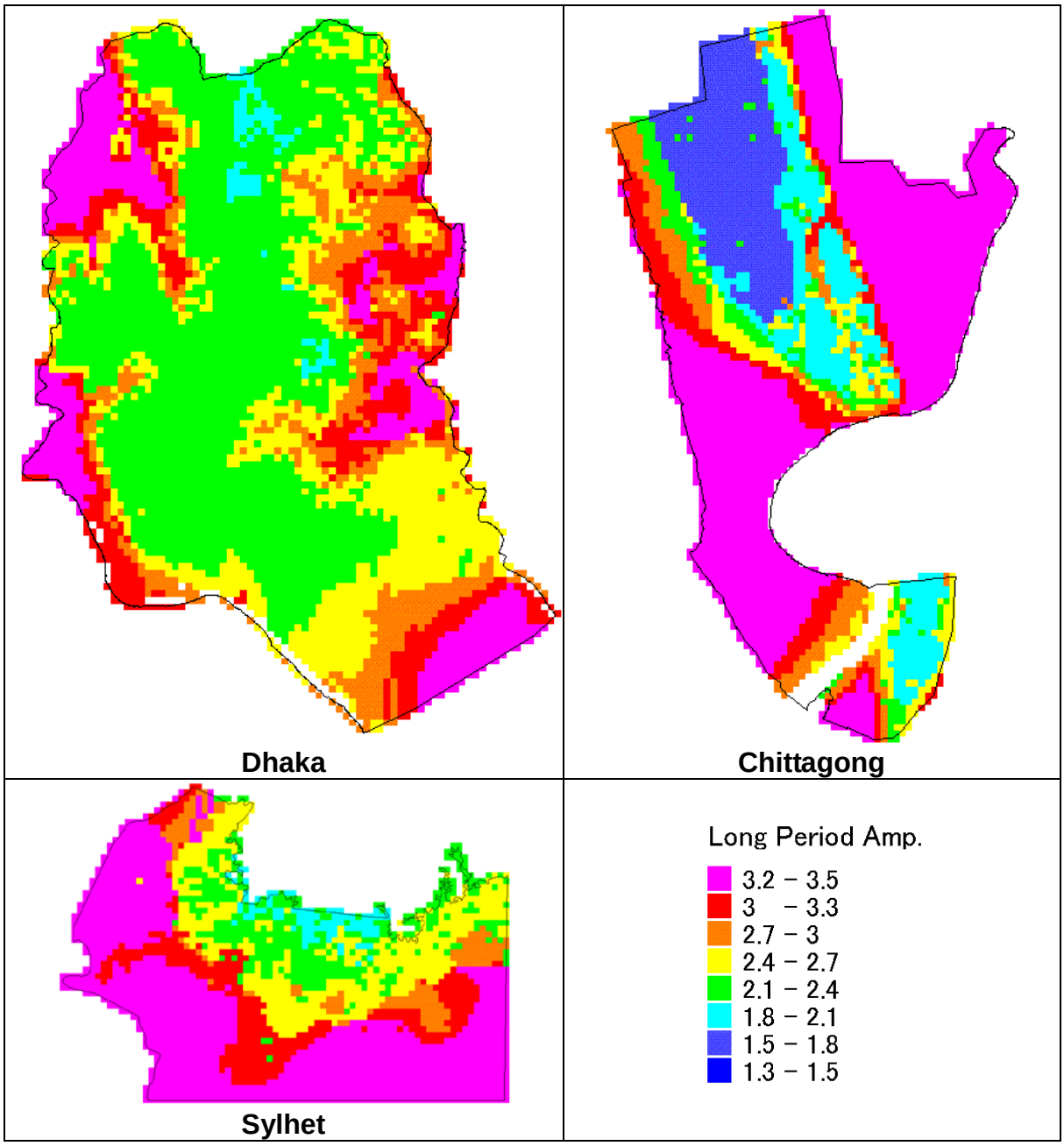

Figure A-6 PGV and Sa(1.0 sec) Amplification for M6 Earthquake occurring directly Underneath

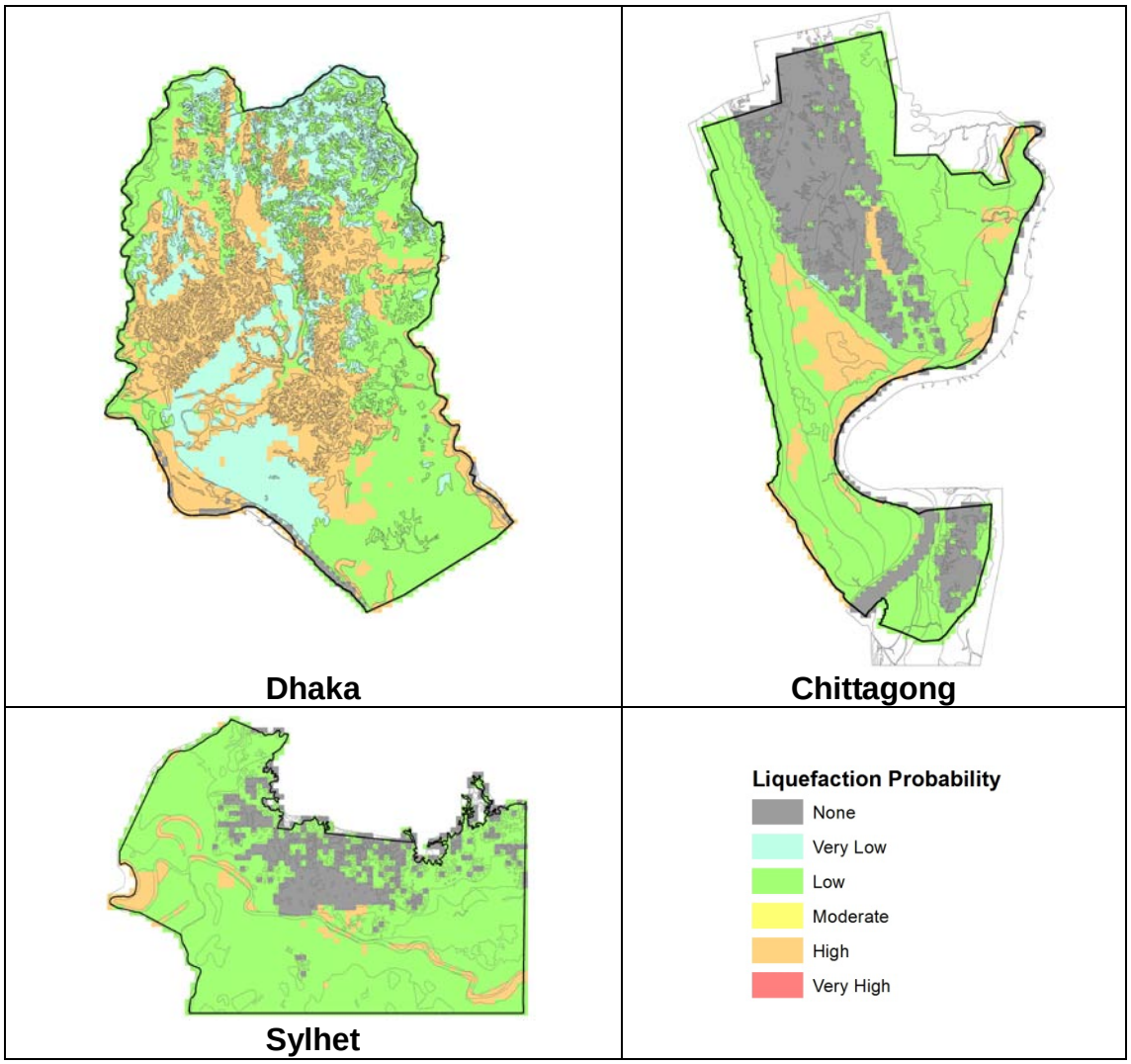

Figure A-7 Liquefaction Probability for M6 Earthquake occurring directly Underneath

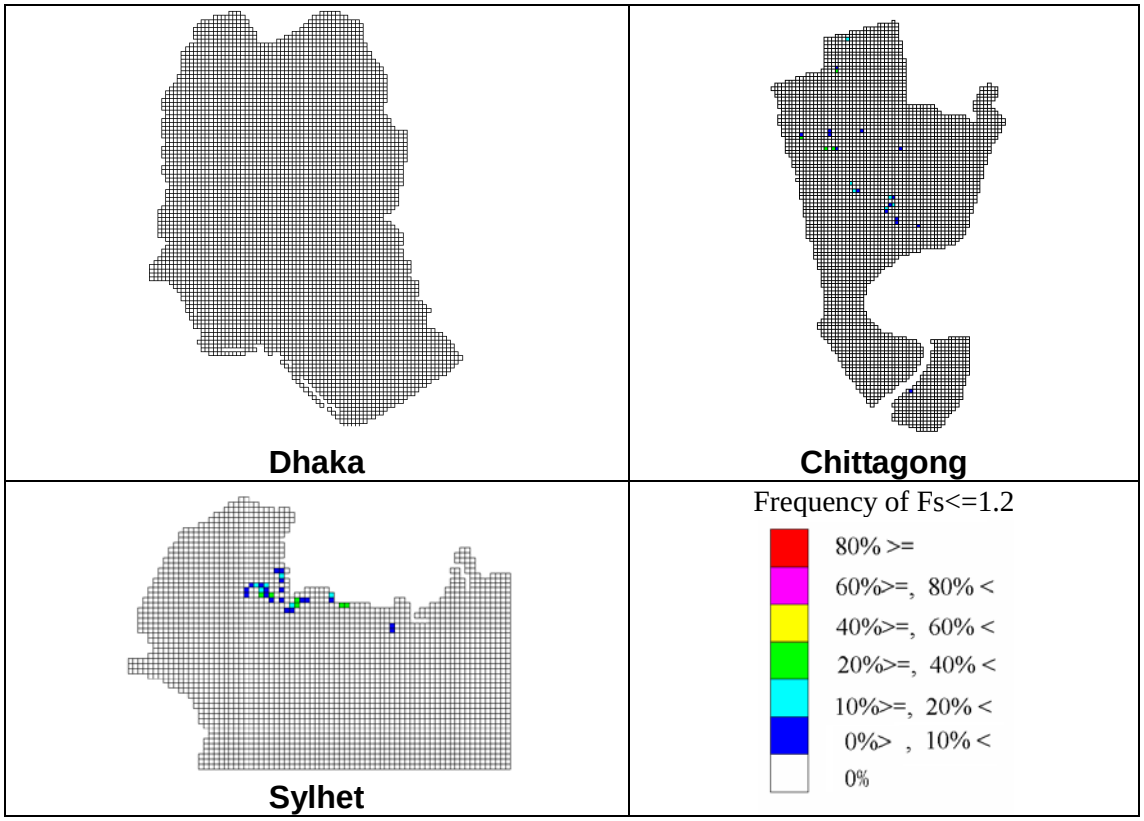

[The Frequency of Fs<=1.2 by Wilson's Method]

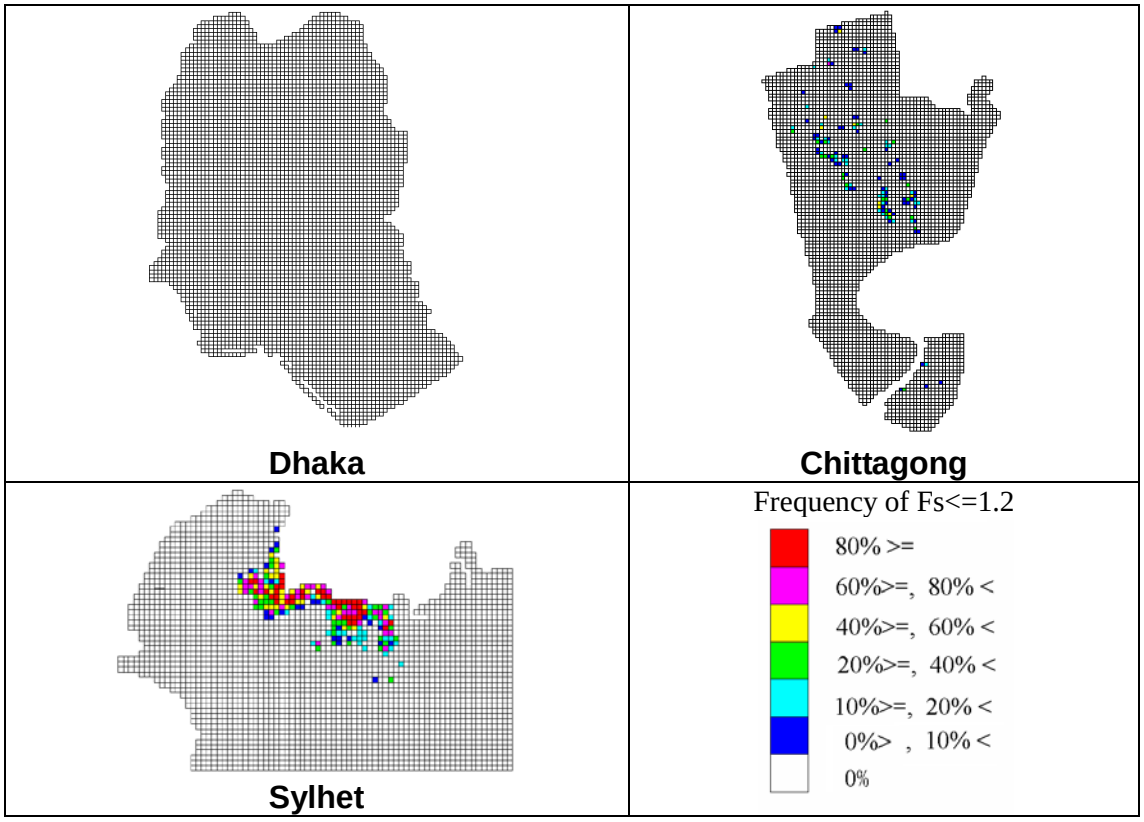

[The Frequency of Fs<=1.2 by Koppula's Method]

Figure A-8 Slope Hazard Probability

Technical Assistance: adpc Asian Disaster Preparedness Center
OYO International Corporation